

Peak-to-Average Power Ratio Reduction Techniques for Wavelet Packet Modulation

Berna Torun

Master of Science Thesis

Microwave Technology and Systems for Radar (MTSR)
Department of Telecommunications
Faculty of Electrical Engineering, Mathematics and Computer Science
Delft University of Technology

Peak-to-Average Power Ratio Reduction Techniques for Wavelet Packet Modulation

MASTER OF SCIENCE THESIS

For the degree of Master of Science in
Microwave Technology and Systems for Radar (MTSR)
at Department of Telecommunications
at Delft University of Technology

Berna Torun

27 October 2010

Faculty of Electrical Engineering, Mathematics and Computer Science
Delft University of Technology
Delft, The Netherlands





All rights reserved.

Copyright © Berna Torun

Telecommunications Department

Faculty of Electrical Engineering, Mathematics and Computer Science

Delft University of Technology

Delft, The Netherlands

DELFT UNIVERSITY OF TECHNOLOGY
DEPARTMENT OF
TELECOMMUNICATIONS

The undersigned hereby certify that they have read and recommend to the Faculty of
Electrical Engineering, Mathematics and Computer Science for acceptance a thesis
entitled

PEAK-TO-AVERAGE POWER RATIO
REDUCTION TECHNIQUES FOR
WAVELET PACKET MODULATION

by

BERNA TORUN

in partial fulfillment of the requirements for the degree of
MASTER OF SCIENCE.

Dated: 27 October 2010

Supervisor:

Dr. H. Nikookar

Readers:

Prof.dr. O. Yarovyj

Dr. G. Leus

M. K. Lakshmanan, MSc

Abstract

Multi-carrier Modulation (MCM) is a popular transmission technique for high speed data communication. In MCM, transmission is carried out in parallel on different frequencies. This technique is desirable for the transmission of digital data through the multipath fading channels. By parallel transmission of data, the deleterious effect of fading is spread over many bits, therefore, instead of a few adjacent bits being completely destroyed by the fading it is more likely that several bits are marginally affected by the channel. Another advantage of this technique is its spectral efficiency. In the MCM method the sub-channels are orthogonal and their spectra overlap over one-another. Therefore more carriers (and hence data) can be packed in a given bandwidth leading to a very high spectral efficiency. Because of the parallel transmission in MCM the symbol duration is increased which is also an advantage in channels having impulsive noise characteristics. In the conventional MCM implementations such as Orthogonal Frequency Division Multiplexing (OFDM), the carriers are static sine/cosine functions. As an alternative to OFDM, other orthogonal bases could be used for multi-carrier systems. For example, Wavelet Packet Modulation (WPM) has been shown to be an efficient technique with interesting features like adaptation and flexibility and improved characteristics in comparison to OFDM.

The WPM is still a developmental system and there are a lot of open questions left for research and understanding. One open research question is its Peak-to-Average Power Ratio (PAPR) performance of the system. The peak of the MCM signal can be up to number of subcarriers times the average power. Multi-carrier systems such as WPM or the classical OFDM combine many independently modulated sub-carriers to obtain a composite signal. If the sub-carriers add coherently then the peak power of the composite OFDM/WPM signal can be many times larger than the average power. This can lead to non-linear distortions and degradation of system performance. A large PAPR brings disadvantages like an increased complexity of the analog-to-digital and digital-to-analog converters and a reduced efficiency of the RF power amplifier. These large peaks increase the amount of inter modulation distortion resulting in an increase in the error rate. The average signal power must be kept low in order to ensure

that the transmitter amplifier operates in the linear region. This however will have a detrimental effect on the efficiency of power utilization particularly in mobile systems where battery lifetime is a premium resource. Minimizing the PAPR allows a higher average power to be transmitted for a fixed peak power, improving the overall signal to noise ratio at the receiver. Usually, the systems are constrained to a limited peak power due to the limitation of the dynamic range over which the transmitter amplifier operates linearly. It is therefore important to study the power fluctuations associated with multi-carrier systems.

While the impact of PAPR on OFDM operation is well understood, the literature on similar analysis for WPM is extremely thin. Furthermore, practically no material exists on the reduction of PAPR for WPM systems. In this regard, it is imperative to know if any of the PAPR reduction techniques available for OFDM can be applied for WPM and if so what are the adjustments required, if any, to make the technique suitable for WPM. Moreover, what are the effects of the wavelet parameters on the PAPR reduction and how could we optimize the PAPR reduction techniques. We have to find answers to these questions to reach our goal to mitigate the PAPR of WPM.

This thesis presents several original contributions to the field of PAPR reduction in the developmental multi-carrier WPM systems. In this thesis, after presenting the analysis of the PAPR effect in WPM system, we expand on the stochastics of the WPM signals. The envelope of the WPM signal follows the Gaussian distribution and its power has Chi-squared distribution. We show how the wave-shapes properties impact the PAPR performance. In this thesis, we mainly focused on the selected mapping techniques since they are distortionless and their complexity is lower compared to other techniques. After studying the selected mapping with scrambling technique to reduce PAPR, we present a novel WPM architecture that employs our proposed secure PAPR reduction technique. Since wireless transmission can easily be eavesdropped, the message is encrypted in most of the wireless communication systems. Generally, stream ciphers are employed for encryption thanks to their performance. Encryption using stream ciphers operates similar to scrambling. Therefore, instead of scrambling, stream cipher may also be employed in selected mapping technique where replicas of the original message are generated by encrypting the message with different keys. In terms of cost and complexity, secure PAPR reduction does not introduce additional complexity to the WPM system while producing almost similar PAPR reduction gains. Furthermore, to the best of our knowledge, employing stream ciphering to reduce PAPR has not been applied in the literature which adds an additional novelty dimension to this thesis. Besides scrambling techniques, phase modification is another technique and in this thesis we present how selected mapping with phase modification can be applied to reduce PAPR. In all instances the proposed technique reduces the PAPR between 1.5 and 2.5 dB. In terms of the BER performances, all the selected mapping techniques have the same BER performance except the multiplicative scrambling based PAPR reduction. Multiplicative scrambling produces a larger BER since multiplicative scramblers diffuse the bit errors into other bit positions proportional with the number of taps in their characteristic polynomials.

Since selected mapping relies on creating replicas of the original signal and selecting

the one producing the least PAPR, their performances are similar. These techniques can roughly be described as greedy search in the phase space where the number of replicas can be regarded as the number of random search points in the phase space. A smarter approach can be developed to optimize this greedy search algorithm using neural networks or some local search techniques. Consequently, we introduce an optimized WPM architecture that employs optimized selected mapping with phase modification technique. The designed optimization algorithm improves the PAPR reduction performance further than the selected mapping with phase modification. For a complementary cumulative distribution function (CCDF) value of 10^{-2} , the PAPR of the original frame is around 10 dB; whereas, optimized phase-shifted frame produces a PAPR value around 8.2 dB. While, a PAPR value below 8.7 dB cannot be reached with the selected mapping techniques, which depends on randomization such as randomly phase-shifting or random scrambling.

Acknowledgements

I would like to acknowledge those who have supported me throughout the thesis process. First, I would like to express my sincere thanks to my supervisor, Dr. H. Nikookar, for his guidance, encouragement and continuous support throughout the completion of the thesis. I also would like to thank my mentor, M.K. Lakshmanan for his helpful suggestions and assistance. I want to thank my thesis committee, Prof.dr. O. Yarovyi and Dr. G. Leus, for taking the time to give feedback on my thesis. I am also grateful to Dr.ir. W.G.M. Groenevelt, for our interesting discussions which have contributed to the theoretical background of this thesis. Further, I wish to thank all the IRCTR and MTSR members and all of my fellow students, for the pleasant and stimulating working atmosphere.

Additionally, I would like to express my gratitude to Prof.dr.ir. A.T. de Hoop for his invaluable motivation and encouragement. Moreover, my special thanks go to my dear old friends for their enormous moral support and encouragements.

Finally, last but not least, I am very grateful to my family, who always have encouraged and supported me enormously during every phase of my life with their endless patience and love.

Table of Contents

Acknowledgements	v
1 Introduction	1
1-1 Background	1
1-2 Motivation and Goals	3
1-3 Novelty and Contribution	4
1-4 Thesis outline	4
2 Background Information	7
2-1 Wavelet Fundamentals	7
2-1-1 History of Wavelets	7
2-1-2 Continuous Wavelet Transform (CWT)	9
2-1-3 Discrete Wavelet Transform (DWT)	10
2-1-4 Filter Banks	13
2-1-5 Wavelet Packet Transform (WPT)	17
2-2 Wavelet Packet Modulation	18
2-2-1 MCM	18
2-2-2 Theory on Wavelet Packet Modulation	18
2-3 Summary	21
3 Peak-to-Average Power Ratio of WPM Signal	23
3-1 PAPR Distribution of Multi-Carrier Signal	24
3-2 PAPR Distribution of WPM Signal	25
3-3 Analysis of WPM Signal Characteristics	25
3-3-1 Stochastic of the WPM Signal	26
3-3-2 Stochastic of WPM Power Distribution	26
3-3-3 Stochastic of WPM PAPR Distribution	28
3-4 Summary	30

4	Selected Mapping with Phase Modification	31
4-1	PAPR Reduction Techniques	31
4-1-1	Signal Scrambling Techniques	32
4-1-2	Signal Distortion Techniques	34
4-1-3	Selection Criteria for PAPR Reduction Technique	35
4-2	Selected Mapping with Phase Modification	36
4-3	Numerical Results	37
4-3-1	Impact of choice of number of replications	39
4-3-2	Choice of distribution of the Phase Sequences	39
4-3-3	Impact of choice of phase alphabet	41
4-3-4	Impact of choice of wavelet families	41
4-3-5	Influence of the PAPR reduction technique on the Bit Error Rate (BER) performance	42
4-4	Summary	43
5	Selected Mapping with Scrambling	45
5-1	Scrambling Based PAPR Reduction in WPM	46
5-1-1	Selected Mapping Using Multiplicative Scrambling	48
5-1-2	Selected Mapping Using Additive Scrambling	50
5-1-3	Numerical Results of Comparison of Scrambling-Based PAPR Reduction Techniques	51
5-2	Secure PAPR Reduction with RC4	57
5-2-1	System Model	57
5-2-2	Numerical Results of Secure Scrambling-Based PAPR Reduction Technique	59
5-3	Comparison of the Selected Mapping with Scrambling Techniques	62
5-4	Summary	64
6	Optimization of Selected Mapping with Phase Modification	65
6-1	PAPR Reduction as an Optimization Problem	66
6-1-1	Hopfield neural network (HNN)	67
6-1-2	Hill Climbing	68
6-2	Hill Climbing Based PAPR Reduction for WPM Systems	70
6-3	Numerical Results	74
6-4	Convergence and Complexity	77
6-4-1	Time Complexity of the Algorithm	77
6-4-2	Convergence of the Algorithm	78
6-5	Summary	78

7 Conclusions and Future Research	81
7-1 Conclusions	81
7-2 Future Research Topics	83
Bibliography	85
Publications	91
Glossary	93
List of Acronyms	93

List of Figures

1-1	Organization of the thesis.	5
2-1	Translation-Scale Representation of a Signal.	9
2-2	2-Channel Analysis Filter Bank.	15
2-3	2-Channel Synthesis Filter Bank.	16
2-4	Inverse Discrete Wavelet Packet Transform	19
2-5	Discrete Wavelet Packet Transform	20
2-6	Wavelet Packet Modulation Transmitter Architecture.	20
2-7	Wavelet Packet Modulation Receiver Architecture.	20
3-1	Cumulative Distribution Function (CDF)-distribution of PAPR for (left to right) number of subcarriers: 16, 32, 64, 128, 256, 512, 1024 (dashed is simulated Daubechies WPM signals with length 15).	26
3-2	CDF of Gaussian signals are compared with the CDF of Daubechies WPM signals with length 15 for different number of carriers (for 128 carriers).	27
3-3	CDF of power of Gaussian and Wavelet Packet Modulation signals (for 128 carriers).	27
3-4	CDF of power of Wavelet Packet Modulated signals for various families (for 128 carriers).	28
3-5	CDF of PAPR for the WPM system applying several wavelet families. All the configurations are taken to have 128 carriers.	29
3-6	CDF of PAPR for the WPM system applying different filter lengths of the Daubechies wavelet family. All the configurations are taken to have 128 carriers.	29
4-1	Scheme of PAPR Reduction Techniques	33
4-2	WPM Transmitter Block diagram with the PAPR reduction technique	36

4-3	Complementary Cumulative Distribution Function (CCDF) of the PAPR of the WPM signal for different values of L . The wavelet considered is Daubechies 5 (length 10). A reference curve with no PAPR reduction is also plotted. . .	38
4-4	Complementary cumulative distribution function (CCDF) of the PAPR of WPM for different distributions of the phase sequences. The wavelet considered is Daubechies 5 (length 10).	39
4-5	CCDF of the PAPR of WPM using the PAPR reduction technique for different phase sequences. The wavelet considered is Daubechies 5 (length 10). . . .	40
4-6	CCDF of the PAPR for several wavelets.	40
4-7	CCDF of the PAPR for the WPM system with different filter lengths of the Daubechies wavelet family.	41
4-8	BER vs. Signal-to-Noise Ratio (SNR) (dB) for the cases with and without PAPR reduction (phase modification) and for various distributions of the phase. For the case with random phase change two figures are plotted. In the first case (denoted Case-1) the receiver has complete and perfect knowledge of the random phases used at the transmitter. In the second scenario (marked Case-2) the receiver operates with no knowledge of the phases used at the transmitter. For the scenarios when phases with Golay and Hadamard distributions are used, the transmitter and receiver only share the keys of the pseudo-random polynomial.	42
5-1	WPM architecture where the different SLM methods are applied.	46
5-2	WPM Transmitter architecture employing Multiplicative Scrambler without side information for PAPR reduction.	48
5-3	WPM Transmitter architecture employing Additive Scrambler with side information for PAPR reduction.	50
5-4	CCDF of the PAPR for several initialization seeds where additive scrambler is employed.	52
5-5	CCDF of the PAPR for several number of labels where multiplicative scrambler is employed.	52
5-6	CCDF of the PAPR for several wavelet families of the additive scrambler. . .	53
5-7	CCDF of the PAPR for several wavelet families of the multiplicative scrambler. . .	54
5-8	CCDF of the PAPR for the WPM system where additive scrambler is employed with different filter lengths of the Daubechies wavelet family.	55
5-9	CCDF of the PAPR for the WPM system where multiplicative scrambler is employed with different filter lengths of the Daubechies wavelet family. . .	55
5-10	CCDF of the PAPR of the WPM signal for different levels of decomposition, N , where additive scrambler is employed. The wavelet considered is Daubechies 5 (length 10). A reference curve with no PAPR reduction is also plotted. . .	56
5-11	CCDF of the PAPR of the WPM signal for different levels of decomposition, N , where multiplicative scrambler is employed. The wavelet considered is Daubechies 5 (length 10). A reference curve with no PAPR reduction is also plotted.	56
5-12	WPM Transmitter architecture employing secure PAPR reduction technique with RC4.	57

5-13	CCDF of the PAPR for several number of replicas, L where secure PAPR reduction technique is employed.	60
5-14	CCDF of the PAPR for various wavelet families where secure PAPR reduction technique is employed.	60
5-15	CCDF of the PAPR for the WPM system where secure PAPR reduction technique is employed with different filter lengths of the Daubechies wavelet family.	61
5-16	CCDF of the PAPR of the WPM signal for different levels of decomposition, N , where RC4 is employed. The wavelet considered is Daubechies 5 (length 10). A reference curve with no PAPR reduction is also plotted.	62
5-17	BER performance of the selected mapping with scrambling techniques. . .	63
5-18	Comparison of the PAPR reduction performance of the selected mapping with scrambling techniques.	63
6-1	Block diagram of the PAPR reduction method using neural network optimizer.	66
6-2	Block diagram of the hill climbing based PAPR reduction method.	72
6-3	Demonstration of Algorithm 6.2 for various wavelet families.	73
6-4	CCDF of the PAPR of WPM for several reduction techniques. The WPM system is realized using a filter bank structure with 4 levels of decomposition and QPSK modulation scheme. For SLM, the number of phase-shifted replicas of the original frame, $N = 4$. Reference (original) curves are the PAPR CCDFs where no PAPR reduction technique is employed.	75
6-5	CCDF of the PAPR of WPM using Hill Climbing based optimization method. The WPM system is realized using a filter bank structure with 4 levels of decomposition and QPSK modulation scheme, for different wavelet families.	76
6-6	CCDF of the PAPR of WPM using Hill Climbing based optimization method with different filter lengths of the Daubechies wavelet family.	76
6-7	Impact of the initially selected step size, s_i on the PAPR reduction.	77
6-8	Demonstration of the impact of the initially selected step size where $s_j = 0.01, \forall j$ on the PAPR reduction. The wavelet considered is Daubechies 5 (length 10). Algorithm 6.2 converges to a minima in around 2000 epochs which are marked with black dots.	79

List of Tables

3-1	Wavelet Specifications.	28
6-1	The parameter values used in the simulations	74

Chapter 1

Introduction

1-1 Background

Multi-carrier Modulation (MCM) is a popular transmission technique for high speed data communication. In this method, transmission is carried out in parallel on different frequency bands. This technique is desirable for the transmission of digital data through the multipath fading channels. By parallel transmission of data, the deleterious effect of fading is spread over many bits, therefore, instead of a few adjacent bits being completely destroyed by the fading it is more likely that several bits are marginally affected by the channel. Another advantage of this technique is its spectral efficiency. In the MCM method the sub-channels are orthogonal and their spectra overlap over one-another. Therefore more carriers (and hence data) can be packed in a given bandwidth leading to a very high spectral efficiency. Because of the parallel transmission in MCM the symbol duration is increased which is also an advantage in channels having impulsive noise characteristics.

In the conventional MCM implementations such as Orthogonal Frequency Division Multiplexing (OFDM), the carriers are static sine/cosine functions. As an alternative to OFDM other orthogonal bases could be used for multi-carrier systems. For example, Wavelet Packet Modulation (WPM) has been shown to be an efficient technique with interesting features like adaptation and flexibility and improved characteristics in comparison to OFDM [1]. Though the principle of multi-carrier modulation is not recent, its actual use in commercial systems had been delayed until the technology required to implement it became available at reasonable costs. Similarly, the idea of using more advanced transform, like wavelet packet analysis, than Fourier as the core of a multi-carrier system though introduced more than a decade ago thus have received very little attention. With the current demands for efficiency and high performance in wireless communication systems, one is entitled to wonder about the possible improvements that wavelet-based modulation could exhibit compared to OFDM systems.

Several objectives motivate the current research on WPM. The greatest motivation for pursuing WPM systems lies in the freedom they provide to communication systems designers. Unlike the Fourier bases which are static sine/cosine, WPM uses wavelets which offer flexibility and adaptability that can be tailored to satisfy an engineering demand. By altering the design specifications, a wavelet based system that is more robust, against intercarrier interference (ICI), intersymbol interference (ISI), could be developed without compromising on spectral efficiency or receiver complexity. While WPM can take advantage of all those advanced functionalities designed for multi-carrier systems, it also benefits from its inherent flexibility.

The WPM is still a developmental system and there are a lot of open questions left for research and understanding. One of it is its Peak-to-Average Power Ratio (PAPR) performance. The peak of the MCM signal can be up to M times the average power (where M is the number of subcarriers). A MCM signal consists of a number of independently modulated subcarriers, which can give a large PAPR when added up coherently. When M signals are added with the same phase, they produce a peak power that is M times the average power.

A large PAPR brings disadvantages like an increased complexity of the analog-to-digital and digital-to-analog converters and a reduced efficiency of the RF power amplifier. These large peaks increase the amount of inter modulation distortion resulting in an increase in the error rate. The average signal power must be kept low in order to ensure that the transmitter amplifier operates in the linear region. This however will have a detrimental effect on the efficiency of power utilization particularly in mobile systems where battery lifetime is a premium resource. Minimizing the PAPR allows a higher average power to be transmitted for a fixed peak power, improving the overall signal to noise ratio at the receiver. Usually, the systems are constrained to a limited peak power due to the limitation of the dynamic range over which the transmitter amplifier operates linearly.

Reliable cellular wireless service requires clean and consistent transmission from base stations under widely and rapidly changing conditions. The base station's radio frequency (RF) power amplifiers (PA) are key in guaranteeing this reliability. Spectral efficiency has always been important in mobile communications. Nowadays, third and fourth generation digital systems demand that PA linearity and efficiency also be included as crucial performance requirements. These amplifiers are found in cellular base stations that support the OFDM of wireless standards (e.g. 3rd and 4th generation networks) as well as improvements to existing standards (e.g. 2nd generation GSM). Due to the use of Quadrature modulation and multiple sub-carriers the signal power in many of these applications fluctuates significantly over time. This means that the signal has a high PAPR ratio when compared with single carrier systems.

Although the aforementioned systems maintain good spectral efficiency, the varying envelope of the signal generates spectral re-growth in the adjacent channels and in-band distortion. A tradeoff exists between linearity and efficiency; power efficiency is very low when the amplifier operates in its linear region and increases as the amplifier is driven into its compression region. Due to the nature of signal generation, multi-carrier signal, OFDM and WPM have large PAPRs. The PAPR values set high demands for the

linearity of the power amplifiers since it is desirable for the PA to operate in its linear region, this leads to low power efficiency.

It is therefore important to minimize the PAPR. Several reduction techniques such as clipping, companding, pulse shaping, selected mapping, coding, etc. to reduce the PAPR problem of OFDM have been proposed in the literature which are discussed in Chapter 3. These techniques could be basically divided in two categories. First, there are signal distortion techniques, which reduce the peak amplitudes simply by nonlinearly distorting the OFDM signal at or around the peaks. Examples of distortion techniques are clipping, peak windowing, companding, etc. The second category is based on scrambling each OFDM symbol with different scrambling sequences and selecting that sequence gives the smallest PAPR. These signal scrambling methods are all variations on how to modify the phases of OFDM subcarriers to decrease the PAPR. Moreover, there are also coding techniques, e.g. special forward-error correcting, which are used in combination with the previous mentioned techniques to reduce the BER.

1-2 Motivation and Goals

While the impact of PAPR on OFDM operation is well understood, the literature on similar analysis for WPM is extremely thin. In fact, practically no material exists on the reduction of PAPR for WPM systems. In this regard it is imperative to know if any of the PAPR reduction techniques available for OFDM can be applied for WPM and if so what are the adjustments required, if any, to make the technique suitable for WPM. Moreover, what are the effects of the wavelet parameters on the PAPR reduction and how could we optimize the PAPR reduction techniques. We have to find answers to these questions to reach our goal to mitigate the PAPR of WPM.

Through this thesis work we conduct a study on the effect of PAPR on the WPM system and pursue techniques to mitigate it. The primary goals of the thesis work are:

- To analyze the PAPR effect in WPM transmission system.
- To establish a simulation setup in MATLAB to analyze WPM PAPR characteristics.
- To investigate the stochastics of the WPM signals and influence of the wave-shape properties on their PAPR performances.
- To propose a method to mitigate the PAPR and implement this method.
- To present other PAPR reduction techniques which are mainly oriented on the security aspects to improve the proposed method.
- To design an optimization algorithm to improve the presented PAPR reduction method.
- To evaluate the performances of the several presented PAPR reduction techniques.

1-3 Novelty and Contribution

This thesis presents several novelties and original contributions to the field of PAPR reduction in the developmental multi-carrier WPM systems. The novelty aspects of this thesis work and the contributions are:

- Analysis of the PAPR effect in WPM system.
- Analysis of the stochastics of the WPM signals.
- Analysis of the influence of the wave-shape properties on their PAPR performances.
- Study on selected mapping with scrambling technique to reduce PAPR.
- Designing a novel WPM architecture that employs secure PAPR reduction technique.
- Study on selected mapping with phase modification to reduce PAPR.
- Designing a novel WPM architecture that employs optimized selected mapping with phase modification technique. The designed optimization algorithm improves the PAPR reduction performance further than the selected mapping with phase modification.
- Evaluation of the performances of the studied PAPR reduction techniques.

Figure 1-1 illustrates the organization of the thesis report.

1-4 Thesis outline

The thesis is organized as follows. In Chapter 2, a literature review of WPM system will be presented. This part will introduce the novel promising alternative multi-carrier WPM system focussing on wavelet representation of signals and where properties and main aspects will be examined. A discussion on the distribution of PAPR in WPM is provided in Chapter 3. In Chapter 4, we propose a method which works on the principle of selected mapping to reduce the high PAPR in WPM. As a consequence of the huge amount of side information which should be sent with the transmitted data for the method proposed in Chapter 4, we will examine in Chapter 5 some other methods which are based on the scrambling techniques, where no side information (or at least encrypted secure side information) is transmitted. In Chapter 6 we propose to optimize the phase shifts of the selected mapping method by introducing the hill climbing based optimization technique. Finally, the conclusions and future work research opportunities are listed in Chapter 7.

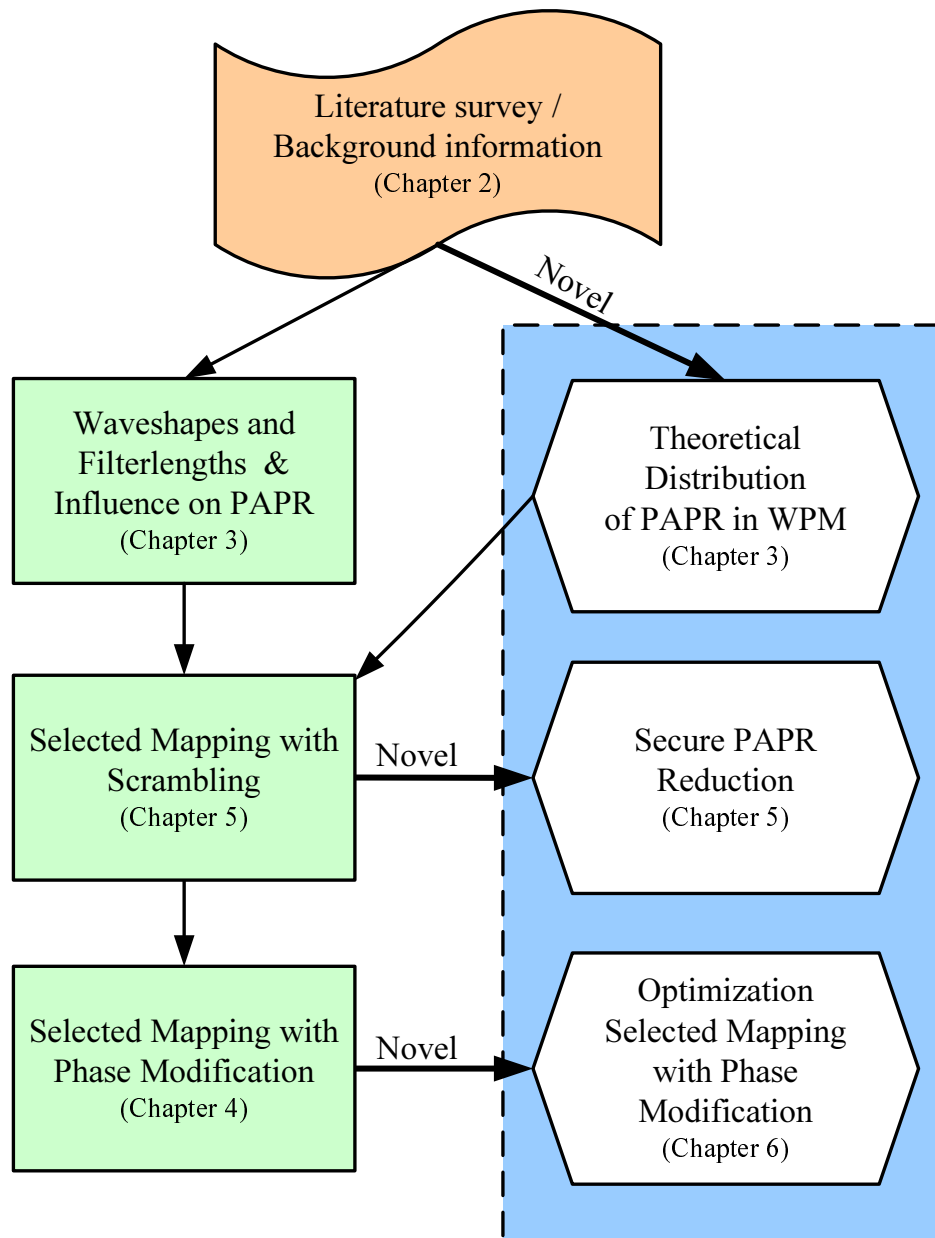


Figure 1-1: Organization of the thesis.

Background Information

Wavelet Packet Modulation (WPM) systems offers an alternative to the well-established Orthogonal Frequency Division Multiplexing (OFDM) as an efficient multicarrier modulation technique for data transmission [2]. It has strong advantage of being generic transmission scheme whose actual characteristics can be widely customized to fulfill several requirements and constraints of advanced communication systems. In the last decades wavelets have been favorably applied in signal and image processing fields but they just recently attracted attention of the telecommunication community. Therefore, some research questions remain to be addressed before novel WPM can be used in practice.

In this chapter, we provide material to understand the contents in Chapter 3 and later. The material is divided into two halves: the first half describing wavelet fundamentals. The second one details how the Wavelet Packet Modulation can be build upon the theory of wavelets.

2-1 Wavelet Fundamentals

2-1-1 History of Wavelets

The wavelets theory can be viewed as an extension of Fourier analysis. The basic idea of both transformations is the same: representing a function by a set of other functions. It all started in 1800s when Joseph Fourier discovered that he could superpose cosines and sines to represent other functions. Since then Fourier analysis has been used extensively by scientists and engineers for all kind of problems and applications. However, Fourier analysis does not work equally well for each problem. Linear problems and stationary signals are well suited for Fourier analysis but representation of brief, unpredictable and non-stationary signals on the other hand is much more difficult. The engineers sought for a solution and found it in Wavelet Transform.

The wavelets are a relatively new concept that has been introduced in the 1980s although some pioneering work had been done earlier. Since the 1980s wavelets have attracted considerable interest from the theoreticians and engineers where wavelets have promising applications. Because of the large interest, the wavelet theory has been well developed over the past years and several books on this subject have appeared as a large volume of research articles. Barbara Burke Hubbard describes the birth, the history, and the seminal concepts in [3]. The wavelet domain is growing very quickly. Many papers on wavelets and practical trials are published every month.

Chronology of developments in the wavelets theory as follows.

- 1805 Fourier analysis developed.
- 1965 Fast Fourier Transform (FFT) algorithm appeared.
- 1980s Beginnings of wavelet theory, modest understanding why/when do wavelets work.
- 1985 Morlet & Grossman work on continuous wavelet transform trying to get perfect reconstruction without redundancy.
- 1987 Mallat unified the work done individually by different researchers.
- 1987 Mallat developed multi-resolution theory, discrete wavelet transform, wavelet construction techniques, but there was still lack of compact support wavelets.
- 1988 Daubechies found compact, orthogonal wavelets with arbitrary number of vanishing moments.
- 1990s Wavelets took off, attracting both mathematicians and engineers.

After the completion of basic theory for wavelet transform, diverse fields have recognized the potential of wavelets. Some of the fields of wavelets applications may be enumerated as follows.

- Image processing
- Data compression
- Acoustics
- Signal processing
- Astrophysics
- Sub-band coding

It has been also foreseen that wavelets are going to play an important role in many areas of future telecommunication systems [4].

2-1-2 Continuous Wavelet Transform (CWT)

The CWT is defined as a sum of a signal multiplied by scaled and shifted version of wavelet basis function. Using different scaling factors the wavelet is stretched or compressed accordingly, while a translation parameter causes delay or hastening of the wavelet's onset. The value of translation parameter affects only the location of the wavelet and has no influence on wavelet duration or bandwidth. For increasing scale, wavelet becomes more dilated and considers the long time/low frequency behavior of the input signal while for the decreasing scale wavelet becomes more compressed and considers short time/high frequency behavior of the input signal. Therefore the scale parameter is inversely proportional to frequency, i.e. low scales correspond to high frequencies and high scales correspond to low frequencies.

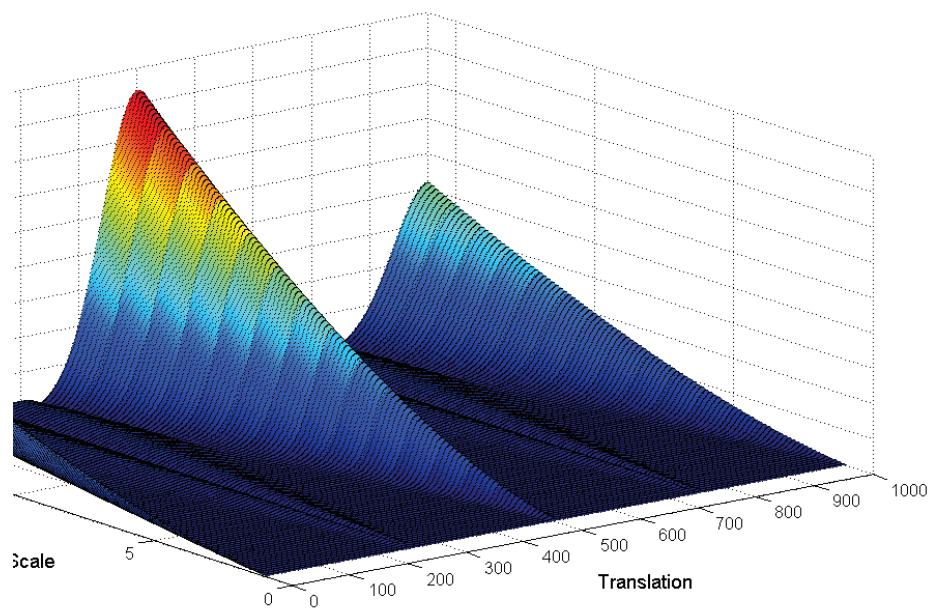


Figure 2-1: Translation-Scale Representation of a Signal.

The CWT encodes a given time signal in terms of wavelet coefficients that are function of two variables. As a result of wavelet transformation we get a collection of two-dimensional time-scale representation, similar to one illustrated in Figure 2-1. The large amplitude in Figure 2-1 corresponds to high frequency-correlation of the signal

with wavelet function at certain scale and time instance.

The CWT is defined as

$$\Upsilon(\kappa, \chi) = \int_{-\infty}^{\infty} f(t)\psi_{\kappa, \chi}^*(t)dt, \quad (2-1)$$

where an input function $f(t)$ is decomposed into a set of wavelet coefficients $\Upsilon(\kappa, \chi)$. The complex conjugate of the wavelet is given by ψ^* . The parameters κ and χ denote scale and translation respectively, and they represent new dimensions of the wavelet transform. The wavelets functions used in (2-1) are generated using single mother wavelet by changing the scaling parameter and translating the wavelet along the time axes by amount χ :

$$\psi_{\kappa, \chi}(t) = \frac{1}{\sqrt{\kappa}}\psi\left(\frac{t - \chi}{\kappa}\right). \quad (2-2)$$

As majority of the transforms also CWT is reversible. Under suitable assumptions about $f(t)$ and κ , the original signal can be reconstructed from wavelet coefficients by applying the formulae for inverse wavelet transform:

$$f(t) = \frac{1}{c_\psi} \int_{\kappa} \int_{\chi} \gamma(\kappa, \chi) \frac{1}{\kappa^2} \psi\left(\frac{t - \chi}{\kappa}\right) d\chi d\kappa, \quad (2-3)$$

where

$$c_\psi = \int_{\mathbb{R}} \frac{|\hat{\psi}(\omega)|^2}{|\omega|} d\omega, \quad (2-4)$$

and $\hat{\psi}(\omega)$ denotes the Fourier transform of $\psi(\omega)$.

2-1-3 Discrete Wavelet Transform (DWT)

Discrete Variables

For practical problems the wavelet transform as discussed in previous paragraph is not always useful because obtained wavelet coefficients are highly redundant and they have to be calculated analytically. In this form the calculation of the wavelet transform would take a lot of time and computational power, depending on the input signals. Therefore the discrete wavelets are more suited for practical problems.

As the name already indicates, the discrete wavelets does not use continuously scalable and translatable wavelets but ones that are scaled and translated in discrete steps. The equation for mother wavelet (2-2) can be rewritten for discrete scale and translation as follows.

$$\psi_{\alpha, \beta}(t) = \sqrt{\kappa_0^\alpha} \psi(\kappa_0^\alpha t - \beta \chi_0) \quad (2-5)$$

where κ_0 stands for fixed dilation step and χ_0 is translation factor. The integers α and β denote scale and translation indices, respectively. The most natural choice for dilation step is 2 as this result in octave bands, also known as dyadic scales. In this case for each subsequent value of scale index, wavelet is compressed in frequency domain by a

factor 2 and consequently stretched in time domain by the same factor. The translation factor is usually set to 1 in order to get dyadic sampling of the time axes, as well.

The output of wavelet transform when discrete wavelets are utilized would be series of wavelet coefficients:

$$\gamma(\alpha, \beta) = \int_{-\infty}^{\infty} f(t)\psi_{\alpha,\beta}^*(t)dt \quad (2-6)$$

To be able to reconstruct the original signal from wavelet coefficients, the energy of the wavelet coefficients should be bounded by two positive bounds ($A > 0$) and ($B < \infty$) [5]. Therefore,

$$A\|f\|^2 \leq \sum_{\alpha} \sum_{\beta} |\langle f, \psi_{\alpha,\beta} \rangle|^2 \leq B\|f\|^2 \quad (2-7)$$

where $\|f\|^2$ denotes the energy of input signal $f(t)$.

The wavelets functions $\psi_{\alpha,\beta}$ with $\alpha, \beta \in \mathbb{Z}$ should form a frame bounded by A and B . If the bound A is not equal to the bound B the decomposition wavelet differs from the reconstruction wavelet and we speak of a dual frame. More favorable situation is obtained for so-called tight frame where two bounds are equal to each other. Furthermore, if $A = B = 1$ the tight frame becomes an orthogonal basis.

The basis function of a wavelet is called orthogonal if the wavelets generated by dilations and translations are orthogonal to each other, i.e.:

$$\int \psi_{\alpha,\beta}(t)\psi_{p,r}^*(t)dt = \begin{cases} 1 & \text{if } \alpha = p \text{ and } \beta = r \\ 0 & \text{otherwise} \end{cases} \quad (2-8)$$

In the sequel of this chapter, we consider in general orthonormal wavelets. The reconstruction of original signal for orthonormal wavelet basis function can be simply obtained by:

$$f(t) = \sum_{\alpha} \sum_{\beta} \gamma(\alpha, \beta)\psi_{\alpha,\beta}(t). \quad (2-9)$$

Multi-Resolution Analysis (MRA)

The complete representation of a signal $f(t)$ requires an infinite number of wavelet functions $\psi_{\alpha,\beta}(t)$, as each following wavelet at increased scale covers only a part of the remaining spectrum. This can be overcome by introducing a low-pass complementary function $\varphi(t)$, called scaling function.

$$\varphi_{\alpha,\beta}(t) = 2^{\alpha/2}\varphi(2^{\alpha}t - \beta) \quad \beta \in \mathbb{Z} \quad \varphi \in L^2 \quad (2-10)$$

where L^2 implies the integral of the square of the modulus is defined.

MRA describes the construction of orthonormal wavelets using family of subspaces that has to satisfy certain properties. The closed subspaces spanned by the scaling functions over integers $-\infty < \beta < \infty$ are defined by:

$$V_{\alpha} = \overline{\text{Span}}_{\beta} \{\varphi_{\beta}(2^{\alpha}t)\} = \overline{\text{Span}}_{\beta} \{\varphi_{\alpha,\beta}(t)\} \quad (2-11)$$

The small values of α represent coarse detail of a signal while larger values represent the finer detail. MRA requires the spanned spaces by scaling functions V_α to have finite energy and that they are ordered by inclusion as $0 \cdots \subset V_{-2} \subset V_{-1} \subset V_0 \subset V_1 \subset V_2 \cdots L^2$ [6], that is:

$$V_\alpha \subset V_{\alpha+1} \quad \text{for all } \alpha \in \mathbb{Z}$$

$$\begin{aligned} \bigcap_{\alpha \in \mathbb{Z}} V_\alpha &= \{0\} \\ \bigcup_{\alpha \in \mathbb{Z}} V_\alpha &= L^2(\mathbb{R}) \end{aligned} \quad (2-12)$$

According to equation (2-12) the space that contains high resolution signal will also contain information about lower resolution of the signal; e.g., V_2 contains V_1 which contains V_0 .

The scaling function $\varphi(t)$ which span V_0 can be defined as a weighted sum of shifted $\varphi(2t)$ which span V_1 using refinement equation,

$$\varphi(t) = \sum_n h(n) \sqrt{2} \varphi(2t - n), \quad n \in \mathbb{Z} \quad (2-13)$$

where $h(n)$ denotes the scaling function coefficients. This equation shows that scaling function can be constructed by the sum of its half-length translations.

The wavelets in MRA are defined as orthogonal bases that span the differences between the spaces spanned by the scaling functions at various scales. Let the subspace spanned by the wavelet be W_{j-1} then spans V_1 and V_2 can be written as:

$$\begin{aligned} V_1 &= V_0 \oplus W_0 \\ V_2 &= V_1 \oplus W_1 = (V_0 \oplus W_0) \oplus W_1 \\ &\vdots \\ V_{\alpha+1} &= V_\alpha \oplus W_\alpha = \bigoplus_{l=0}^{\alpha} W_l \quad \forall \alpha \in \mathbb{Z} \end{aligned} \quad (2-14)$$

The space W_0 spanned by a wavelet is actually a subspace of V_1 ($W_0 \subset V_1$), and therefore similarly to equation (2-13) also the wavelet functions can be represented by a weighted sum of shifted scaling function $\varphi(2t)$.

$$\psi(t) = \sum_n g(n) \sqrt{2} \varphi(2t - n), \quad n \in \mathbb{Z}, \quad (2-15)$$

where $g(n)$ denotes the wavelet function coefficients. Because of the orthogonality condition $V_0 \perp W_0 \perp W_1 \perp \cdots \perp W_\alpha$ the scaling and wavelet coefficients are related to each other by

$$g(n) = (-1)^n h(L - 1 - n) \quad \text{for } h(n) \text{ of length } L \quad (2-16)$$

The reconstruction formulae for DWT using finite resolution of wavelet and scaling function can now be expressed as

$$f(t) = \underbrace{\sum_{\beta=-\infty}^{\infty} \lambda(\alpha_0, \beta) 2^{\alpha_0/2} \varphi(2^{\alpha_0} t - \beta)}_{V_{\alpha_0}} + \underbrace{\sum_{\alpha=\alpha_0}^{\infty} \sum_{\beta=-\infty}^{\infty} \gamma(\alpha, \beta) 2^{\alpha/2} \psi(2^{\alpha} t - \beta)}_{\subset W_{\alpha}} \quad (2-17)$$

The parameter α_0 in (2-17) sets the coarsest scale which is spanned by the scaling function. The rest is spanned by the wavelets which provide the higher resolution details of the signal. Provided that a wavelet system is orthogonal, the DWT coefficients may be defined as (2-18) and (2-19), respectively:

$$\lambda(\alpha, \beta) = \langle f(t), \varphi_{\alpha, \beta}(t) \rangle = \int f(t) 2^{\alpha/2} \varphi(2^{\alpha} t - \beta) dt \quad (2-18)$$

$$\gamma(\alpha, \beta) = \langle f(t), \psi_{\alpha, \beta}(t) \rangle = \int f(t) 2^{\alpha/2} \psi(2^{\alpha} t - \beta) dt \quad (2-19)$$

2-1-4 Filter Banks

The discrete wavelet transform can be efficiently represented by filtering operations. The weights $h(n)$ given by scaling function coefficients in (2-13) can be represented by low-pass filter H . Similarly the weights of wavelet function $g(n)$ corresponds to high-pass filter G . Therefore the equations (2-13) and (2-15) can be viewed as discrete time filtering with filters H and G , respectively [6, 7]. In the sequel of this thesis, we will refer to filter H as scaling filter and to filter G as wavelet filter.

Filtering a signal can be viewed as the convolution of signal with filter's coefficients. For a Finite Impulse Response (FIR) filter H of length L and an input signal $x(n)$ the filtering operation is given by:

$$x(n) * h(n) = \sum_{k=0}^{L-1} x(k) h(n - k) \quad (2-20)$$

Due to orthogonality condition wavelet and scaling filter are related to each other according to equation (2-15). In frequency domain, the spectrum of wavelet filter can be seen as the mirror image at frequency of $\pi/2$ of scaling filter's spectrum. The scaling filter is actually half band Low-Pass Filter (LPF) and complementary wavelet filter is half band High-Pass Filter (HPF).

Filtering of a signal with perfect half band pass filter removes exactly half of the frequency components from the input signal meaning that the number of samples in the filtered signal has now became redundant. In order to remove redundancy we can perform subsampling. For half-band pass filter the filtered signal should be subsampled by 2 in order to remove redundant information. If the signal is subsampled by a larger factor we will lose information and the frequency components will be mixed up. The

subsampling by factor 2 can be seen as taking every other sample of the input signal and discarding the rest of the samples, i.e.:

$$y(n) = x(2n) \quad (2-21)$$

The opposite operation to subsampling is upsampling. Upsampling increases the length of a signal by inserting zeros between each pair of samples. In contrast to subsampling, upsampling does not discard information and therefore it can always be inverted.

The upsampling by a factor 2, doubles the number of samples in a signal by inserting one zero between each pair of samples. This can be mathematically illustrated by

$$y(m) = \begin{cases} x\left(\frac{m}{2}\right) & \text{for } m = 2n \\ 0 & \text{Otherwise} \end{cases} \quad (2-22)$$

Analysis Filter Bank

The refinement equations given in (2-13) and (2-15) can be rewritten so that the lower scale representations of the wavelet and scaling functions can be expressed in those of higher scale as [8],

$$\begin{aligned} \varphi(2^\alpha t - \beta) &= \sum_n h(n) \sqrt{2} \varphi(2(2^\alpha t - \beta) - n) \\ &= \sum_n h(n) \sqrt{2} \varphi(2^{\alpha+1} t - 2\beta - n) \\ &= \sum_{m=2\beta+n} h(m - 2\beta) \sqrt{2} \varphi(2^{\alpha+1} t - m) \end{aligned} \quad (2-23)$$

$$\begin{aligned} \psi(2^\alpha t - \beta) &= \sum_n g(n) \sqrt{2} \psi(2(2^\alpha t - \beta) - n) \\ &= \sum_n g(n) \sqrt{2} \psi(2^{\alpha+1} t - 2\beta - n) \\ &= \sum_{m=2\beta+n} g(m - 2\beta) \sqrt{2} \psi(2^{\alpha+1} t - m) \end{aligned} \quad (2-24)$$

Using derivation carried above for wavelet and scaling function, we can express similarly DWT coefficients at scale α by coefficients at the higher scale $\alpha + 1$ as follows:

$$\begin{aligned} \lambda(\alpha, \beta) &= \langle f(t), \varphi_{\alpha, \beta}(t) \rangle \\ &= \int f(t) 2^{\alpha/2} \varphi(2^\alpha t - \beta) dt \\ &= \sum_m h(m - 2\beta) \int f(t) 2^{\alpha+1/2} \varphi(2^{\alpha+1} t - m) dt \\ &= \sum_m h(m - 2\beta) \lambda(\alpha + 1, m) \end{aligned} \quad (2-25)$$

$$\begin{aligned}
\gamma(\alpha, \beta) &= \langle f(t), \psi_{\alpha, \beta}(t) \rangle \\
&= \int f(t) 2^{\alpha/2} \psi(2^{\alpha}t - \beta) dt \\
&= \sum_m g(m - 2\beta) \int f(t) 2^{\alpha + 1/2} \psi(2^{\alpha+1}t - m) dt \\
&= \sum_m g(m - 2\beta) \gamma(\alpha + 1, m)
\end{aligned} \tag{2-26}$$

Equations (2-25) and (2-26) imply that wavelet and scaling DWT coefficients at the certain scale can be calculated by taking a weighted sum of DWT coefficients from higher scales. This can be viewed as convolution between the DWT coefficients at scale $\alpha + 1$ with wavelet and scaling filter coefficients and subsequently subsampling each output with factor 2 to obtain new wavelet and scaling DWT coefficients at scale α . Therefore, we can describe (2-25) and (2-26) by a 2-channel filter bank illustrated in Figure 2-2.

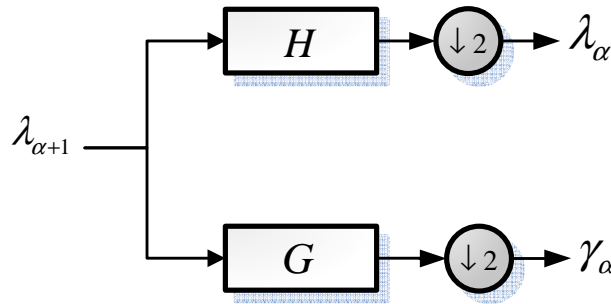


Figure 2-2: 2-Channel Analysis Filter Bank.

The 2-channel filter bank first splits the input signal in two parts and filters one part with filter H and other with filter G . Both filtered signals are then subsampled by 2 and resulting signals are forwarded to the output of the 2-channel filter bank. Each output signal will therefore contain half the number of samples and will span half of the frequency band compared to the input signal. It should be noticed that the number of samples at the input of the filter bank equals the number of samples at the output.

The complete representation of the DWT can be obtained by iteration of the 2-channel filter bank and taking repeatedly scaling DWT coefficients λ as input. The iteration process starts with λ at the largest scale which is equal to the original signal. The number of stages in iteration process will determine the DWT resolution and therefore the number of channels.

Synthesis Filter Bank

The reconstruction formula for DWT is given in equation (2-17). If we now substitute the refinement equations for wavelet and scaling function, (2-15) and (2-13), respectively,

into reconstruction equation (2-17) we get:

$$f(t) = \sum_{\beta} \lambda(\alpha, \beta) \sum_n h(n) 2^{(\alpha+1)/2} \varphi(2^{\alpha+1}t - 2\beta - n) + \sum_{\beta} \gamma(\alpha, \beta) \sum_n g(n) 2^{(\alpha+1)/2} \varphi(2^{\alpha+1}t - 2\beta - n) \quad (2-27)$$

Multiplying both sides of equation (2-27) by $\varphi(2^{\alpha+1}t - \beta')$ and taking the integral allows us to describe the DWT coefficients at higher scales by those of the lower scale as [7]

$$\lambda(\alpha + 1, \beta) = \sum_m \lambda(\alpha, m) h(\beta - 2m) + \sum_m \gamma(\alpha, m) g(\beta - 2m) \quad (2-28)$$

which implies that the DWT coefficients at certain scale level $\alpha + 1$ can be reconstructed by taking a combination of weighted wavelet and scaling DWT coefficients at previous scale α . This process can be described by the 2-channel synthesis filter bank, illustrated in Figure 2-3.

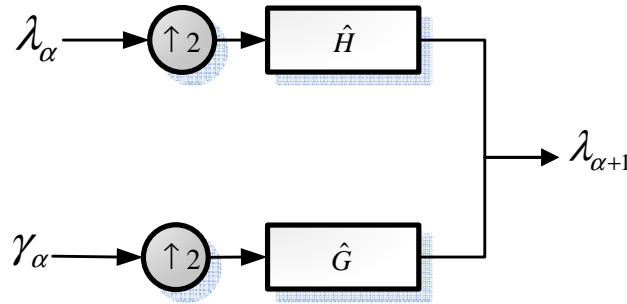


Figure 2-3: 2-Channel Synthesis Filter Bank.

The 2-channel synthesis filter bank performs exactly opposite operation compared to previously discussed analysis filter bank. The wavelet and scaling DWT coefficients are first upsampled by factor 2 and after that the wavelet function DWT coefficients are filtered with HPF \hat{G} while scaling function DWT coefficients are filtered with LPF \hat{H} . The two filtered signals are then added to each other to construct DWT coefficients at higher scale. The filters \hat{H} and \hat{G} are according to equation (2-28) and equations (2-25) and (2-26) time reversed version of filters H and G , respectively.

The decomposition of a signal in terms of coefficients is called discrete wavelet transform. In order to reconstruct the original signal from coefficients we can apply inverse wavelet transform, abbreviated Inverse Discrete Wavelet Transform (IDWT). The IDWT can be efficiently implemented by iterating the 2-channel synthesis filter bank in the same manner like we have done in the previous paragraph for the 2-channel analysis filter bank.

If our primal assumption of orthogonality (2-16) is valid the reconstructed signal is simply delayed version of the input signal ($x(n) = y(n)$). The filter banks that satisfy this property are called perfect reconstruction filter banks.

2-1-5 Wavelet Packet Transform (WPT)

The resolution of DWT, as described so far, depends on the frequency bands. Because we are iterating the 2-channel filter bank only for the low pass output (scaling function branch), at the end of decomposition the high frequencies will have wide bandwidths while low frequencies will have narrow bandwidths.

The WPT on the contrary performs the iteration of the 2-channel filter bank on both sides: low pass (scaling function branch) and high pass (wavelet function branch). Because the high frequencies are decomposed in the same manner as low frequencies the wavelet packet transform has evenly spaced frequency resolution.

The filter bank structure for wavelet packet transform expands to a full binary tree. In order to make clear distinction between different sets of coefficients we will label each wavelet packet ξ by the level l which corresponds to the depth of the node in the tree and by the current position p of the node at a given level.

Wavelet packet decomposition recursively splits each parent node in two orthogonal subspaces W_l^p located at the next level:

$$W_l^p = W_{l+1}^{2p} \oplus W_{l+1}^{2p+1} \quad (2-29)$$

in which the subspaces are those spanned by the basis functions of wavelet packets:

$$W_l^p = \overline{\text{span} \{2^{l/2} \zeta_l^p(2^l t - \beta)\}} \quad (2-30)$$

Wavelet packet coefficients ζ at a certain level are calculated by convolving the wavelet and scaling filter with wavelet packets coefficients from previous level. This action is performed repeatedly for all wavelet packets until the full binary tree is obtained with desired depth. The equation (2-31) shows the recursive equation for wavelet packets generation. The wavelet packets coefficients $\zeta_{l+1}^{2p}(\beta)$ are generated using the scaling filter and coefficients $\zeta_{l+1}^{2p+1}(\beta)$ are created using the wavelet filter.

$$\begin{aligned} \zeta_{l+1}^{2p}(\beta) &= \sum_m h(m - 2\beta) \zeta_l^p(m) \\ \zeta_{l+1}^{2p+1}(\beta) &= \sum_m g(m - 2\beta) \zeta_l^p(m) \end{aligned} \quad (2-31)$$

In the regular DWT decomposition for each additional level we need only to perform single iteration of 2-channel filter bank while in wavelet packet transform the number of iterations is exponentially proportional to the number of levels. Therefore, the wavelet packet transform has higher computational complexity when compared to regular DWT. By utilization of fast filter bank algorithm wavelet packet transform requires $O(N \log(N))$ operation, similar to Fast Fourier Transform (FFT) while DWT needs only $O(N)$ calculation [8].

The reconstruction of wavelet packets is also performed in an iterative method. For each pair of wavelet packets coefficients at level l of the tree we can calculate wavelet packets coefficients at the previous level $l - 1$ by:

$$\zeta_l^p(\beta) = \sum_m \zeta_{l+1}^{2p}(m) h(\beta - 2m) + \sum_m \zeta_{l+1}^{2p+1}(m) g(\beta - 2m) \quad (2-32)$$

2-2 Wavelet Packet Modulation

2-2-1 Multi-carrier Modulation (MCM)

MCM subdivides the total bandwidth in N narrow channels, which are transmitted in parallel. The original data stream at rate R_s is divided into N streams each having data rate of R_s/N and therefore N times longer symbol duration, i.e. $T_{MC} = NT$.

Each data symbol in single-carrier systems occupies the entire available bandwidth while an individual data symbol in multicarrier system only occupies a fraction of the total bandwidth. Therefore, narrow band interference or strong frequency band attenuation can cause single-carrier transmission to completely fail but in MCM they only affect subcarriers located at particular frequencies.

MCM can be implemented using several techniques. The first multicarrier systems realized was Frequency Division Multiplexing (FDM). In FDM, the composite multicarrier signal is obtained by shifting baseband parallel data streams upwards in frequency by modulating them on different sinusoidal carriers. The FDM signal must consist of subcarriers which do not spectrally overlap. Otherwise, crosstalk would occur between different subchannels. In practical systems, guard bands are inserted between subcarriers to accommodate for local oscillator imperfections and/or channel effects like Doppler spread.

The growth of high data rate applications has caused spectrum to become scarce. Therefore, systems that make use of available bandwidth more efficiently received a lot of attention. One of the spectrally efficient multicarrier methods is OFDM. Although the principle of OFDM existed since the early sixties the first real life systems appeared only in the past decade. Presently, OFDM is the most commonly used multicarrier modulation technique and is widely adopted across the world. One of the first systems to use OFDM was European Digital Audio Broadcasting (DAB) back in 1995 and in short time other standards such as Digital Video Broadcasting (DVB) [9], IEEE 802.11a/g/j/n [10–12], IEEE 802.16 (WiMax) [12], Ultrawideband (UWB) Wireless Personal Area Network (PAN) (IEEE 802.15.3a) [13] and Mobile Broadband Wireless Access (MBWA) (IEEE 802.20) [14] followed.

The high spectral efficiency of OFDM is due to its orthogonal subcarriers which allow their spectrums to overlap. Adjacent subcarriers do not interfere with each other as long as they preserve their orthogonality. Furthermore, the guard bands like those used in FDM are no longer necessary.

2-2-2 Theory on Wavelet Packet Modulation

Wavelet Packet Modulation (WPM) is a multiplexing method that makes use of orthogonal wavelet packet bases to combine a collection of parallel signals into a single composite signal. Fundamentally, OFDM and WPM have many similarities as both use orthogonal waveforms as subcarriers and they achieve high spectral efficiency by allowing subcarriers' spectra to overlap one another. The adjacent subcarriers do not

interfere with each other as long as the orthogonality between subcarriers is preserved. The difference between OFDM and WPM is the shape of the subcarriers and in the way they are created. OFDM makes use of Fourier bases which are static sines/cosines while WPM uses wavelets which offer much more flexibility. By altering the properties of the filter banks, the shape of the subcarriers can be altered and subsequently the characteristics of the transmission system can change. This leads to the possibility of customizing the WPM system characteristics based on system requirements.

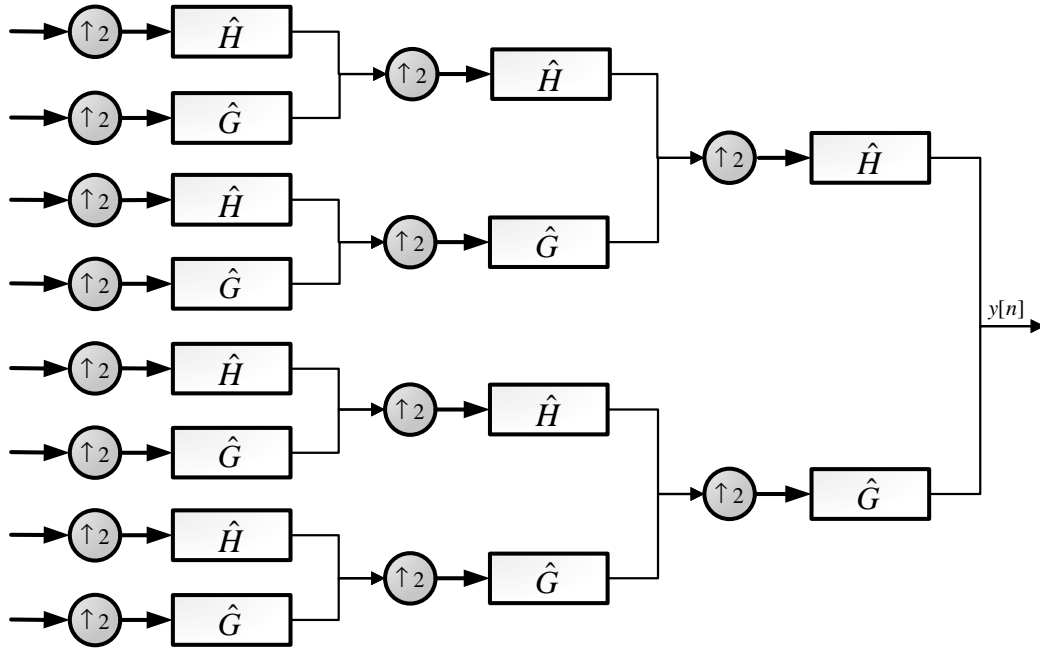


Figure 2-4: Inverse Discrete Wavelet Packet Transform

WPM is implemented by utilization of the inverse discrete wavelet packet transformation (IDWPT), which is illustrated in Figure 2-4, at the transmitter and discrete wavelet packet transformation (DWPT), which is illustrated in Figure 2-5, at the receiver, analogous to the Inverse Discrete Fourier Transform (IDFT) and the Discrete Fourier Transform (DFT) in OFDM systems. MRA of wavelet theory allows us to represent wavelet and scaling functions by high- and low-pass filters (LPF and HPF), respectively, with coefficients $h[n]$ and $g[n]$. Therefore, the wavelet transformation can be easily implemented using discrete time filters. In this work, we derive the carriers of the multi-carrier modulation (MCM) system through a wavelet packet transform (WPT). The WPT is just like the wavelet transform except that it decomposes even the high frequency bands, which are kept intact in the wavelet transform.

WPM is implemented with orthogonal wavelet packet bases derived from a MRA [15–17]. The starting point of the process to derive these orthogonal bases is to consider a pair of Quadrature Mirror Filters (QMF) which consists of a half-band high and low pass filter duo (represented by their impulse responses $h[n]$ and $g[n]$, respectively) of length L . These filters share a tight relationship given as [5]- [18]:

$$g[L - 1 - n] = (-1)^n h[n] \quad (2-33)$$

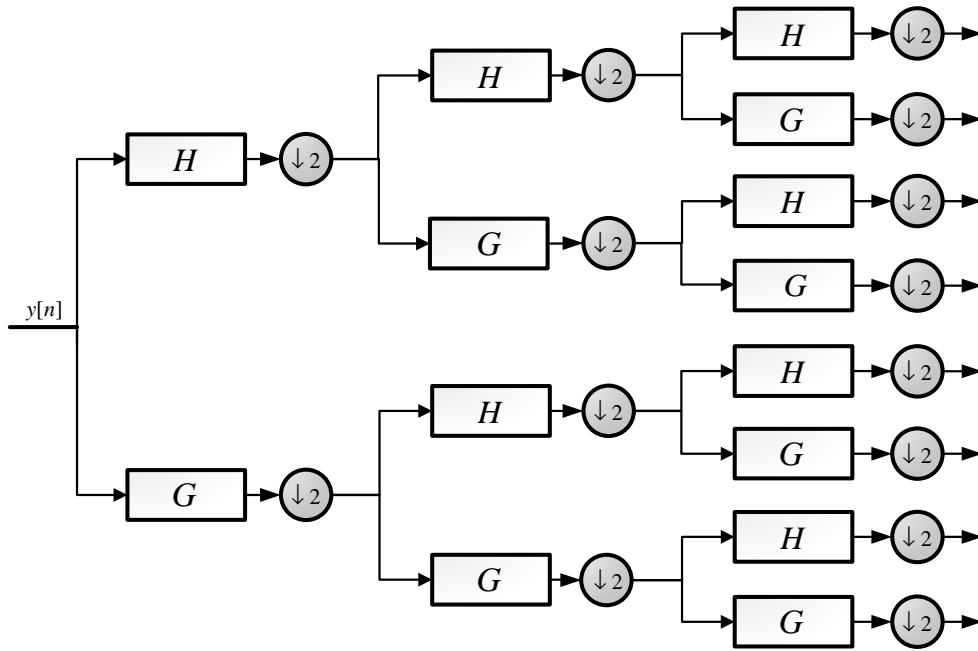


Figure 2-5: Discrete Wavelet Packet Transform

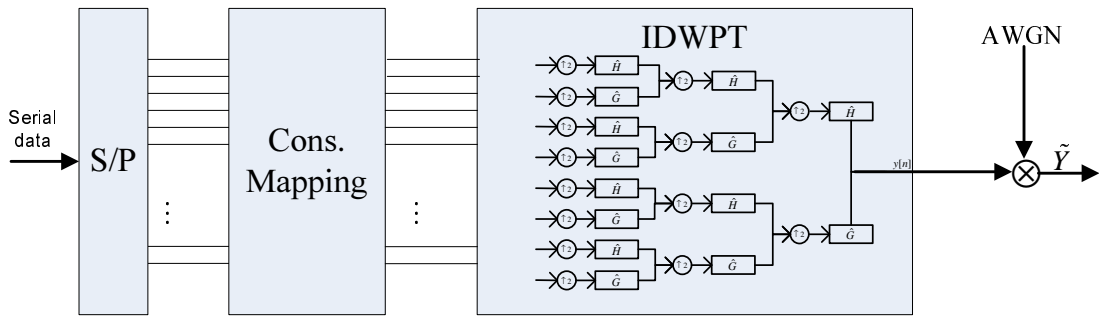


Figure 2-6: Wavelet Packet Modulation Transmitter Architecture.

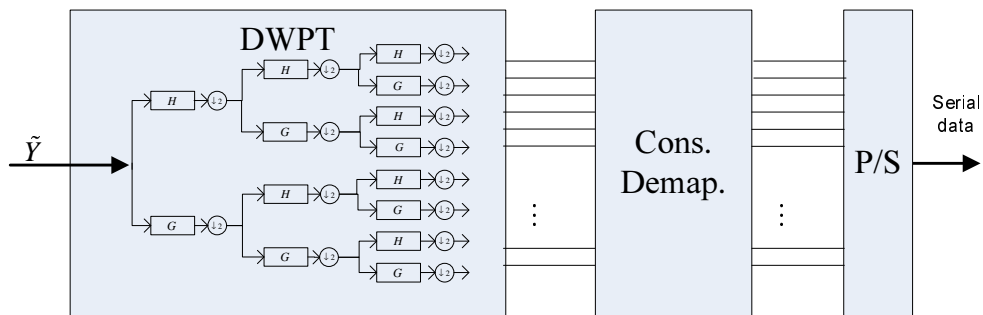


Figure 2-7: Wavelet Packet Modulation Receiver Architecture.

Furthermore, they also have adjoints or duals which are their complex conjugate time reversed variants given by [18]:

$$h'[n] = h^*[-n] \text{ and } g'[n] = g^*[-n] \tag{2-34}$$

The pair $\{h'[n], g'[n]\}$ is called the analysis filter-pair and is used to generate the wavelet packet carriers for modulation of data at the transmitter end. On the other hand the combination $\{h[n], g[n]\}$ is called the synthesis filter-pair and is used to derive the wavelet packet carrier duals for demodulation of data at the receiver end. Denoting the magnitude responses of these four filters in the frequency domain as $H(\omega), G(\omega), H'(\omega)$ and $G'(\omega)$ the filters have been shown to satisfy the perfect reconstruction conditions [18]:

$$\begin{aligned} H^*(\omega + \pi)H'(\omega) + G^*(\omega + \pi)G'(\omega) &= 0 \\ H^*(\omega)H'(\omega) + G^*(\omega)G'(\omega) &= 0 \end{aligned} \quad (2-35)$$

These filters can hence be used for applications as varied as compression techniques in image/speech processing to transceiver design in communication theory. The wavelet packet bases $\{\Upsilon_l^p\}$ obtained from these QMF filters can be derived recursively through a MRA as [18]:

$$\begin{aligned} \Upsilon_{l+1}^{2p}(t) &= \sqrt{2} \sum_n h[n] \Upsilon_l^p(2t - n) \\ \Upsilon_{l+1}^{2p+1}(t) &= \sqrt{2} \sum_n g[n] \Upsilon_l^p(2t - n) \end{aligned} \quad (2-36)$$

In (2-36) the superscript p stands for subcarrier index at any given tree depth l . The number of WPM carriers M that can be derived from l iterations is given by $M = 2^l$. Finally, the WPM modulation signal $y[n]$ which is obtained from a linear combination of the wavelet packet bases weighted with complex data symbols $a_{u,k}$ of different parallel streams p , and data index l can be given as:

$$y[n] = \sum_u \sum_{k=0}^{M-1} a_{u,k} \Upsilon_l^k(n - uM) \quad (2-37)$$

At the transmitter in Figure 2-6 the data is modulated with the bases obtained through the synthesis filter pair, and at the receiver in Figure 2-7 the data is demodulated with duals of these bases obtained through a process mentioned above, albeit, with the synthesis filter pair $\{h[n], g[n]\}$. The processes are referred to as inverse discrete wavelet packet transformation (IDWPT) at the transmitter and discrete wavelet packet transformation (DWPT) at the receiver, analogous to the inverse discrete Fourier Transform (IDFT) and the DFT, respectively, in OFDM systems [15]. We recommend [1]- [15] for further details.

2-3 Summary

In this chapter, we have discussed the basic theory of the wavelet transform and we have explained how discrete wavelet transform can be calculated with utilization of filter banks. Due to efficient implementation and the freedom they provide, wavelets have emerged in many different fields. Recently, wavelets have been also proposed as a candidate for MCM. In this chapter we have presented WPM transceiver, which is one of the possible wavelet based implementation of orthogonal multicarrier system.

Peak-to-Average Power Ratio of WPM Signal

A major drawback of multicarrier systems is their high Peak-to-Average Power Ratio (PAPR). In the literature several methods are reported to reduce the PAPR problem of Orthogonal Frequency Division Multiplexing (OFDM). These techniques are mainly divided into two categories namely, signal scrambling and signal distortion. The signal scrambling methods are all variations on how to modify the phases of OFDM subcarriers to decrease the PAPR. The signal distortion techniques are mainly developed to reduce the high peaks directly by distorting the signal prior to amplification. An elaborate note on these topics can be found in [19–34]. In this chapter, we conduct a study on the PAPR of MCM and Wavelet Packet Modulation (WPM) systems. Then the stochastics of WPM signals and their power is studied. Furthermore, the variation of PAPR with different wavelets and pulse shapes is gauged. Subsequently, the influence of the pulse shaping characteristics on the PAPR is investigated. This study shows that the envelope of the WPM signal is Gaussian and its power distribution Chi-squared. The novelty of the work is in the investigation of the stochastics of the WPM signals and influence of the wave-shapes properties on their PAPR performances. Several well-known wavelets such as Daubechies, Symlets, Coiflets, Discrete Meyer and biorthogonal wavelet are applied. The results of this research show how these wavelet-based systems cope with PAPR.

This chapter is organized as follows. After introducing the topic in the next section, we introduce the distribution of PAPR of OFDM in Section 3-1. The theoretical distribution of PAPR of WPM is discussed in Section 3-2. Furthermore, the analysis of WPM signal characteristics and results are presented in Section 3-3. Finally, a short summary will be given in Section 3-4.

3-1 PAPR Distribution of Multi-Carrier Signal

A multicarrier signal consists of a number of independently modulated subcarriers, which can give a large peak-to-average-power ratio when added up coherently. When M signals are added with the same phase, they produce a peak power that is M times the average power. The peak power is defined as the power of sine wave with an amplitude equal to the maximum envelope value. Knowing that a multicarrier signal is the sum of many independent symbols modulated onto subchannels of equal bandwidth. Let X_m , $m = 0, 1, \dots, M - 1$ be the number of data symbols, given as a vector $X = [X_0, X_1, \dots, X_{M-1}]$ which will be termed a frame. Then for one OFDM symbol with M subcarriers, the complex baseband of the continuous time-varying representation can be written as

$$x(t) = \frac{1}{\sqrt{M}} \sum_{m=0}^{M-1} X_m e^{j2\pi m \Delta f t}, \quad 0 \leq t \leq T \quad (3-1)$$

where $j = \sqrt{-1}$, Δf is the subcarrier spacing and T is the symbol duration. The orthogonality is established with a carrier subspacing Δf of $\frac{1}{MT}$. And the discrete time-varying equation of the baseband signal can be written as

$$x[n] = \frac{1}{M} \sum_{m=0}^{M-1} X_m e^{j\frac{2\pi m n}{M}}, \quad n = 0, 1, \dots, Ml - 1 \quad (3-2)$$

It can be seen that the sequence $x[n]$ can be interpreted as the inverse discrete Fourier transform (IDFT) of the OFDM data block X with $(l - 1)M$ zero padding. The PAPR is one way to measure the variation of transmitted signal about its mean and the PAPR computed from the l -times oversampled time-domain signal samples is given by

$$\text{PAPR} = \frac{\max_{0 \leq n \leq Ml} (|x[n]|^2)}{E(|x[n]|^2)} \quad (3-3)$$

where $E(|\cdot|)$, the expected value, denotes the average. The Cumulative Distribution Function (CDF) of the PAPR is one of the most frequently used performance measures for PAPR reduction techniques [29, 35]. From the central limit theorem it follows that for large number of subcarriers M , the real and imaginary components of $x(t)$ (time domain signal) follows the Gaussian distribution, each with a zero mean and variance of M times the variance of one complex sinusoid. The amplitude of the OFDM signal therefore has a Rayleigh distribution and its power distribution becomes a central chi-square distribution with two degrees of freedom and zero mean [29, 36]. The CDF of the power is given as [29]

$$F(z) = \int_0^z \frac{1}{2\sigma^2} e^{-\frac{u}{2\sigma^2}} du = 1 - e^{-\frac{z}{2\sigma^2}} \quad (3-4)$$

where $z \geq 0$. From the power distribution the theoretical CDF for PAPR per OFDM symbol can be derived. Assuming the samples to be mutually uncorrelated (which is

true when there is no over sampling) the probability that PAPR is below some threshold level z , can be written as [29]:

$$Prob\{PAPR \leq z\} = [F(z)]^N = \left(1 - e^{-\frac{z^2}{2\sigma^2}}\right)^N \quad (3-5)$$

3-2 PAPR Distribution of WPM Signal

There is a fundamental difference in the calculation of PAPR between OFDM as expressed in (3-3) and WPM. The PAPR in OFDM is usually calculated per symbol. This is not possible in WPM because WPM symbols overlap in the time-domain and therefore the PAPR has to be calculated per frame. A WPM signal, like the OFDM signal, is the sum of many information bearing sub-carriers which are statistically independent. WPM is implemented with orthogonal wavelet packet bases derived from a Multi-Resolution Analysis (MRA) [15] as explained in Chapter 2. The PAPR of a multicarrier modulated signal is given as:

$$PAPR = \frac{\max_n(|y[n]|^2)}{E(|y[n]|^2)} \quad (3-6)$$

where $y[n]$ as defined in (2-37) stands for the transmitter output signal, which is usually a frame of M symbols, $\max_n()$ represents the maximum value over all instances of time index n , and $E(|\cdot|)$ denotes ensemble averaging.

The algorithm to calculate the PAPR for WPM signals is given below:

Algorithm 3.1 Calculate the PAPR for WPM signals

- 1: **for** $i = 1$ to K where K is number of iterations. **do**
 - 2: Create a random WPM signal $x[n]$ with M carriers and M symbols per frame.
 - 3: Calculate PAPR per frame (in dB) $PAPR = \frac{\max_n(|y[n]|^2)}{E(|y[n]|^2)}$.
 - 4: **end for**
 - 5: From the list of all PAPR values ($PAPR_i, i = 1, 2, \dots, K$) find the CDF.
-

3-3 Analysis of WPM Signal Characteristics

In this section, we present the results of our study. We start by analyzing the stochastics of WPM signal and its power distribution. Then we conduct a preliminary analysis of the PAPR variations of WPM. The investigations are carried out using computer simulations and the performance metric of choice is the CDF. In Figure 3-1 the theoretical derivation is plotted against simulated values from WPM for different number of subcarriers M . We see in Figure 3-1 that equation (3-5) is quite accurate for $M > 128$. Here we can see, the higher the number of carriers, the better the simulated lines fit the theoretical derivations. For this reason, the WPM system is realized using a filter bank structure with 7 levels of decomposition yielding 128 carriers (which is significantly large). The modulation scheme used is Binary Phase Shift Keying (BPSK).

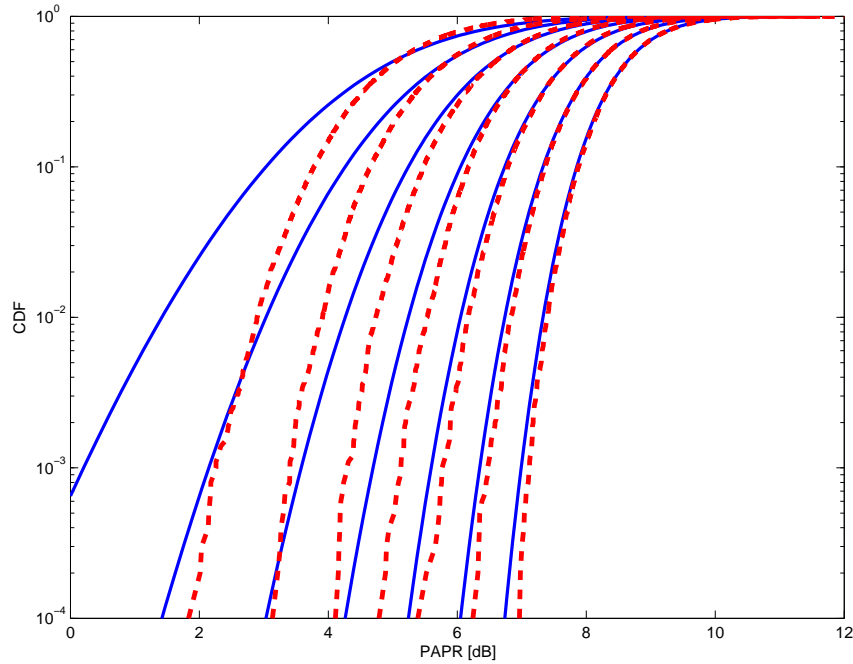


Figure 3-1: CDF-distribution of PAPR for (left to right) number of subcarriers: 16, 32, 64, 128, 256, 512, 1024 (dashed is simulated Daubechies WPM signals with length 15).

3-3-1 Stochastic of the WPM Signal

Unlike OFDM which is a complex signal with real and imaginary parts, the WPM signal only has real components. OFDM signal has a Rayleigh distribution and it would be interesting to check the distribution of WPM signal. Figure 3-2 plots the simulated CDF curves for WPM systems along with Gaussian and Rayleigh distributions. The WPM setup uses Daubechies wavelets with length 15. It is clear from the figure that the patterns of the WPM signal variations follow the Gaussian distribution.

3-3-2 Stochastic of WPM Power Distribution

The Central Limit Theorem (CLT) states that the mean of a sufficiently large number of independent random variables, each with finite mean and variance, will be normally distributed. Based on CLT, when large number of subcarriers are employed in a WPM system; i.e., large number of levels in the Inverse Discrete Wavelet Packet Transform (IDWPT), the amplitude of WPM signal follows Gaussian distribution. It is well known from the stochastic theory that the distribution of power of Gaussian signals is Chi-squared. This means that the power distribution of WPM signals should also be Chi-squared. This fact is corroborated in Figure 3-3. In Figure 3-3 where the curves for the power distribution of WPM signal are fitted along with Gaussian, Rayleigh and Chi-Square distributions are plotted. And in Figure 3-4 the power distributions for WPM

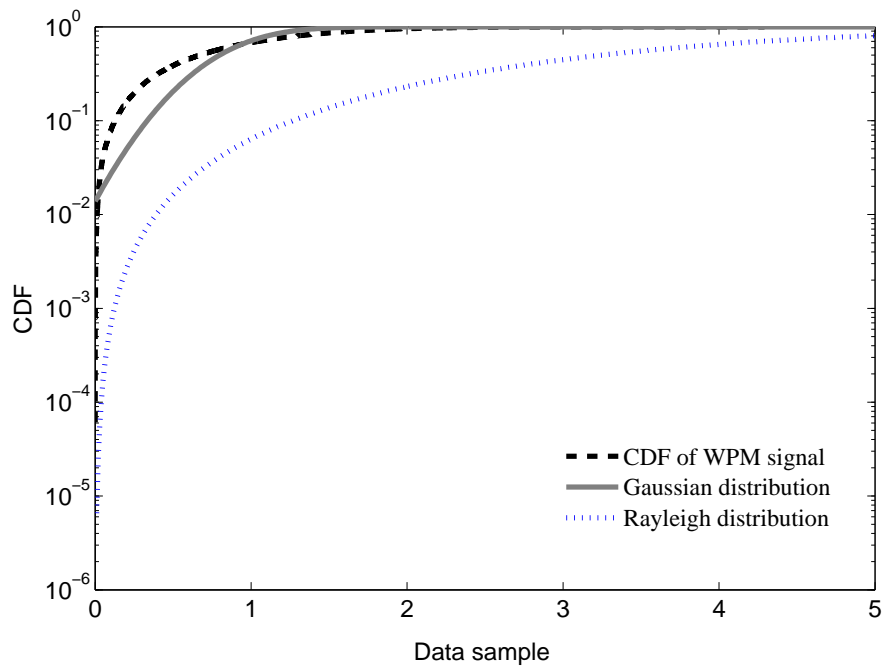


Figure 3-2: CDF of Gaussian signals are compared with the CDF of Daubechies WPM signals with length 15 for different number of carriers (for 128 carriers).

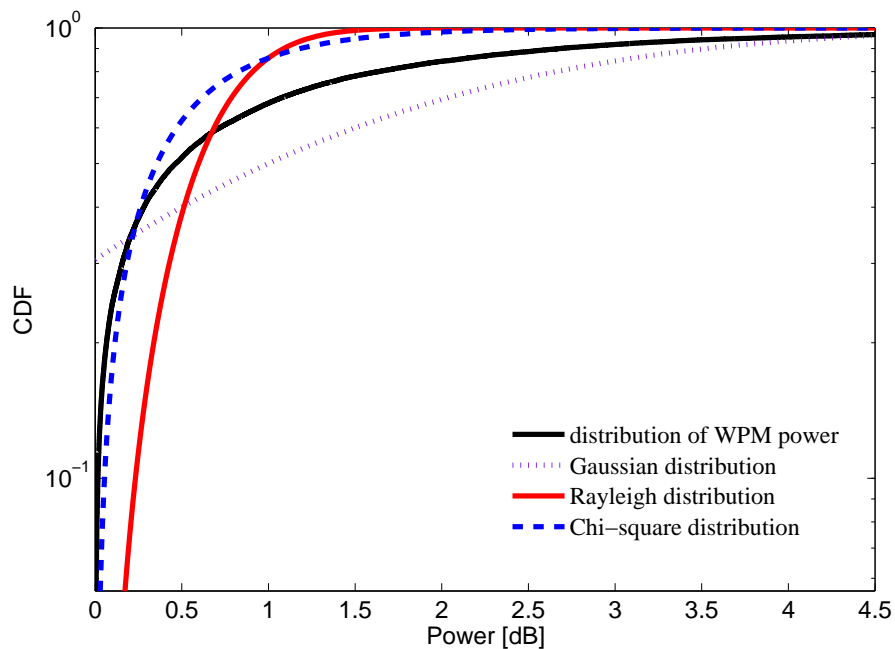


Figure 3-3: CDF of power of Gaussian and Wavelet Packet Modulation signals (for 128 carriers).

signals applying different wavelet families are shown. Almost all the wavelet families have a power distribution which is Chi-squared. The specifications of the wavelets

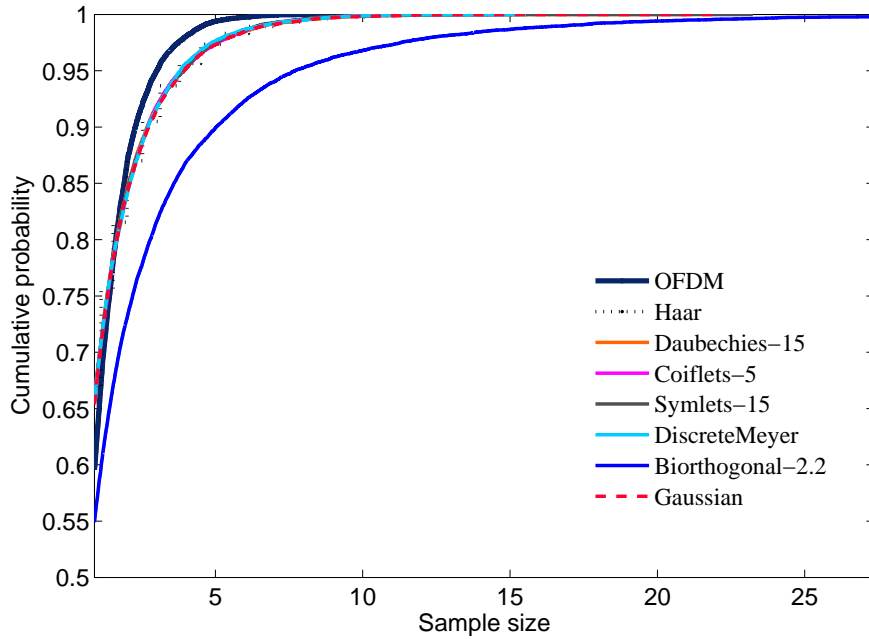


Figure 3-4: CDF of power of Wavelet Packet Modulated signals for various families (for 128 carriers).

Table 3-1: Wavelet Specifications.

Name	Orthonormal?	Length
Daubechies	Yes	30
Coiflet	Yes	30
Symlet	Yes	30
Discrete Meyer	Yes	102
Bi-Orthogonal	No	(5,3)

(Daubechies 15, Coiflet 5, Symlet 15 (all of length 30), Discrete Meyer (of length 102) and Bi-Orthogonal 2.2) which are considered are given in Table3-1.

3-3-3 Stochastic of WPM PAPR Distribution

Finally, we present results on the PAPR variations of the WPM signal. In OFDM the PAPR is usually calculated per symbol. This is not possible in WPM because WPM symbols overlap in the time-domain therefore the PAPR has to be calculated per frame.

Figure 3-5 and Figure 3-6 show the PAPR performance curves for various wavelet families and various filter lengths, respectively. From Figure 3-5 we can deduce that apart from the bi-orthogonal wavelet, all the other wavelets follow a similar CDF pattern for the PAPR. And from Figure 3-6 it is clear that even with increasing lengths of the wavelet, from Daubechies 2 to Daubechies 45, the PAPR distribution doesn't vary much.

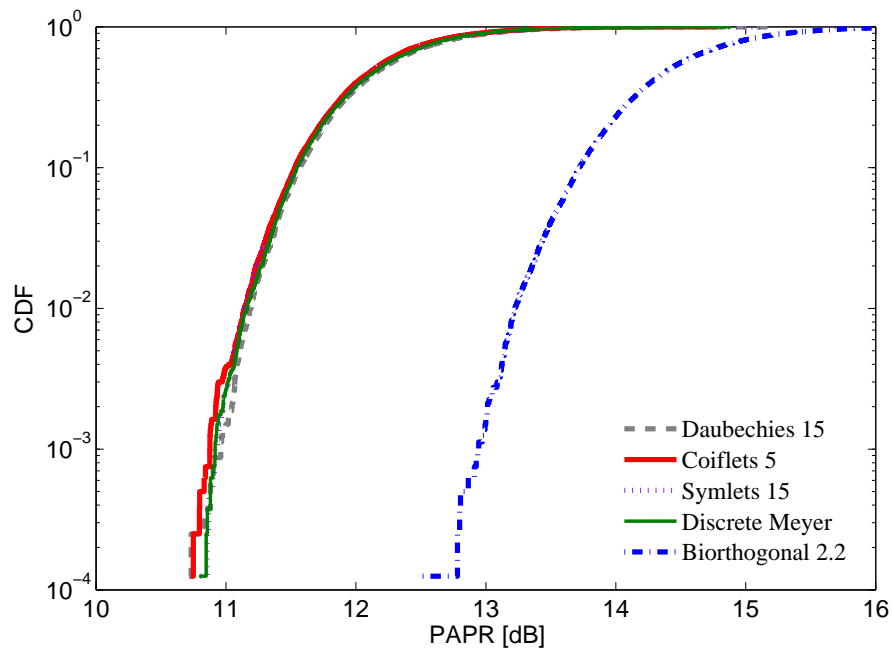


Figure 3-5: CDF of PAPR for the WPM system applying several wavelet families. All the configurations are taken to have 128 carriers.

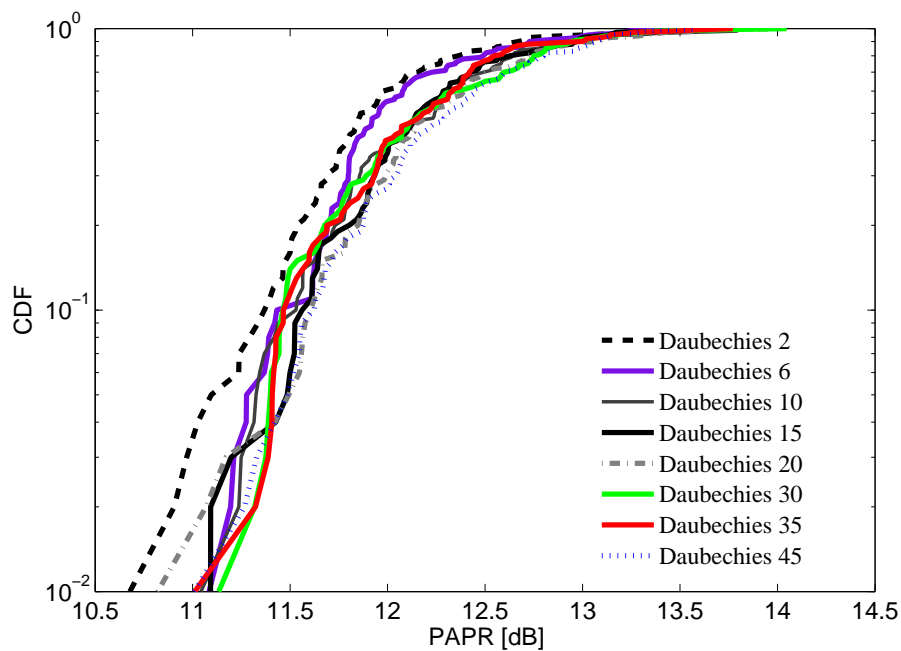


Figure 3-6: CDF of PAPR for the WPM system applying different filter lengths of the Daubechies wavelet family. All the configurations are taken to have 128 carriers.

3-4 Summary

In this chapter, a study on the effect of PAPR on the "developmental" Wavelet Packet Modulation scheme was presented. To this end, the stochastic of WPM signal and its power variations were analyzed. Studies showed that the envelope of the WPM signal is Gaussian and its power had a Chi-squared distribution. Furthermore, the PAPR for WPM systems with different wavelets, pulse shapes and lengths were studied. In the considered scenarios, almost all the wavelets performed similarly with regard to their PAPR performance.

Selected Mapping with Phase Modification

We showed in Chapter 3 [37] that the WPM signal follows Gaussian distribution and its power distribution is Chi-square. In this chapter, we propose a method to reduce the Peak-to-Average Power Ratio (PAPR) in the developmental Wavelet Packet Modulation (WPM) system. The method is called as selected mapping with phase modification. The key idea behind phase modifications is that the PAPR of a multicarrier system can be adjusted by varying the phase-shifts of the subcarriers. Selected mapping with phase modification technique is applied after the constellation mapping. Hence different PAPR values for the same information can be obtained by randomly altering the phases of the sub-carriers used to modulate the data. The WPM frame with the least PAPR is then identified and transmitted. The attraction of the method is its simplicity, the elegance of implementation and the notable gains it yields with minimal increase in complexity.

The contents of the chapter, are organized as follows. The first part of this chapter presents a literature survey on existing PAPR reduction techniques in Section 4-1. In the second part, we introduce selected mapping technique with phase modification, then we present the WPM architecture in Section 4-2 which elucidates the PAPR reduction technique proposed in this chapter. Furthermore, the results of the simulation studies are discussed in Section 4-3. Finally, the chapter is summarized in Section 4-4 by drawing on the inferences of the study.

4-1 PAPR Reduction Techniques

High Peak-to-Average Power Ratio (PAPR) has been recognized as one of the major practical problems involving multi-carrier modulation. High PAPR results from the nature of the modulation itself where multiple sub-carriers are added together to form the signal to be transmitted. When M sub-carriers add, could be as high as M times

the average. The average might be quite low due to the destructive interference between the sub-carriers. High PAPR signals are usually undesirable for it usually strains the analog circuitry. High PAPR signals would require a large range of dynamic linearity from the analog circuits which usually results in expensive devices and high power consumption with lower efficiency (for e.g. power amplifier has to operate with larger back-off to maintain linearity). The high PAPR could cause problems when the signal is applied to a transmitter which contains non-linear components such as High Power amplifier (HPA) in the transmitter chain. The non-linear effects on the transmitted OFDM symbols/frames are spectral spreading, inter-modulation and changing the signal constellation. In other words, the nonlinear distortion causes both in-band and out-of-band interference to signals. The in-band interference increases the bit error rate (BER) of the received signal, while the out-of-band interference causes adjacent channel interference through spectral spreading. A better solution is to prevent the occurrence of such nonlinear distortion by reducing PAPR of the transmitted signal with some manipulation of the OFDM signal itself.

In the literature several techniques have been proposed to reduce the PAPR of OFDM. These techniques can mainly be categorized in signal scrambling techniques and signal distortion techniques. Fig. 4-1 shows a scheme of the PAPR reduction techniques. Signal scrambling techniques are all variations on how to scramble the codes or on how to modify the phases to decrease the PAPR. Coding techniques can be used for signal scrambling. Golay complementary sequences, Shapiro-Rudin sequences, Barker codes can be used efficiently to reduce the PAPR. However with the increase in the number of carriers the overhead associated with exhaustive search of the best code would increase exponentially. More practical solutions of the signal scrambling techniques are block coding, selected mapping (SLM) and partial transmit sequences (PTS). Signal scrambling techniques with side information reduce the effective throughput since they introduce redundancy.

The signal distortion techniques are mainly developed to reduce the high peaks directly by distorting the signal prior to amplification and introduce both in-band and out-of-band interference and complexity to the system. Clipping the OFDM signal before amplification is a simple method to limit PAPR. However clipping may cause large out-of-band (OOB) and in-band interference, which results in the system performance degradation. More practical solutions are peak windowing, peak cancellation, peak power suppression, weighted multi-carrier transmission, companding etc. Basic requirement of practical PAPR reduction techniques include the compatibility with the family of existing modulation schemes, high spectral efficiency and low complexity.

4-1-1 Signal Scrambling Techniques

Block Coding

Jones and Wilkinson [19] propose a block coding scheme for the reduction of the peak to mean envelope power ratio of multi-carrier transmission systems. The main idea behind this approach is that PAPR can be reduced by block coding the data such that set of permissible code words does not contain those which result in excessive peak

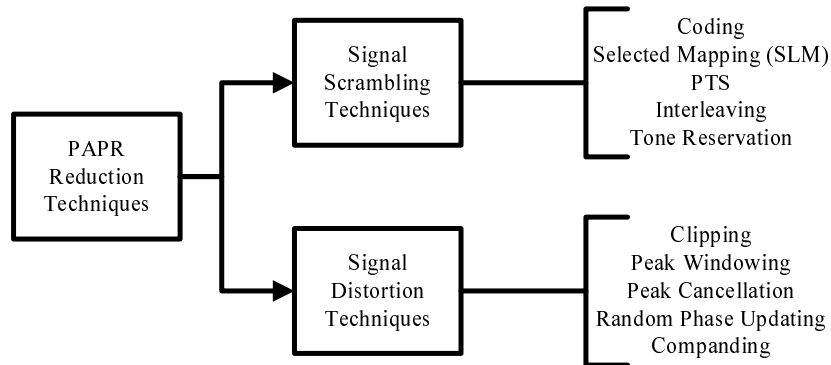


Figure 4-1: Scheme of PAPR Reduction Techniques

envelope powers (PEPs). There are three stages in the development of the block coding technique. The first stage is the selection of suitable sets of code words for any number of carriers, any M-ary phase modulation scheme, and any coding rate. The second stage is the selection of the sets of code words that enable efficient implementation of the encoding /decoding. The third stage is the selection of sets of code words that also offer error deduction and correction potential.

Selected Mapping (SLM)

Bauml et.al. [20] propose a method for the reduction of peak to average transmit power of multi-carrier modulation systems with selected mapping. In the selected mapping (SLM) method a whole set of candidate signals is generated representing the same information, and then the most favorable signal as regards to minimum PAPR is chosen and transmitted. Information about this choice needs to be explicitly transmitted along with the chosen candidate signal. SLM scheme is one of the initial probabilistic approaches for reducing the PAPR problem, with a goal of making occurrence of the peaks less frequent, not to eliminate the peaks. The scheme can handle any number of sub-carriers and drawback associated with the scheme is the overhead of side information that needs to be transmitted to the receiver.

Partial Transmit Sequences (PTS)

Muller and Huber [22] propose an effective and flexible peak power reduction scheme for OFDM system by combining partial transmit sequences (PTS). The main idea behind the scheme, is that, the data block is partitioned into non-overlapping sub blocks and each sub block is rotated with a statistically independent rotation factor. The rotation factor, which generates the time domain data with the lowest peak amplitude, is also transmitted to the receiver as side information. PTS scheme can be interpreted as a structurally modified case of SLM scheme, and is found that the PTS schemes performs better than SLM schemes but is much more complex. When differential modulation is used in each sub block, no side information needs to be transmitted to the receiver.

Interleaving

Jayalath and Tellambura [38] present an interleave based technique for improving the peak to average power ratio of an OFDM signal. Highly correlated data frames have large PAPR, which could thus be reduced, if long correlation patterns were broken down. The paper proposes a data randomization technique for the reduction of the

PAPR of the OFDM system. The most important aspect of this method is that it is less complex than the PTS method but achieves comparable results. This method is most effective for data frames with moderate PAP values (very high PAP values which are nearly M can't be reduced by this method). Therefore, higher order error correction method should be used in addition to this scheme.

Tone Reservation

The tone reservation method in [30] is suggested to reduce the PAPR. In this method a fraction of the bandwidth is used to synthesize signals that are of opposite polarity and shape a peak in the OFDM signal. Subtraction of peaks reduces the PAPR without great effect on the transmission capability of OFDM. The basic idea is to reserve a small set of tones for PAPR reduction. The problem of computing the values for these reserved tones that minimize the PAPR can be formulated as a convex problem and can be solved exactly. The amount of PAPR reduction depends on the numbers of reserved tones, their location within the frequency vector, and the amount of complexity.

4-1-2 Signal Distortion Techniques

Clipping

The simplest way to reduce the PAPR is the envelope clipping [26], such that the peak amplitude becomes limited to some threshold. Nevertheless, by distorting the OFDM signal amplitude, a kind of self-interference is introduced that degrades the BER. Furthermore, nonlinear distortion of the OFDM signal significantly increases the level of both in-band distortion and out-of-band radiation.

Peak Windowing

Nee and Wild [24] infer that since large PAP ratios occur only infrequently, it is possible to remove these peaks at the cost of a slight amount of self interference. Clipping is one example of a PAPR reduction technique creating self interference. Peak Windowing technique provides better PAPR reduction with better spectral properties than clipping. In windowing technique a large signal peak is multiplied with a certain window, such as Gaussian shaped window, cosine, Kaiser and Hamming window. Since the OFDM signal is multiplied with several of these windows, the resulting spectrum is a convolution of the original OFDM spectrum with the spectrum of the applied window.

Peak Cancellation

The peak cancellation method introduced in [39], suggests using a time-shifted and scaled reference function is subtracted from the signal, such that each subtracted reference function which reduces the peak power of at least one signal sample. By selecting an appropriate reference function with approximately the same bandwidth as the transmitted signal, it can be assured that the peak power reduction does not cause any out-of-band interference. Peak cancellation can be done digitally after generation of the digital OFDM symbols. However, the peak cancellation is in fact almost identical to clipping followed by filtering.

Random Phase Updating

Nikookar and Lidsheim [32] propose a novel random phase updating algorithm for the

peak to average power ratio (PAPR) reduction of the OFDM signal. In the random phase updating algorithm, a random phases generated and assigned for each carrier. The random phase update is continued till the peak value of the OFDM signal is below the threshold. The threshold can be dynamic and the number of iterations for the random phase update is limited. After each phase update, the PAPR is calculated and the iteration is continued till the minimum threshold level is achieved or the maximum number of iterations has been reached.

Companding

Wang et.al. [27] propose a simple and effective companding technique to reduce the PAPR of OFDM signal. The OFDM signal can be assumed Gaussian distributed, and the large OFDM signal occurs infrequently. So the companding technique can be used to improve OFDM transmission performance. This technique is used to compand the OFDM signal before it is converted into analog waveform. The OFDM signal after taking IFFT, is companded and quantized. Companding technique improves the quantization resolution of small signals at the price of the reduction of the resolution of large signals, since small signals occur more frequently than large ones.

4-1-3 Selection Criteria for PAPR Reduction Technique

There are many factors that should be considered before a specific, PAPR reduction technique is chosen. These factors include PAPR reduction capability, power increase in the transmit signal, BER increase at the receiver, loss in data rate, computation complexity increase etc. Sometimes these requirements are contradictory and cannot be met at the same time. For example the amplitude clipping technique clearly removes the time domain signal peaks but results in in-band distortion and out-of-band radiation. Some techniques require a power increase in the transmitted signal after using PAPR reduction techniques. For example Tone reservation (TR) requires more signal power because some of its power must be used for the peak reduction carriers. Some techniques may have an increase in BER at the receiver if the transmit signal power is fixed or equivalently may require large transmit power to maintain the BER after applying the PAPR reduction techniques. In some techniques such as SLM, PTS and Interleaving, the entire data block may be lost if the side information is received in error. This also may increase BER at the receiver. Some techniques require the data rate to be reduced. In block coding technique one out of four information symbols is to be dedicated to controlling PAPR. In SLM, PTS and Interleaving, the data rate is reduced due to the side information used to inform the receiver of what has been done in the transmitter. In these techniques the side information may be received in error, unless some form of protection such as channel coding is employed. Computational complexity is yet another important consideration in choosing a PAPR reduction technique. Techniques such as PTS find a solution for the PAPR reduced signal by using many iterations. The PAPR reduction capability of Interleaving technique is better for large number of Interleavers, which on the other hand slows the computation capacity. According to the above mentioned criteria we found that the selected mapping technique is a simple, feasible and reliable method which could be applied to WPM extended to achieve better PAPR performances.

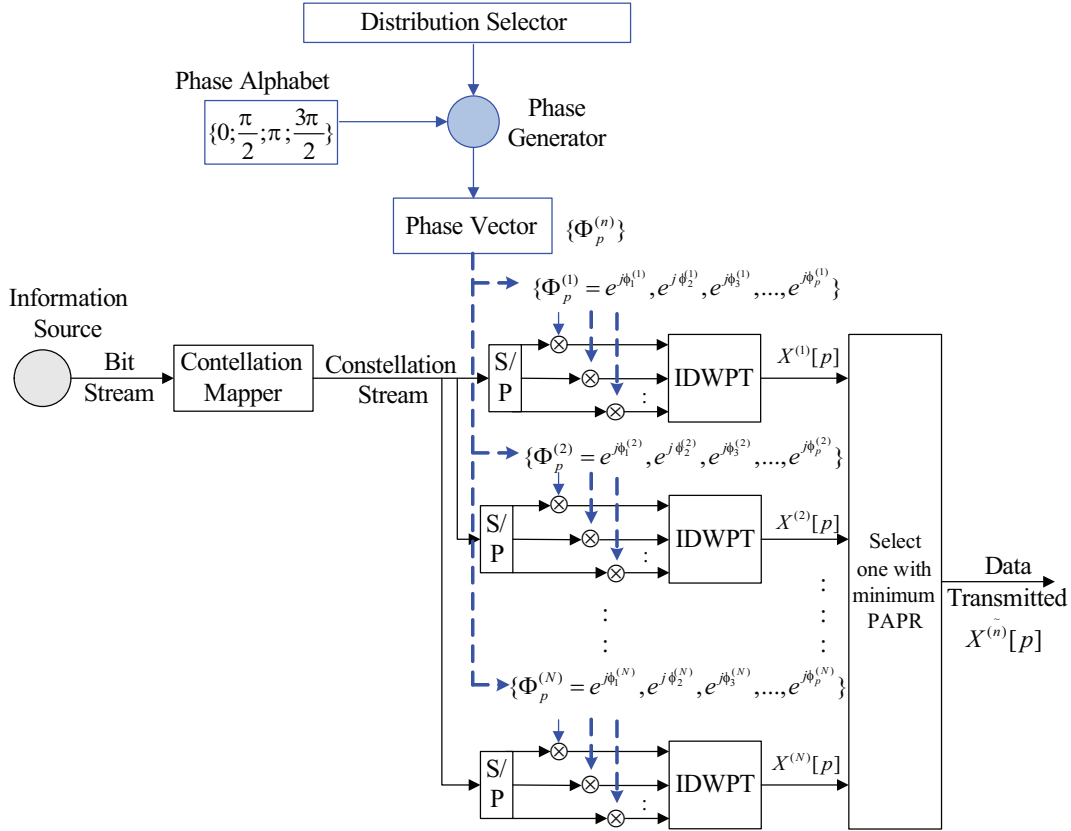


Figure 4-2: WPM Transmitter Block diagram with the PAPR reduction technique

4-2 Selected Mapping with Phase Modification

As the number of carriers M increases the PAPR of the signal also increases. Chances are that the power fluctuations of the WPM system, with large number of carriers, will spill into the non-linear region of the transmitter amplifier operation resulting in distortion and spectral spreading of the signal. It is therefore important to reduce the PAPR. The methods currently available in the literature for PAPR reduction of the WPM signal are either too complicated or yield marginal gains [40] and [41].

We now present a simple approach to reduce PAPR. This is done by mapping a finite information set into multiple WPM frames with different PAPRs. Then the WPM frame that has the least PAPR is selected for transmission. In order to generate the frames out of the same information, the WPM carriers are randomly rotated with a value chosen from an alphabet of finite number of identically spaced phase-shifts. The fundamental idea of the method is that PAPR of any multi-carrier signal can be adjusted by altering the phases of the sub-carriers and hence by varying the phases of the sub-carriers, frames with different PAPRs, albeit representing the same information, can be obtained [20] and [32].

Fig. 4-2 shows the blocks of the proposed WPM system with the PAPR reduction structure. The bit stream from the information source is first converted to a constellation

(Quadratic Phase Shift Keying (QPSK)/Binary Phase Shift Keying (BPSK)) stream and then replicated to obtain a finite number of copies, say L . Each of the replicated set is then serial-to-parallel (S/P) converted and then phase-shifted by a random phase sequence.

The phase sequences are generated by a phase generator which chooses between different phase alphabets ϕ and stochastic distributions and creates a phase vector $\Phi_p^{(n)}$. Here n ($= 1, 2, 3, \dots, L$) stands for the index of the frame and p ($= 1, 2, 3, \dots, M$) connotes the sub-carrier index. The phase vector thus contains L rows each with M columns. Denoting the information bearing WPM frame by the notation $\mathbf{X}[p]$, the L different WPM frames $\mathbf{X}^{(n)}[p]$ obtained by sub-carrier wise multiplication with the phase-vector $\Phi_p^{(n)}$ can be given as:

$$\mathbf{X}^{(n)}[p] = \mathbf{X}[p] \times \Phi_p^{(n)} = \mathbf{X}[p] \times e^{j\phi_p^{(n)}} \quad (4-1)$$

The phase-shifted information bearing streams are then transformed by an Inverse Discrete Wavelet Packet Transform (IDWPT) operation and the PAPR of the transformed composite signal is calculated. Amongst the set of L PAPR values, the one with the least value is selected and transmitted. Note that all of the frames carry identical information. In order to achieve PAPR reduction, the WPM frame with the lowest PAPR is transmitted. Defining the candidate time domain WPM frame as $x = \mathbf{IDWPT}(\mathbf{X}^{(n)}[p])$, the index of this frame can be given as:

$$\hat{n} = \underset{1 \leq n \leq L}{\operatorname{argmin}}(\operatorname{PAPR}(x^{(n)})) \quad (4-2)$$

In order to ensure that the transmitter and receiver operate harmoniously, the chosen index of the frame \hat{l} is sent to the receiver as a side information. Typically for a size L vector, the number of bits required to send \hat{l} will be $\log_2(L)$. However, to prevent corruption of this precious message, more bits may be used to encapsulate this message by channel coding.

The algorithm to calculate and select the minimum PAPR for WPM is summarized in Algorithm 4.1.

4-3 Numerical Results

In this section we present results of the studies and evaluate the performance of WPM system with the PAPR reduction technique. The investigations are carried out using computer simulations and the performance metric of choice is the Complementary Cumulative Distribution Function (CCDF). In Orthogonal Frequency Division Multiplexing (OFDM) the PAPR is usually calculated per symbol. This is not possible in WPM because WPM symbols overlap in the time-domain therefore the PAPR has to be calculated per frame. The WPM system is realized using a filter bank structure with 7 levels of decomposition. The modulation scheme used is QPSK. The phase alphabet is taken to be $\phi \in (0, \pi/2, \pi, 3\pi/2)$ which is randomly chosen while generating the phase

Algorithm 4.1 Pseudocode for calculating and selecting the minimum PAPR for WPM

- 1: Obtain the source message.
- 2: Replicate it a finite number of times, say L .
- 3: Generate statistically independent phase sequences from the chosen phase alphabet (e.g. $\phi \in (0, \pi/2, \pi, 3\pi/2)$).
- 4: Multiply frame sequences element/carrier-wise by M -length phase sequences. Here M is also the number of WPM carriers.
- 5: Do the IDWPT transform for each resulted frame sequence for each replicated copy of the data.
- 6: Calculate the PAPR per frame of the signal for each replicated copy of the data and find the PAPR.
- 7: List all the PAPR values; select the minimum PAPR and transmit.
- 8: Send as side information the index of the frame with minimum PAPR, \hat{l} to recover the data in the receiver.

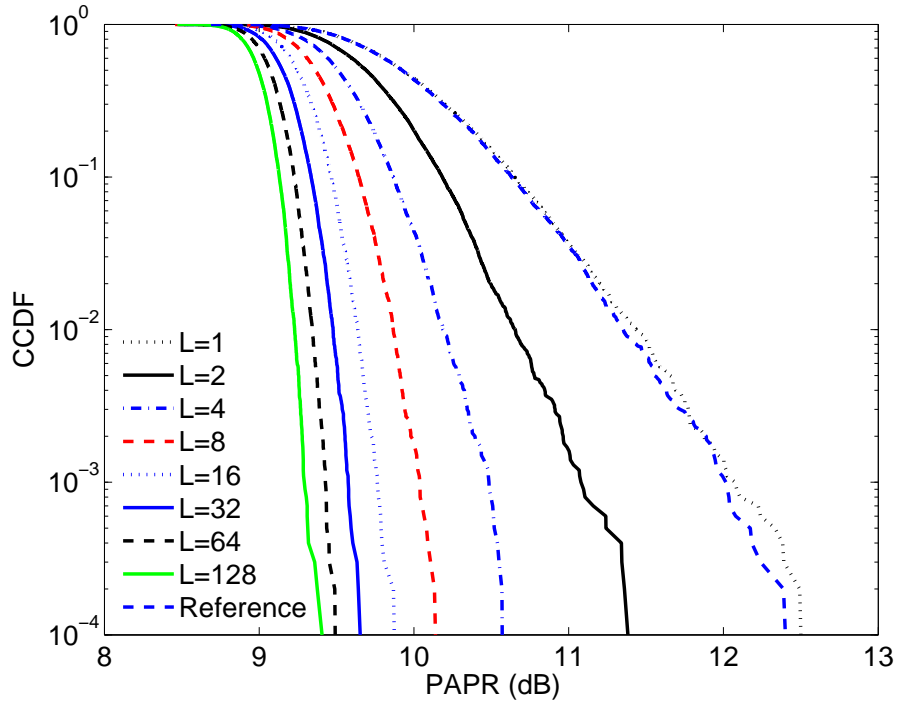


Figure 4-3: CCDF of the PAPR of the WPM signal for different values of L . The wavelet considered is Daubechies 5 (length 10). A reference curve with no PAPR reduction is also plotted.

vector. The wavelet of choice is Daubechies 5 (denoted db5) which is of length 10. These simulation parameters will be used through out the experiments unless stated otherwise. To properly evaluate the improvements due to the PAPR reduction technique, a reference PAPR-CCDF curve obtained for db5 wavelet for the case without PAPR reduction (i.e. no phase modification) will also be provided.

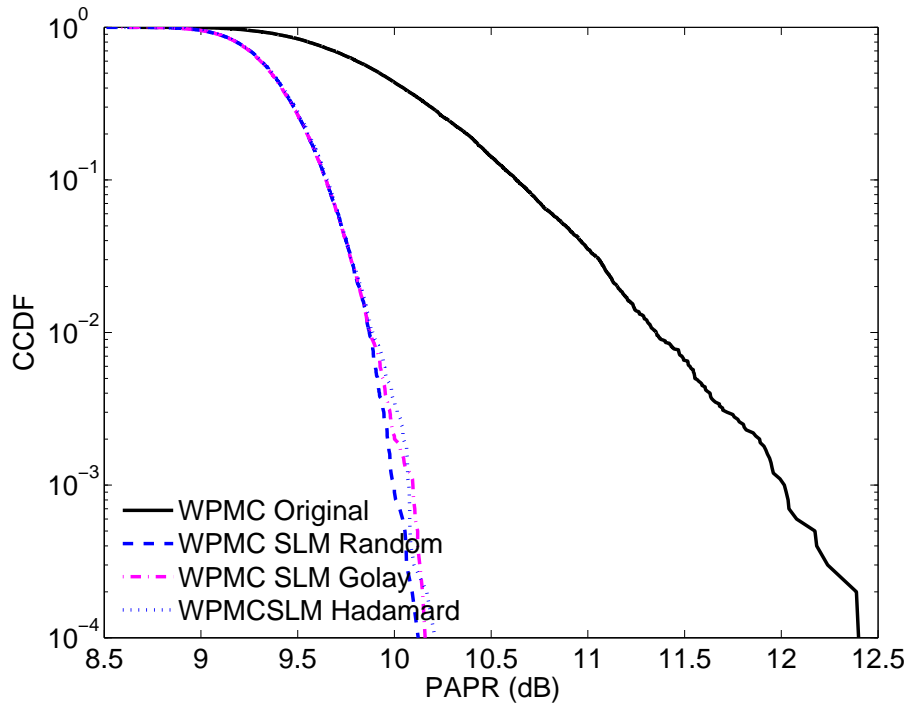


Figure 4-4: Complementary cumulative distribution function (CCDF) of the PAPR of WPM for different distributions of the phase sequences. The wavelet considered is Daubechies 5 (length 10).

4-3-1 Impact of choice of number of replications

In the first set of results we verify the impact of the PAPR reduction technique. Figure 4-3 shows the CCDF curves for the variation of PAPR under the PAPR reduction technique for different number of replications, L . It is evident from the plots that the improvements are significant and bring in up to 3dB reduction in PAPR in comparison to the case when no PAPR reduction technique is used.

4-3-2 Choice of distribution of the Phase Sequences

To gauge the impact of the distribution of the phase sequences we now consider different stochastic distributions, namely, the random sequences, the Golay sequences [42, 43] and the Hadamard sequences where the number and length of all the sequences are the same. The phase alphabet is taken to be $\phi \in (0, \pi/2, \pi, 3\pi/2)$ and the value of L is fixed at 8. Figure 4-4 shows the respective plots and it can be deduced from the figures that though all the distributions yield notable improvements, there is no perceivable differences in their performances.

These results are important because the imperceivable difference in the performances when using pseudo-random and random sequences means that the former can be used in place of the later. Thus the receiver end only needs to know the key used to generate the pseudo-random phase sequences used at the transmitter (and not the entire

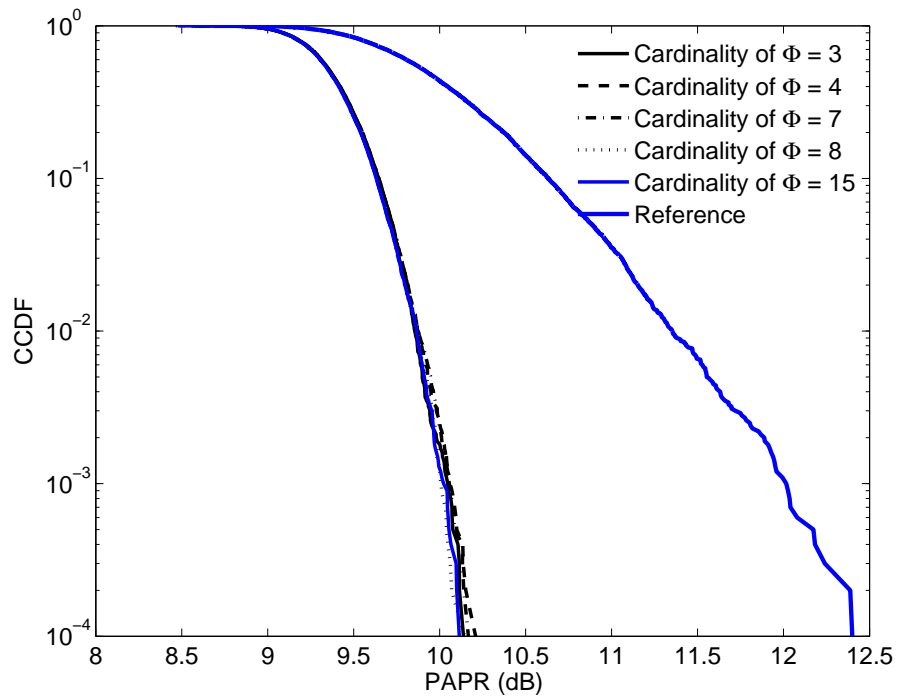


Figure 4-5: CCDF of the PAPR of WPM using the PAPR reduction technique for different phase sequences. The wavelet considered is Daubechies 5 (length 10).

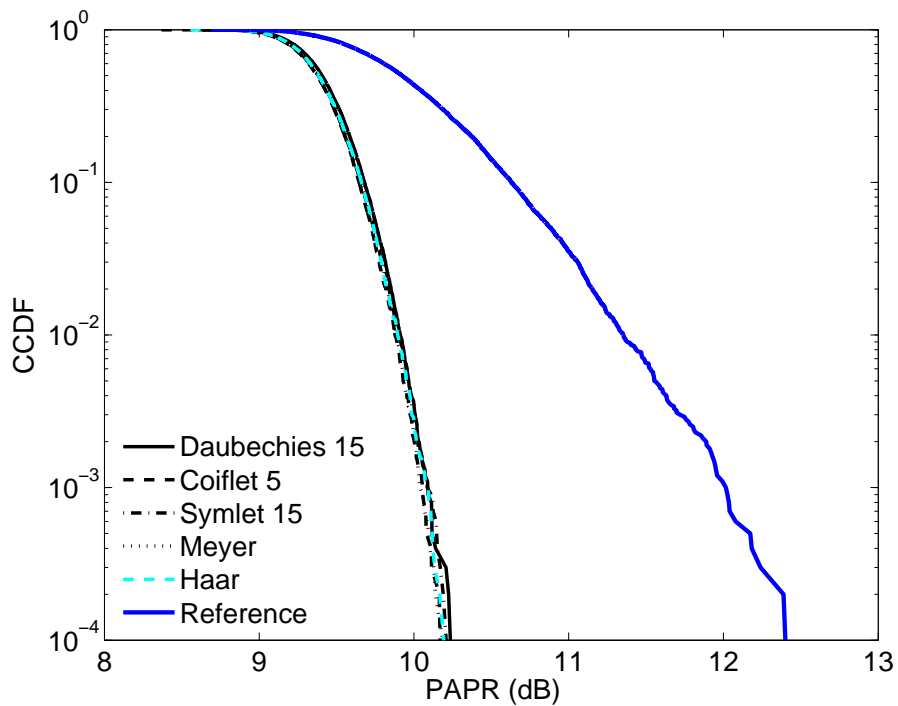


Figure 4-6: CCDF of the PAPR for several wavelets.

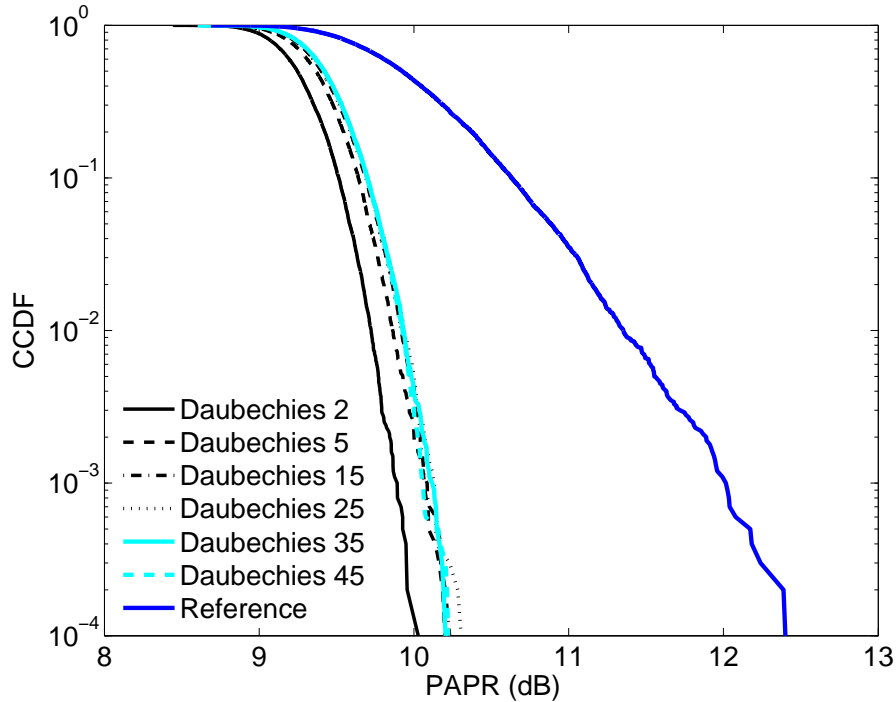


Figure 4-7: CCDF of the PAPR for the WPM system with different filter lengths of the Daubechies wavelet family.

phase sequence). This paves the way for a significant reduction in the transfer of side information.

4-3-3 Impact of choice of phase alphabet

We now evaluate the impact of the phase alphabet on the PAPR reduction mechanism. The results are plotted in Figure 4-5 where a range of cardinalities for the phases are considered. The results show that the choice of the phase alphabet does not affect the performance of the PAPR reduction technique.

4-3-4 Impact of choice of wavelet families

We now analyze the conduct of the PAPR reduction technique for different wavelet families and for different filter lengths. In these set of experiments the value of L is taken to be 8. The various wavelet families considered are Daubechies 15, Coiflet 5, Symlet 15 (all of length 30), Meyer (of length 102) and Haar. Figure 4-6 and Figure 4-7 show the PAPR performance curves for various wavelet families and various filter lengths, respectively. From Figure 4-6 we can deduce that all the wavelets follow a similar CCDF pattern for their PAPR performances. And from Figure 4-7 it is clear that even with increasing lengths of the wavelet filter, from Daubechies 2 to Daubechies 35, the PAPR distribution is limited to a variation of about 0.8 dB. In all instances the proposed technique reduces the PAPR between 1.5 and 2.5dB.

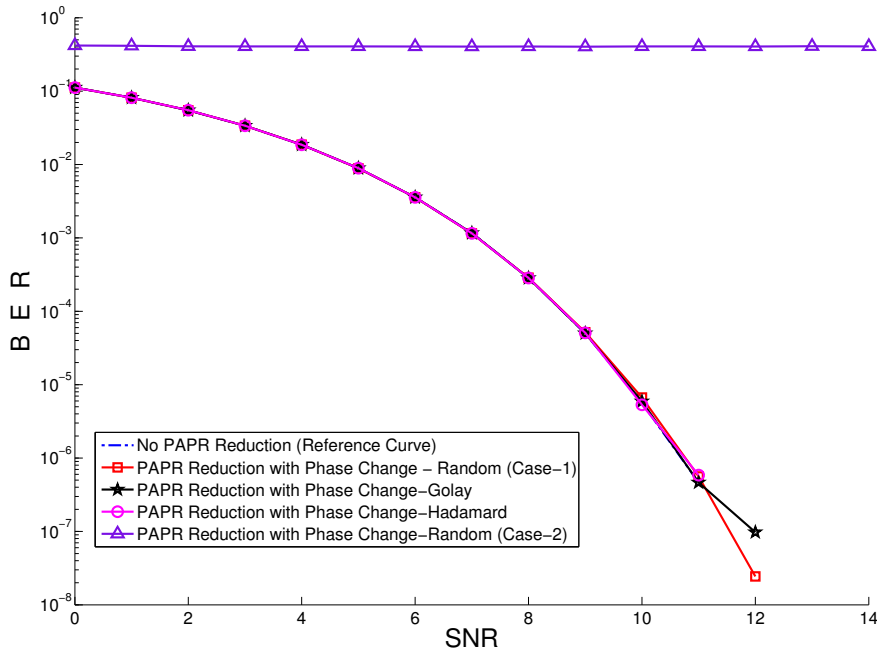


Figure 4-8: BER vs. SNR (dB) for the cases with and without PAPR reduction (phase modification) and for various distributions of the phase. For the case with random phase change two figures are plotted. In the first case (denoted Case-1) the receiver has complete and perfect knowledge of the random phases used at the transmitter. In the second scenario (marked Case-2) the receiver operates with no knowledge of the phases used at the transmitter. For the scenarios when phases with Golay and Hadamard distributions are used, the transmitter and receiver only share the keys of the pseudo-random polynomial.

4-3-5 Influence of the PAPR reduction technique on the BER performance

We finally plot the BER performances of the WPM system (Figure 4-8). The curves plotted are for the cases when the phase sequences are generated randomly (two cases are considered where in the first case the receiver has complete and perfect knowledge of the random phases used at the transmitter and in the second case where the receiver operates with no knowledge of the phases used at the transmitter) and pseudo-randomly (when the receiver only knows the key used by the transmitter to generate the pseudo-random sequence). As a reference the BER plot for the case when no PAPR reduction technique is used is also plotted. The results show the importance of having complete knowledge on the phase sequences. Even a slight mismatch in the phase information at the receiver deteriorates the system performance significantly given the sensitivity of WPM systems (or for that matter any multi-carrier system) to phase errors. Since a perfect replication of randomly generated phases is not possible at the receiver, the application of pseudo-random generators can be mooted. This is supported by the results plotted in Figure 4-4 where the PAPR reduction due to pseudo-random codes is shown to be as good as that of random phase generators and in Figure 4-8 where the BER curves show that using PAPR reduction mechanism with pseudo-random phase generators does not result in any loss in performance.

4-4 Summary

In this chapter, we proposed and presented a method to reduce the PAPR in the developmental Wavelet Packet Modulation system. The method exploited the fact that by altering the phase of the WPM sub-carriers one can alter the PAPR of the transmitted signal. By randomly altering the phases of the sub-carriers that modulate the information, one can obtain different WPM frames with different PAPRs. And by transmitting the WPM frame with least PAPR, the possibility of the WPM system slipping into non-linear region is considerably reduced.

The importance of the method is in its simplicity and elegance of implementation. Furthermore, this method can be tagged with other PAPR reduction techniques, selecting the best tree structure, which is proposed in [40] and [41], to fine tune the level of PAPR reduction that can be achieved. Future efforts in this area can broadly be in the lines of: (a) obviating the need to send side information (or the index of the phase vector with least PAPR), which is studied in Chapter 5 by encoding it as a part of the transmitted data using scramblers and de-scramblers at the transmitter and receiver, respectively. (b) finding the optimum set of phase values that result in the lowest possible PAPR at all instances, which we delve on in Chapter 6.

Selected Mapping with Scrambling

In the selected mapping technique, replicas of the original message are randomly determined and the one producing the frame with the least Peak-to-Average Power Ratio (PAPR) value is transmitted. The replicas of the original message is distinct from each other; however, they carry the same information as that of the original message. One way to implement selected mapping based PAPR reduction technique is to generate various scrambled replicas of the source message. Another way is to shift the phase of the replicas of the signal [44–47]. In Chapter 4, we showed how to employ selected mapping technique with phase modifications. Scrambling based techniques work on the source coding stage before constellation mapping, which is shown in Figure 5-1. In this chapter, we introduce and discuss the Wavelet Packet Modulation (WPM) architecture where scrambling based PAPR reduction techniques are employed. In the literature, to the best of our knowledge, encryption based PAPR reduction has never been employed before. In this chapter, we also present how to reduce the PAPR of the WPM signal in a secure fashion. The scrambling (also referred to as a randomizing process) is a process which manipulates a data stream by transposing signals at the transmitter to make the message undecidable at a receiver which cannot appropriately descramble the received signal. Scrambling is often used in telecommunication systems to eliminate the dependence of a signal's power spectrum upon the actual transmitted data. There are two types of scrambling techniques: additive or multiplicative. In the additive scrambling techniques, a pseudo random sequence is added to the signal. In this case, both the transmitter and receiver must be able to generate the same pseudo sequence. In the multiplicative scrambling technique, the signal is multiplied with the scrambler's transfer function. In this technique, the signal is used to change the state of the registers used to generate the scrambling sequences.

Scrambling techniques can also be used to reduce the PAPR. Multiple copies of the original input signal is scrambled with different states if additive scrambler is used or with different prefixes inserted at the beginning of the input signal if multiplicative scrambler is used. Among these generated scrambled signals containing the original

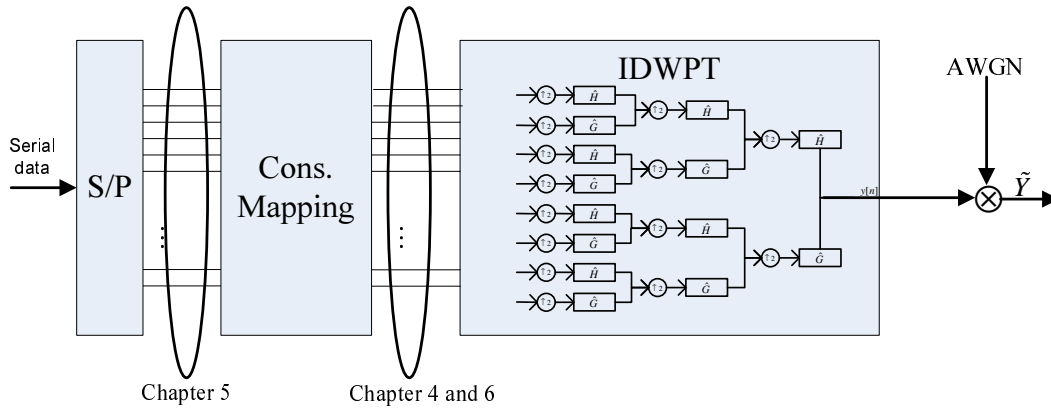


Figure 5-1: WPM architecture where the different SLM methods are applied.

signal, the one producing the least PAPR is selected after modulation and transmitted. When additive scrambler is employed, additional side information, namely, the initialization state (seed) is to be transmitted to the receivers. When multiplicative scrambler is used, no side information is required. However, a prefix has to be inserted in front of the signal to change the output of the scrambler such that various scrambled copies of the same original signal can be generated. Since original signal is used to alter the state of the multiplicative scrambler, the output signal consists of the diffused original signal which implies that a symbol error will also be diffused to the other symbol positions. Multiplicative scramblers lead to error multiplication during descrambling (i.e. a single bit error at the descrambler's input will result into w errors at its output, where w equals the number of the scrambler's feedback taps).

In Section 5-1 we present how the scrambling techniques can be applied in WPM system to reduce the PAPR. As a novelty, we propose to employ an encryption system which is similar to additive scrambling technique to reduce the PAPR. Employing this proposed encryption based system, enhances the security of the system as well as performs same as additive scrambler without any additional cost compared to the scrambling techniques. Since all telecommunications systems employ some kind of stream ciphers to secure the signals transmitted over an insecure channel, using the same block for PAPR reduction does not introduce additional implementation or permutational costs. In Section 5-2, we introduce this novel technique.

5-1 Scrambling Based PAPR Reduction in WPM

In this section, we introduce how scramblers can be used to reduce the PAPR in WPM. The basic idea of symbol scrambling is that, for each symbol, the input sequence is scrambled by a certain number of scrambling sequences. The transmitted signal is the one with the least PAPR. Scrambling based PAPR reduction has already been implemented in the Orthogonal Frequency Division Multiplexing (OFDM) systems [21, 44–46, 48]. Scrambling based PAPR reduction techniques reduce the PAPR in Quadratic Phase Shift Keying (QPSK)-OFDM systems; however, when additive scram-

blers are employed, they incur some redundancy which can be considered negligible [47]. When multiplicative scramblers are employed, no side information is required [46, 49]. Scrambling may reduce the PAPR of the OFDM signals around 2% of the maximum possible value [21].

In [50], Ochiai and Imai propose a simple scheme to reduce the PAPR of the OFDM-CDMA signals. They examine the statistical behavior of the peak power of the OFDM-CDMA signals and employ Walsh-Hadamard and Golay complementary sequences as spreading sequences. For small number of active users, Golay complementary sequences produce a lower PAPR than Walsh-Hadamard sequences. As the number of active users increases, Walsh-Hadamard sequences becomes better. In this paper, a simple scrambling scheme is employed to reduce PAPR for a small number of the active users. Further PAPR reduction is achieved by adaptively selecting the set of the spreading sequences [50].

Scramblers employ Linear Feedback Shift Register (LFSR) to generate pseudo-random sequences which are used to scramble the input signal [51, 52]. Before going into the details of the scrambling techniques, here we recapitulate the LFSRs. Historically, linear feedback registers are used to randomize the transmitted bitstream to prevent repeating sequences (multiple copies of the same symbols in sequence) which may complicate symbol tracking at the receiver. This randomization produced by the scrambler is then removed at the receiver after demodulation. When the LFSR runs at the same rate as the transmitted symbol stream, this technique is called as scrambling [53].

A linear feedback shift register (LFSR) is a shift register whose input bit is a linear function of its previous state. State of a LFSR is the content of the register. XOR is a linear boolean function. Therefore, an LFSR is a shift register whose input bit is calculated by the exclusive-or (xor) of some bits of the overall shift register value. The bit positions are called as taps. The initial value of the LFSR is called the seed (initialization state). The LFSR works in a deterministic fashion, that is the output stream produced by the register is completely determined by its present (or previous) state. The LFSR has a finite number of possible states. Therefore, the LFSR states eventually repeats. However, when the feedback (characteristic) function is chosen carefully, the output stream appears to be random with a very long cycle. The arrangement of taps for feedback in an LFSR can be expressed in Galois field ($GF(2)$) arithmetic as a polynomial modulo 2 in which case the coefficients of the polynomial must be 1's or 0's. This is called the feedback polynomial or characteristic polynomial [53].

The bit positions that affect the next state are called the taps. The rightmost bit of the LFSR is called the output bit. The taps are xor'ed sequentially with the output bit and then fed back into the leftmost bit. The sequence of bits in the rightmost position is called the output stream. If the signal is not used as an input to the characteristic polynomial then the LFSR can be considered as an additive scrambler where the output stream, which is a pseudo random sequence, is added to the input signal. When the signal is used as an input the LFSR, then it acts as a multiplicative scrambler. The output of the LFSR, is the scrambled signal.

In the sequel, we present how such scrambling techniques can be employed to reduce the PAPR.

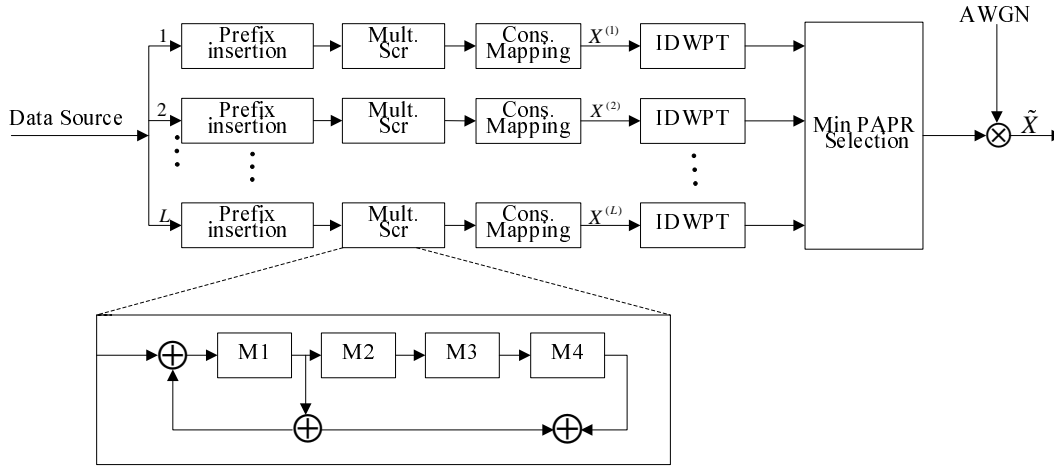


Figure 5-2: WPM Transmitter architecture employing Multiplicative Scrambler without side information for PAPR reduction.

5-1-1 Selected Mapping Using Multiplicative Scrambling Without Side Information

In this section, we describe a scrambling scheme, which abstains from explicit transmission and careful protection of side information. Figure 5-2 shows a block diagram of the multiplicative scrambler transmitter. The multiplicative scrambler can be implemented using a LFSR. A scrambler is used in telecommunications systems to transpose/invert a signal such that the signal is not decipherable if the receiver is not equipped with an adequate descrambler. The scrambler makes the actual transmitted data independent of its signal's power spectrum. To generate L different transmit sequences, representing the same binary information data replicas, prefixes/labels are inserted in front of the replicas of the input signal. The labels are different binary vectors of length and by assuming without loss of generality that prefix $L=0$. The concatenated vector L of the label prefix and the information replica is then fed into a scrambler consisting of a shift register with a feedback branch only as shown in Figure 5-2, which is reset to the zero state before the scrambling takes place. The labels are hence used to drive the scrambler into one of different states before scrambling the data replicas it selves. The scrambled output vector L is then processed as usual, and mapped to a signal constellation. After the Inverse Discrete Wavelet Packet Transform (IDWPT), we obtain the transmit sequence associated with the inserted label. This proceeding is executed, and finally the specific transmit sequence, which processes the lowest peak power, is selected and transmitted.

When a multiplicative scrambler is employed, it is possible to reduce the PAPR without using any side information. The modified signal is then transformed using a multiplicative scrambler. Due to the inserted prefix, different signals of the actual message are produced. The PAPR for these replicas are computed and the one with the smallest PAPR value is transmitted. At the receiver, no side information is required.

The corresponding descrambler can transform the received signal to the actual signal

by employing the reverse operation of the scrambler. The only additional devices are descrambler and prefix removal. The descrambler performs the inverse operation of the scrambler in the transmitter and is hence a shift-register with a feed-forward branch, only. The descrambler is reset to the zero-state before descrambling starts for a WPM frame. If no transmission errors have occurred, the output of the descrambler is the concatenation of the transmitted prefix with the data replica. The prefix remover only needs to strip off the label prefix and output the estimated information data replica. The receiver can explicitly determine the number of the sequence selected for transmission, but it does not need this information for data recovery.

If errors occur during transmission, the descrambler causes a moderate multiplication of these errors. As an example, consider the case that the transmitted binary vector is the all zero-data replica. Then a transmission error manifests itself in the presence of one symbol in data replica before descrambling in the receiver. When shifted through the descrambler, for every clock tic this error can produce an error at the descrambler output. If two or more errors are shifted simultaneously through the descrambler, then they can extinguish each other partially in the descrambler output. Therefore, the total number of errors at the descrambler output is at most equal to the number of errors before descrambling multiplied by the number of taps of the descrambler, i.e. the weight of the (de-)scrambler polynomial. Therefore a scrambler polynomial of low weight should be chosen. In the simulations, we use a multiplicative scrambler with a feedback (characteristic) polynomial of $x^4 + x + 1$, that is, the taps are at the fourth and first symbol positions. The 1 in the feedback polynomial corresponds to the input to the first symbol position.

Although multiplicative scramblers eliminate the side information requirement, they are prone to larger bit error rates (BER) as can be seen in Figure 5-17. Since in a multiplicative scrambler the input is used to change the LFSR states, and LFSR states are used to determine the output symbol in turn, an error in the signal results in multiple errors in the received signal. As can be seen Figure 5-17, the BER is high when multiplicative scrambler is employed.

Moreover, the bits that comprise the label (prefix) are transmitted in the same way as the information data replica bits. Therefore, the prefix bits are also encoded and thereby protected like the data replica bits. In fact, they represent information that has to be transmitted; if is a power of 2, then the information content of every label bit is exactly 1 bit, since the transmission of all candidate sequences is equally probable for the receiver. The information in the bits of the data replica and the selected label is however not transmitted directly. Due to the presence of the scrambler this information is rather contained in the combination of several successive bits after the scrambler. In this way, the information of any bit is smeared over a larger part of the scrambled sequence and eventually the transmit sequence.

When multiplicative scrambler is employed, the input signal is used to change the state of the LFSR. Since in multiplicative scramblers the signal is also used as an argument in the LFSR operations, bit errors diffuse throughout the symbols of the signal. In additive scramblers, a bit error remains as a bit error and does not impact other symbols. To mitigate the disadvantage of the multiplicative scrambler method, an additive scrambler

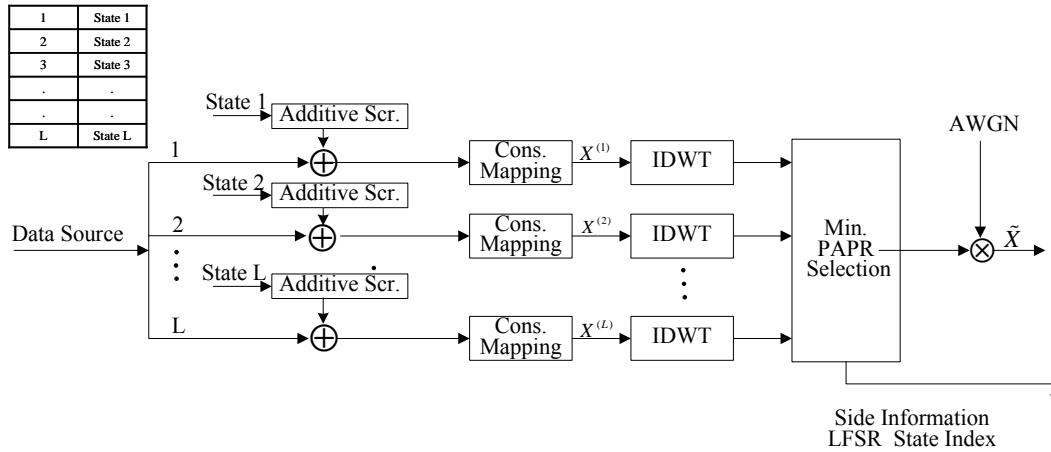


Figure 5-3: WPM Transmitter architecture employing Additive Scrambler with side information for PAPR reduction.

can be preferred.

5-1-2 Selected Mapping Using Additive Scrambling With Side Information

An additive scrambler as shown in Figure 5-3 transforms the signal by xor'ing it with a pseudo random sequence generated by one or more interconnected LFSRs. If additive scrambler is employed, the signals do not intervene in the LFSR cycles; in other words, the input signal does not impact the state of the LFSR. Multiple replicas of the actual signal are transformed by xor'ing them with various pseudo random sequences produced by additive scramblers initialized with different states. PAPR values of the replicated and transformed signals are calculated and the one with the minimum PAPR value is transmitted. In this case, the transmitter has to convey the state used by the scrambler of the selected signal to the receiver as side information.

Instead of randomizing the initialization states (seeds), the side information length can be reduced to $\log_2 L$ where L is the number of replicated signals among which the signal with the minimal PAPR is selected. Assume that the transmitter and receiver initially configures with a table of scrambler states. Then, the index of the selected scrambler's state would be enough to descramble the signal. As can be seen in Figure 5-3, we use a table to manage the initialization seeds of the LFSR of the additive scrambler. The replicas of the original signal is generated using the scrambler initialized with different seeds kept in this table. The same table should be shared by the transmitter and the receiver.

The feedback polynomial that we used in the simulations is $x^{15} + x^4 + x^2 + x$.

This is an example feedback polynomial which we used in the simulations. Different feedback polynomial can also be employed. As long as the feedback polynomial facilitate generating a set of scrambled outputs which are not the same and the size of the set is larger than L . Based on the selected feedback polynomial, the scramblers have a period in which they start repeating the same random sequences. The period of the

scrambler has to be larger than the maximum number of replicas, L . In other words, in the selected mapping technique, all the generated replicas have to be different from each other. If a subset of replicas are the same, they will produce the same PAPR value, which causes waste of computational power. Therefore, selection of the feedback polynomial is of significant concern. However, in this thesis we do not go into the details of how to determine a proper feedback polynomial. Interested reader may refer to [53].

In the selected feedback polynomial, the tap positions are 15,4,2 and 1. Both the transmitter and receiver share a table of initialization states (seeds). The table contains L seeds which are used to generate L different pseudo-random sequences which will be xor'ed with the input signal. The one producing the least PAPR is transmitted along with the index value of the selected seed. The pseudocode of the scrambling based PAPR reduction techniques is presented in Algorithm 5.1.

Algorithm 5.1 Pseudocode of scrambling based PAPR reduction for WPM

- 1: Obtain the source message.
 - 2: Make finite copies of the, say L , same message and scramble each of them with a different code.
 - 3: Do the **IDWPT** transform for each scrambled frame sequence.
 - 4: Calculate the PAPR per frame of the signal for each replicated copy of the data and find the PAPR.
 - 5: Among all the PAPR values select the frame with the least PAPR and transmit.
 - 6: If additive scrambler is used send as side information the index of the seed used the scramble the frame.
 - 7: If multiplicative scrambler is used no side information is required.
-

5-1-3 Numerical Results of Comparison of Scrambling-Based PAPR Reduction Techniques

In this section, we present the simulation results and evaluate the performance of WPM system with the scrambling based PAPR reduction techniques. The study is carried out using MATLAB simulations and the performance metric of choice is the Complementary Cumulative Distribution Function (CCDF). Since WPM symbols overlap in the time-domain, the PAPR calculation is done per frame. The WPM system is realized using a filter bank structure with 7 levels of decomposition which also applies for the reference curve. The modulation scheme used is QPSK and the number of replicas, L , is taken to be 8. The wavelet of choice is Daubechies 5 (denoted db5) which is of length 10. These are the constant values of the simulation parameters used to produce the results throughout this section unless otherwise states. To properly evaluate the improvements due to the PAPR reduction technique, a reference PAPR-CCDF curve obtained for db5 wavelet for the case without PAPR reduction is also provided.

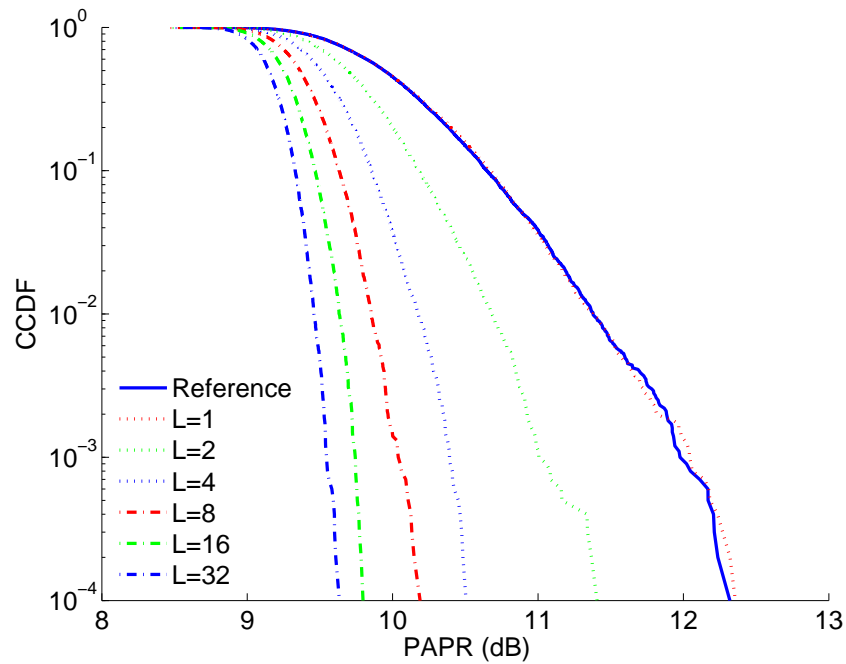


Figure 5-4: CCDF of the PAPR for several initialization seeds where additive scrambler is employed.

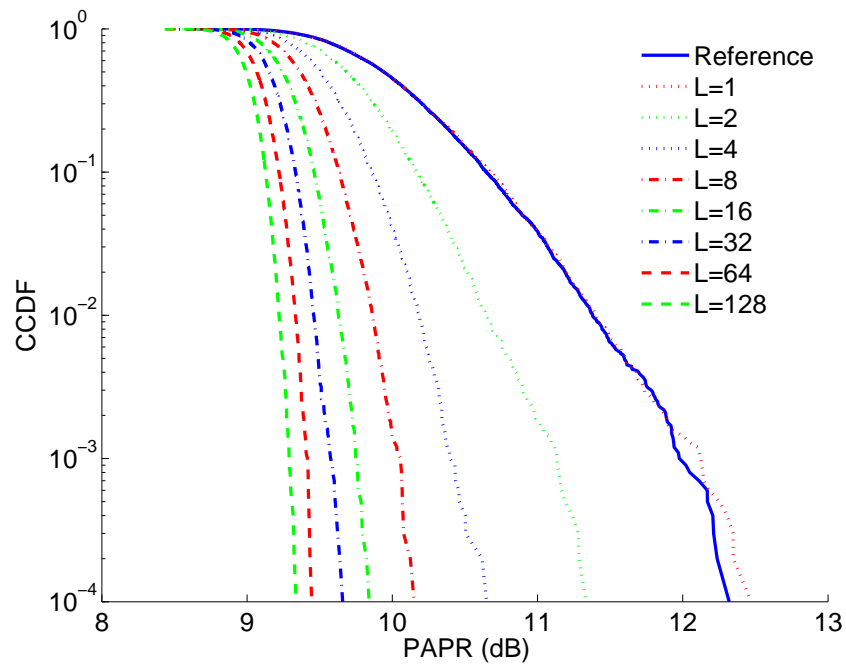


Figure 5-5: CCDF of the PAPR for several number of labels where multiplicative scrambler is employed.

Impact of choice of number of replications

In Figures 5-4 and 5-5, we present the impact of the number of replicas on the PAPR reduction. As L goes to infinity, the scrambling based technique reduces to brute-

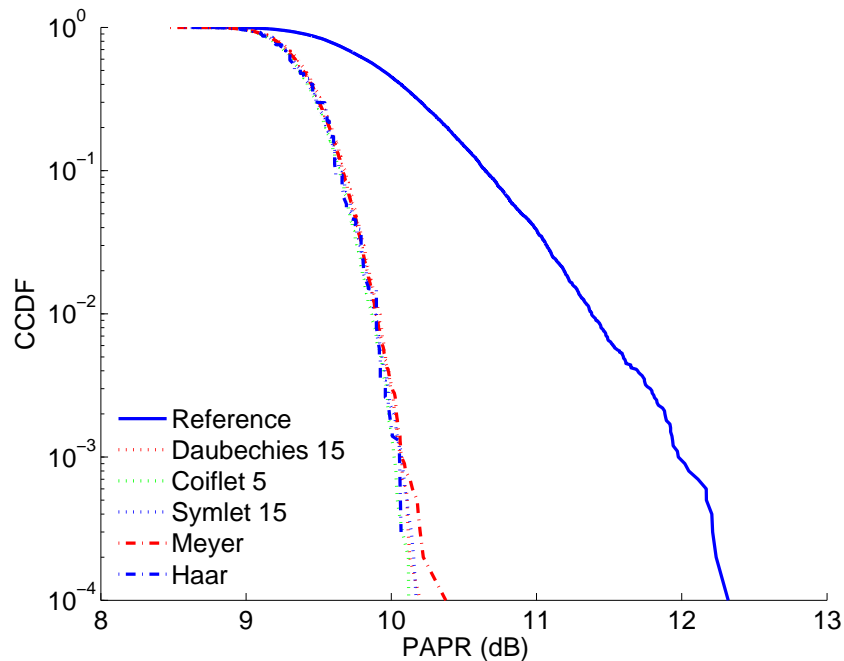


Figure 5-6: CCDF of the PAPR for several wavelet families of the additive scrambler.

force search. Therefore, the probability of finding a replica with a global minimum increases. Consequently, when larger number of replicas, L are employed in the WPM system, the PAPR reduction performs better. However, increasing L requires additional processing power or additional scrambling hardware. When $L = 1$ which means that only one scrambled replica of the original signal is considered, the PAPR reduction does not provide any significant gains. The trends of the CCDF curves for both additive and multiplicative scrambler are almost the same. For example, for a CCDF value of 10^{-2} , the resultant PAPR is around 9.8 dB for both schemes where the reference PAPR (i.e., when no PAPR reduction technique is employed) is around 11.4 dB. The gains by increasing the number of replicas decreases when $L > 16$.

Impact of choice of wavelet families

The PAPR reduction gains when different wavelet families or different filter lengths are employed in the WPM system are shown in Figures 5-6 and 5-7. In these set of experiments the WPM system is realized using a filter bank structure with 7 levels of decomposition. The modulation scheme used is QPSK and the value of L is taken to be 8. The various wavelet families considered are Daubechies 15, Coiflet 5, Symlet 15 (all of length 30), Meyer (of length 102) and Haar. As can be seen in these figures, changing the wavelet families do not impact the PAPR reduction performance significantly.

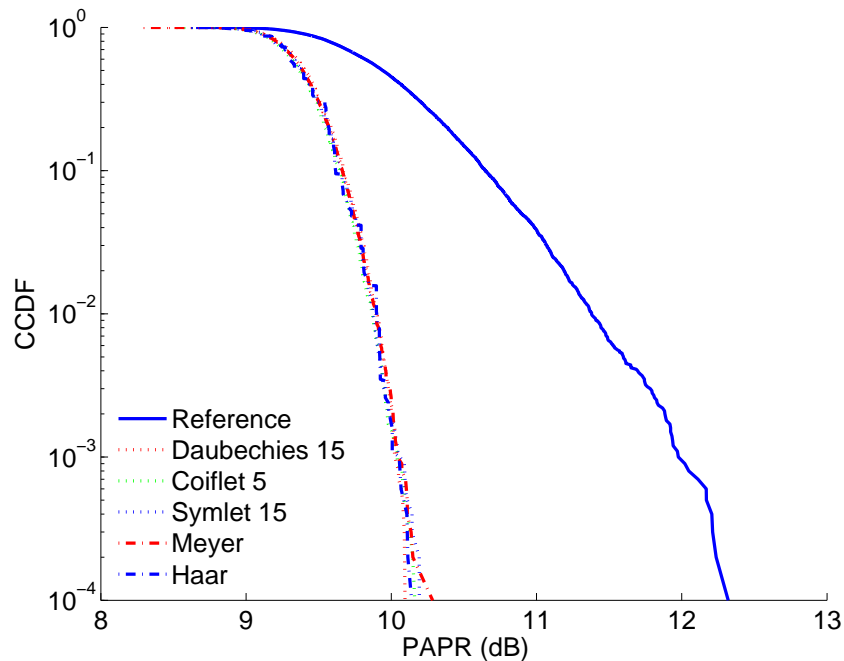


Figure 5-7: CCDF of the PAPR for several wavelet families of the multiplicative scrambler.

Impact of filter lengths

Figure 5-8 and Figure 5-9 show the PAPR performance curves for various filter lengths when Daubechies family is employed in the WPM system. When the filter length is increased, PAPR reduction gains decrease. All wavelets perform the same with Daubechies 2 being the best of the lot.

Impact levels of decomposition of filter bank structure

Figure 5-10 and Figure 5-11 show the PAPR performance curves for various decomposition levels, N employed in the filter bank structure of the WPM system. Both of the scrambling based PAPR reduction techniques perform better when a small number of levels are employed in the filter bank. Increasing the levels of the filter banks causes an increase in the overlaps of the input symbols. Consequently, the elevations in the M -dimensional PAPR surface become less, which will decrease the performance of any PAPR reduction technique. In these results, the considered wavelet is Daubechies 5 with a filter length of 10. If the filter bank of the WPM system is designed to have 2 levels, when additive or multiplicative scrambler based PAPR reduction is employed, the PAPR value becomes 7 dB for both compared to the reference value (i.e., when PAPR reduction is not applied) of 11.4 dB for a CCDF value of 10^{-2} . Here, the difference is around 4.4 dB. When the number of filter bank levels is increased, the gains decrease. For example, the PAPR reduction is around 1.4 dB if $N = 7$.

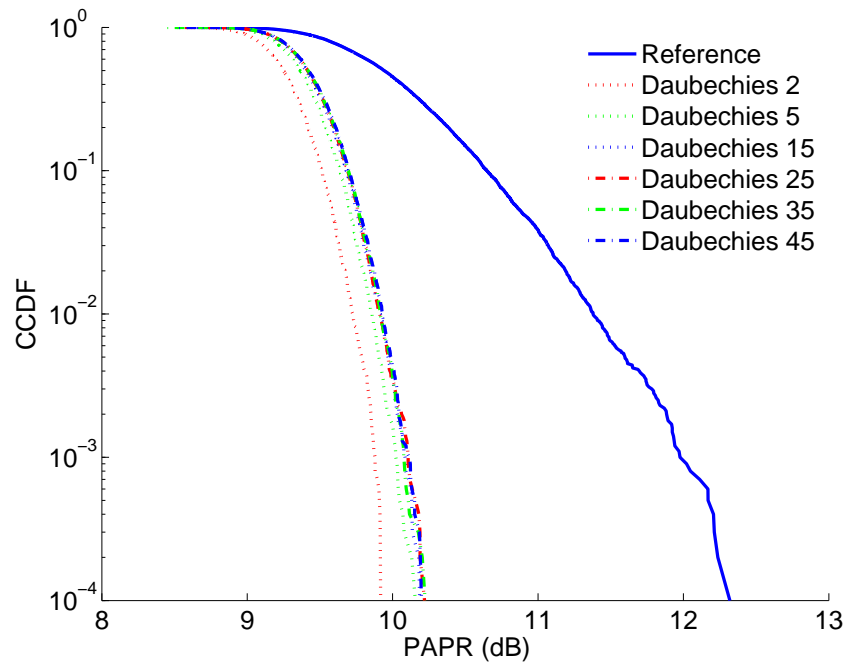


Figure 5-8: CCDF of the PAPR for the WPM system where additive scrambler is employed with different filter lengths of the Daubechies wavelet family.

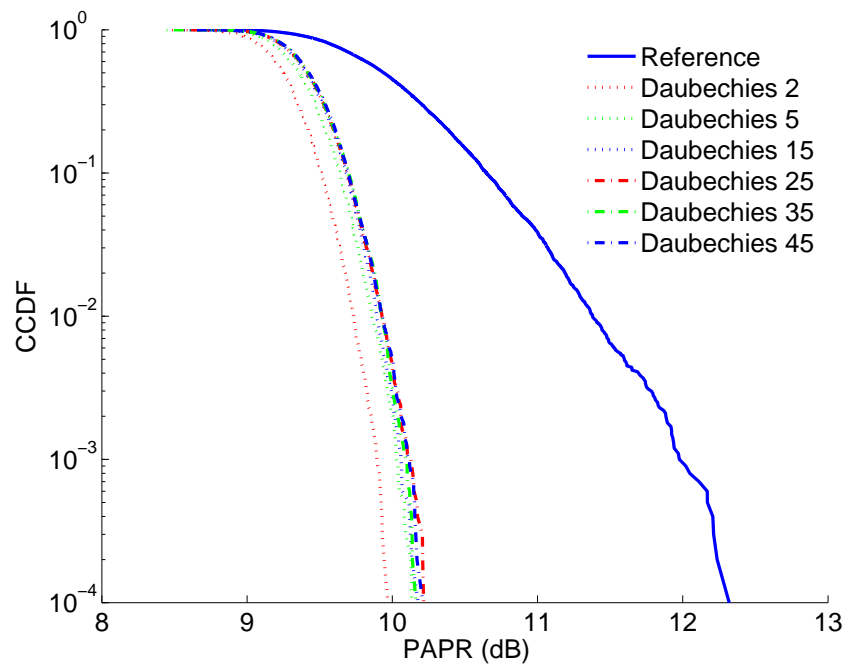


Figure 5-9: CCDF of the PAPR for the WPM system where multiplicative scrambler is employed with different filter lengths of the Daubechies wavelet family.

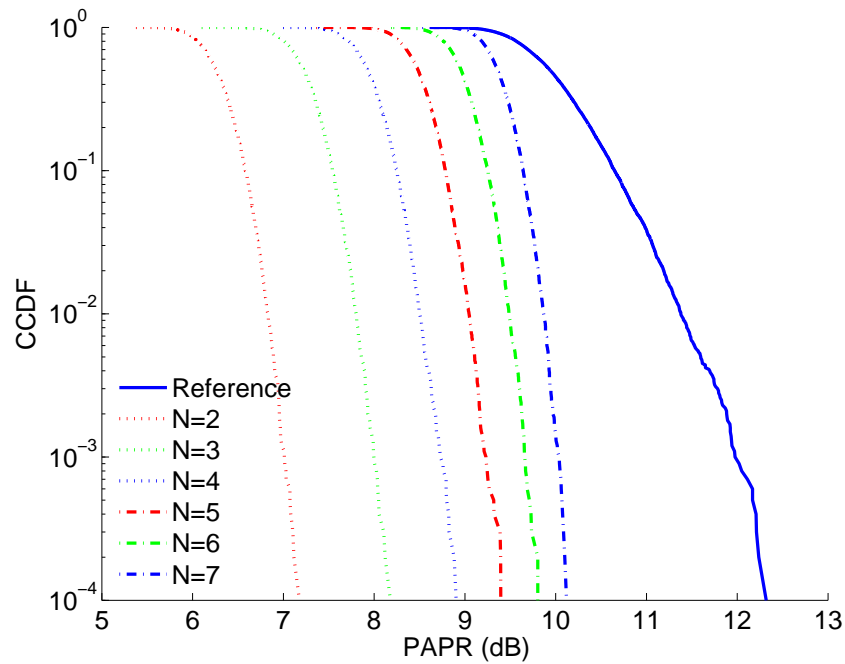


Figure 5-10: CCDF of the PAPR of the WPM signal for different levels of decomposition, N , where additive scrambler is employed. The wavelet considered is Daubechies 5 (length 10). A reference curve with no PAPR reduction is also plotted.

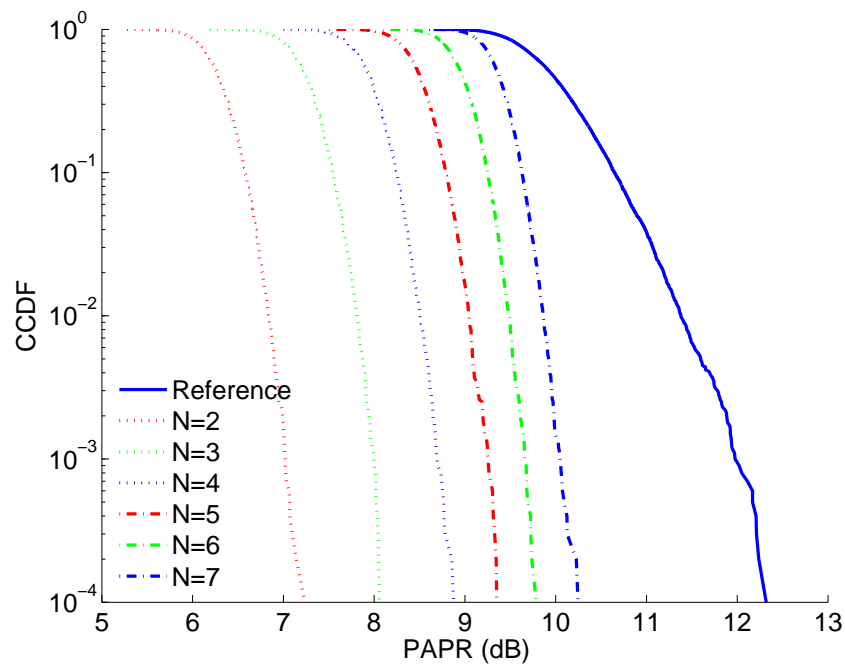


Figure 5-11: CCDF of the PAPR of the WPM signal for different levels of decomposition, N , where multiplicative scrambler is employed. The wavelet considered is Daubechies 5 (length 10). A reference curve with no PAPR reduction is also plotted.

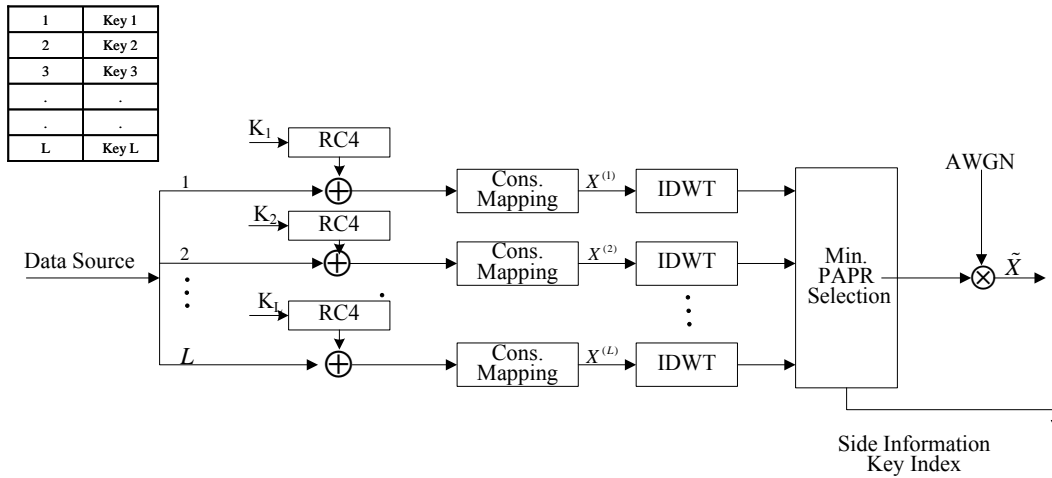


Figure 5-12: WPM Transmitter architecture employing secure PAPR reduction technique with RC4.

5-2 Secure PAPR Reduction with RC4

Scramblers or combinations of LFSRs are also employed in stream ciphers. Stream ciphers (explained in Section 5-2-1) are already being used in wireless communications systems since the broadcast nature of wireless communications makes it prone to eavesdropping. Instead of using scrambler or additional hardware both at the transmitter and receiver, already existing stream cipher implementations can be employed. For example, in WiFi network connections when Wired Equivalent Privacy (WEP) is used, RC4 is the selected stream cipher. As done in scrambling based PAPR reduction techniques, when stream ciphers are employed, various encrypted versions of the same original message can be created using different keys. After this process, the ciphertext that produces the least PAPR is selected as the to-be-transmitted sequence. We call this technique as secure PAPR reduction and it has the same basic idea behind selected mapping based techniques. In this section, we present this novel secure PAPR reduction technique. To the best of our knowledge, this technique has never been employed in OFDM or WPM systems.

5-2-1 System Model

Stream ciphers also produce a pseudo random sequence like additive scramblers. Then, the produced pseudo random sequence is xor'ed with the actual signal to generate the cipher-text. The novelty in this work is to employ L different secret keys and to generate the cipher-texts out of which the one with the minimum PAPR value is to be transmitted. The generated side information is the index of the key of the selected cipher-text. Assuming that transmitter and receiver architectures are sharing the key information. This scheme is illustrated in Figure 5-12. Any kind of stream cipher can be employed in this architecture.

Stream Ciphers

A stream cipher is a symmetric key cipher where plaintext symbols are combined with a pseudorandom cipher symbol stream (keystream), typically by an exclusive-or (xor) operation. In a stream cipher the plaintext symbols are encrypted one at a time, and the transformation of successive symbols varies during the encryption. Stream ciphers represent a different approach to symmetric encryption from block ciphers. Stream ciphers run faster than block ciphers and have lower hardware complexity. However, one of the security problems of the stream ciphers is that the same starting state (seed of the LFSRs) must never be used twice.

Stream ciphers may approximate the action of a proven unbreakable cipher, the One-time Pad (OTP), sometimes known as the Vernam cipher or additive scrambler [54]. An OTP employs a random keystream. The keystream is combined with the message one at a time to form the ciphertext. OTP or Vernam cipher is proven to be unbreakable by Claude Shannon in 1949 in [54]. The random keystream has to be at least the same length as the plaintext, and generated completely at random. Therefore, in practice, it is rather difficult to implement OTP. Instead of OTP, a stream cipher uses a smaller key (e.g., 128 bits). Using this key, an algorithm (e.g., RC4) generates pseudorandom keystream which is then combined with the plaintext. Since the keystream is pseudorandom, stream ciphers are not as secure as the OTP.

A Synchronous Stream Cipher

In a synchronous stream cipher a stream of pseudo-random symbols is generated independently of the plaintext and ciphertext messages, and then combined with the plaintext (to encrypt) or the ciphertext (to decrypt). Mostly, symbols are binary digits, and the keystream is combined with the plaintext using the exclusive-or operation (xor). This is called as binary additive stream cipher. The sender and receiver must be able to create the same keystream synchronously for a successful decryption. If digits are added or removed from the message during transmission, synchronization is lost. To restore synchronization, various offsets can be attempted to obtain the correct decryption. If a symbol error occurs, only a single symbol in the plaintext is affected and the error does not propagate to other parts of the message. This property is useful when the symbol error rate is high. Because of this property, synchronous stream ciphers are very susceptible to active attacks if an attacker can change a digit in the ciphertext, he might be able to make predictable changes to the corresponding plaintext bit. For instance, a bit change in the ciphertext causes the corresponding bit to be altered in the plaintext. Binary stream ciphers are often constructed using linear feedback shift registers LFSRs because they can be easily implemented in hardware and can be readily analyzed mathematically.

5-2-2 Numerical Results of Secure Scrambling-Based PAPR Reduction Technique

In this section, we present the CCDF performances of the secure PAPR reduction technique that we propose in this thesis. The impact of the number of replicated considered in the selected mapping, wavelet families, filter lengths and the number of levels of the WPM system are considered as the influential factors. The WPM system is realized using a filter bank structure with 7 levels of decomposition. The modulation scheme used is QPSK and the value of L is taken to be 8. The wavelet of choice is Daubechies 5 (denoted db5) which is of length 10. These are the constant values of the simulation parameters used to produce the results throughout this section unless otherwise states. To properly evaluate the improvements due to the PAPR reduction technique, a reference PAPR-CCDF curve obtained for db5 wavelet for the case without PAPR reduction is also provided.

Impact of choice of number of replications

In Figure 5-13, we present the impact of the number of replicas on the PAPR reduction when selected mapping over encrypted messages is employed. Similar to what we have seen in scrambling based techniques, as more and more replicas are used for selected mapping (i.e., L increases), the secure PAPR reduction technique reduces to brute-force search and PAPR reduction performance increases because the probability of finding a replica with the least PAPR increases. When larger number of replicas, L are employed in the WPM system, the PAPR reduction performs better; however, this comes with additional cost of processing power or additional scrambling hardware. When $L = 1$ which means that only one scrambled replica of the original signal is considered, the PAPR reduction does not provide any significant gains. For example, for a CCDF value of 10^{-4} , when $L = 32$, the resultant PAPR is around 9.8 dB where the reference PAPR (i.e., when no PAPR reduction technique is employed) is around 12.4 dB. The gains by increasing the number of replicas decreases when $L > 16$.

Impact of choice of wavelet families

The PAPR reduction gains when different wavelet families or different filter lengths are employed in the WPM system are shown in Figure 5-14. In these set of experiments the value of L is taken to be 8. The various wavelet families considered are Daubechies 15, Coiflet 5, Symlet 15 (all of length 30) and Meyer (of length 102) and Haar. As can be seen in Figure 5-14, changing the wavelet families do not impact the PAPR reduction performance significantly and all families yield similar PAPR reduction performances. Which also applies to multiplicative and additive scrambling.

Impact of filter lengths

Figure 5-15 presents the PAPR performance curves for various filter lengths when Daubechies family is employed in the WPM system. When the filter length is increased,

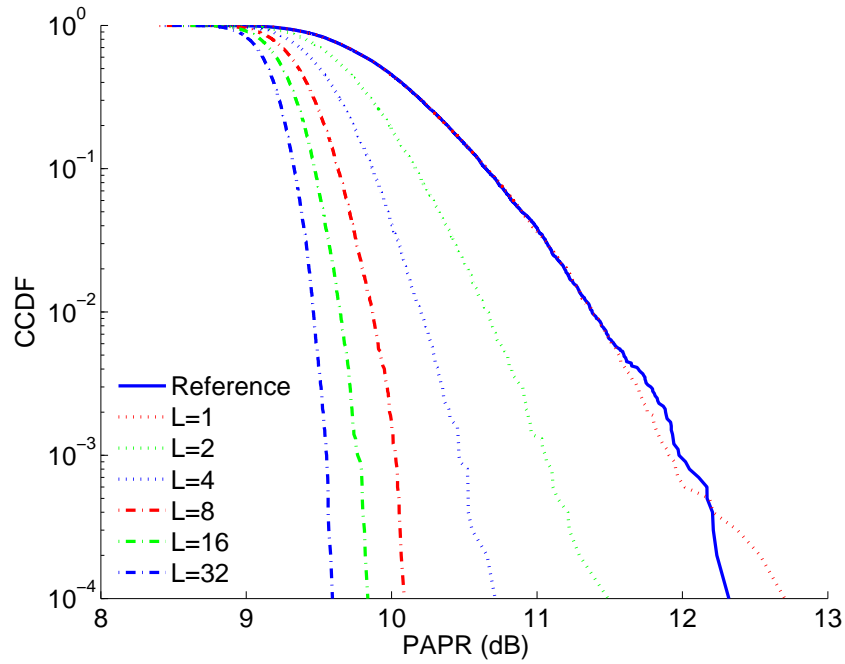


Figure 5-13: CCDF of the PAPR for several number of replicas, L where secure PAPR reduction technique is employed.

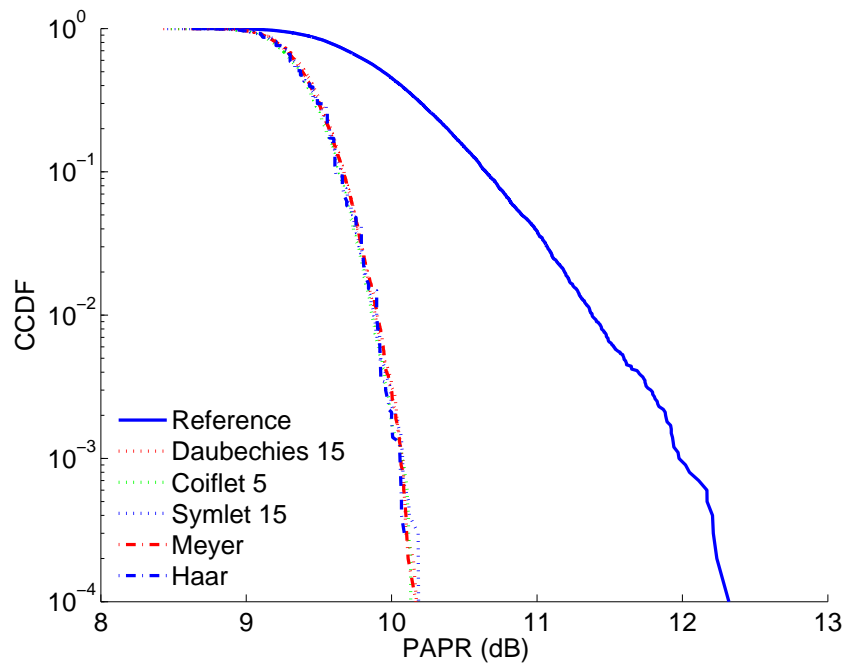


Figure 5-14: CCDF of the PAPR for various wavelet families where secure PAPR reduction technique is employed.

PAPR reduction gains decreases. Daubechies 2 outperforms the other filter lengths of the same family. The reason behind this phenomenon is the overlap of input symbols

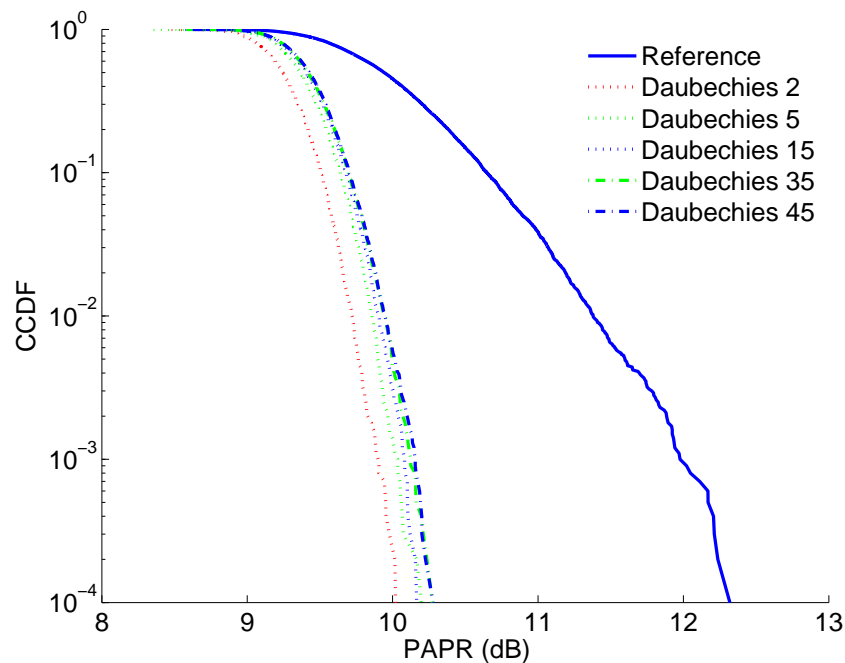


Figure 5-15: CCDF of the PAPR for the WPM system where secure PAPR reduction technique is employed with different filter lengths of the Daubechies wavelet family.

in time when WPM is employed. As the filter length increases, the overlap of symbols in time grows because multiple coefficients are multiplied with the symbols and added onto each other in the frequency domain. In other words, in time domain, multiple symbols proportional to the filter length convolve with each other.

Impact of levels of decomposition of WPM

The same phenomenon, which we observed when we change the filter lengths of the WPM system, is also observed when WPM is designed to have different number of levels as can be seen in Figure 5-16. Increasing, the number of levels, increases the number of subcarriers which yields worse peak powers because of larger number of convolved signals in time domain. Therefore, any PAPR reduction technique provides smaller PAPR reduction gains when the WPM system is designed with larger number of levels. For example, when the WPM system has 2 levels which yields 4 subcarriers; the reduced PAPR is around 7.2 dB for a CCDF value of 10^{-4} . When the same WPM system is designed to have 6 levels which yields 2^6 subcarriers, the reduced PAPR becomes 9.8 dB. For the same CCDF performance, the reference PAPR value (i.e., no PAPR reduction technique is used) is around 12.4 dB.

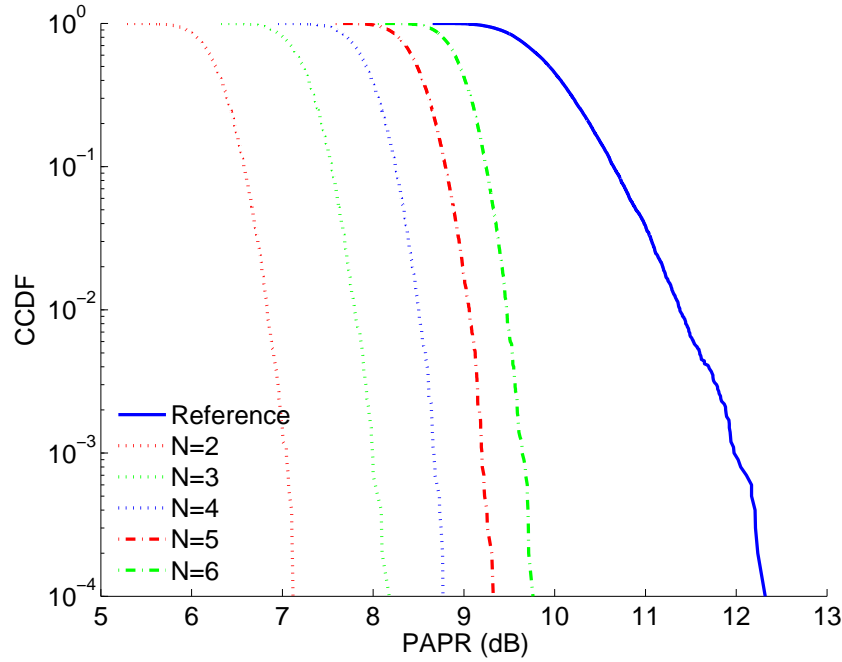


Figure 5-16: CCDF of the PAPR of the WPM signal for different levels of decomposition, N , where RC4 is employed. The wavelet considered is Daubechies 5 (length 10). A reference curve with no PAPR reduction is also plotted.

5-3 Comparison of the Selected Mapping with Scrambling Techniques

In this section, we compare all the techniques proposed in this chapter along with the selected mapping with phase modification which is introduced in Chapter 4. As can be seen in Figure 5-18, the PAPR reduction performances of all variants of the selected mapping with scrambling technique performs almost the same. For a CCDF value of 10^{-3} , the original PAPR value is around 11.6 dB. The selected mapping with scrambling reduces the PAPR around 1.6 dB. In terms of the BER performances, as can be seen in Figure 5-17, all the techniques have the same BER performance except the multiplicative scrambling based technique. Although multiplicative scramblers eliminate the side information requirement, they are prone to larger bit error rates (BER) as can be seen in Figure 5-17. In the multiplicative scrambler, the input impacts the LFSR states. Depending on the length of the LFSR and the tap positions, one error in the message is distributed into several other positions where the distribution ratio is proportional to the number of tap positions. Therefore, an error in the signal results in multiple errors in the received signal. As can be seen Figure 5-17, the BER is high when multiplicative scrambler is employed. In Figure 5-18, we also present the selected mapping technique employing phase shifting which was introduced in Section 4. Since all these techniques rely on creating replicas of the original signal and selecting the one producing the least PAPR, their performances are similar. These techniques can roughly be described as greedy search in the phase space where the number of replicas

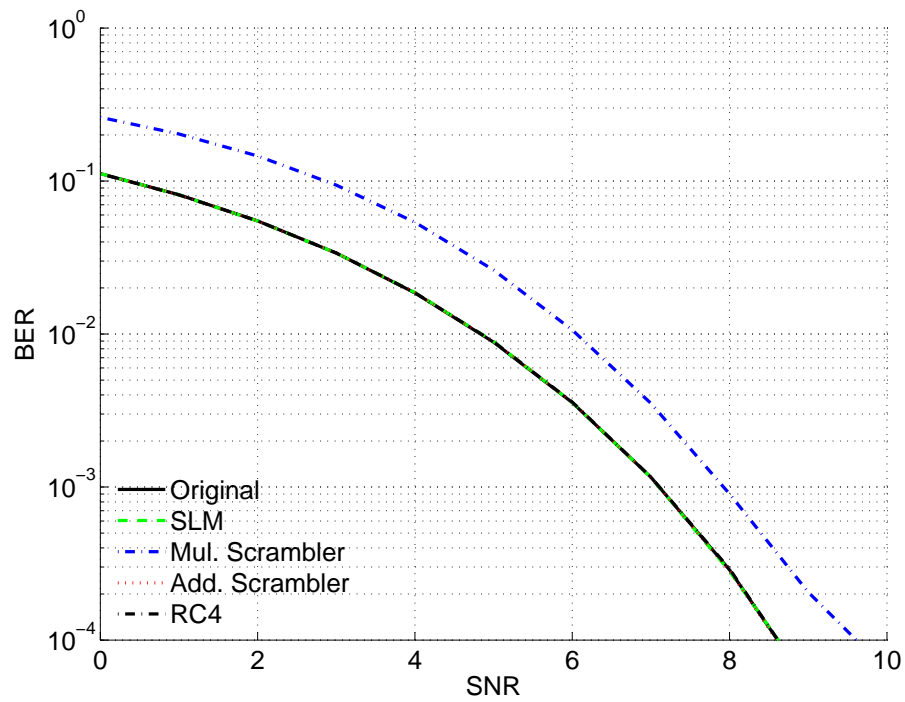


Figure 5-17: BER performance of the selected mapping with scrambling techniques.

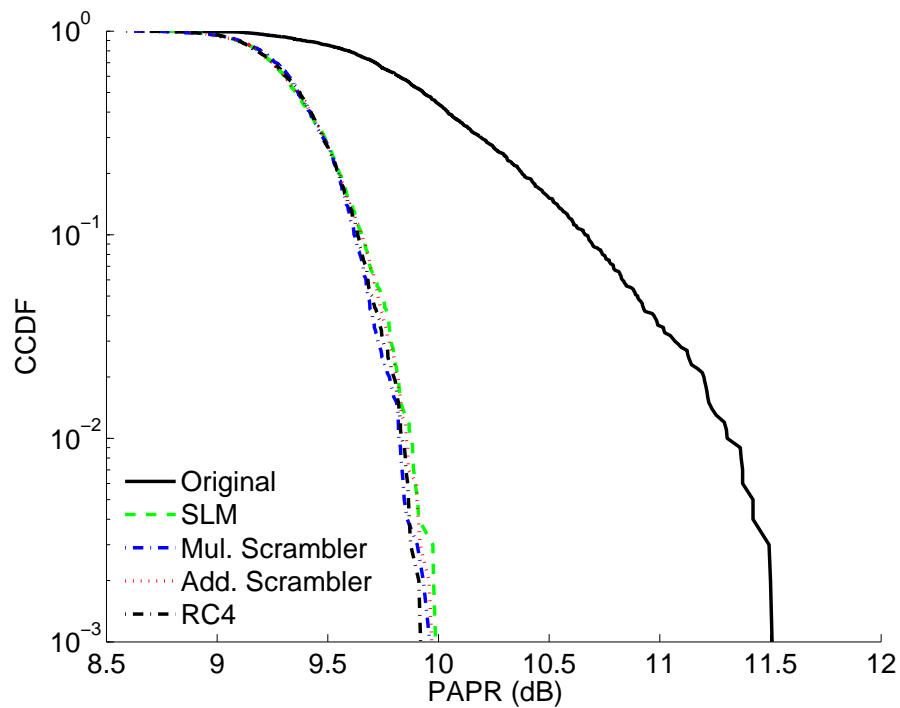


Figure 5-18: Comparison of the PAPR reduction performance of the selected mapping with scrambling techniques.

can be regarded as the number of random search points in the phase space. A smarter approach can be developed to optimize this greedy search algorithm using neural networks or some local search techniques. In the next chapter, we introduce such a local search based technique which outperforms all these techniques presented in Figure 5-18.

5-4 Summary

In this chapter, we presented the selected mapping with scrambling techniques used to reduce the PAPR. In the selected mapping with scrambling based techniques, replicas of the original input signal is created by scrambling the original message with different scrambling techniques. The message is scrambled with LFSR initialized with different states if additive scrambler is used. For the multiplicative scrambler case, the message is scrambled by inserting a prefix in front of the message which lets the scrambler to produce a scrambled output because of the different prefixes inserted at the beginning of the input signal. When secure PAPR reduction technique is used, multiple encrypted replicas of the original message with different keys are used in the selected mapping. Among these generated scrambled signals containing the original signal, the one producing the least PAPR is selected after modulation and transmitted. When additive scrambler or secure PAPR is employed, additional side information, namely, the initialization state (seed) or the index of the ciphering key is to be transmitted to the receivers, respectively. When multiplicative scrambler is used, no side information is required. However, a prefix has to be inserted in front of the signal to change the output of the scrambler such that various scrambled copies of the same original signal can be generated. Since original signal is used to alter the state of the multiplicative scrambler, the output signal consists of the diffused original signal which implies that a symbol error will also be diffused to the other symbol positions. In selected mapping with multiplicative scrambling, a single bit error at the descrambler's input will result into w errors at its output, where w equals the number of the scrambler's feedback taps.

As a novelty of this chapter, we propose to employ an encryption system which is similar to additive scrambling technique to reduce the PAPR. Employing this proposed encryption based system, enhances the security of the system as well as performs same as additive scrambler without any additional cost compared to the scrambling techniques. Since all telecommunications systems employ some kind of stream ciphers to secure the signals transmitted over an insecure channel, using the same block for PAPR reduction does not introduce additional implementation or permutational costs. To the best of our knowledge, this technique has not been employed in OFDM or WPM systems.

Optimization of Selected Mapping with Phase Modification

In Chapter 4 [55] we proposed a simple and elegant method which reduces the PAPR by creating replicas of the original message whose phases are randomly shifted. In Chapter 5, we presented how to employ selected mapping technique with scrambling. We enhanced the selected mapping with scrambling technique by proposing the secure Peak-to-Average Power Ratio (PAPR) reduction technique in Chapter 5. In this chapter, we extend the selected mapping technique by proposing a novel optimization scheme using the phase shifts of the selected mapping technique.

In the selected mapping technique, several phase shifts are determined randomly and the one producing the frame with the least PAPR value is denoted as the selected phase-shift. Instead of random trials, the optimum set of phase-shifts, that guarantee minimization of PAPR can be determined by a local search around the selected phase-shift in the M -dimensional space. Local search is a meta-heuristic that can be employed on problems where a solution is to be determined that maximizes (or minimizes) a criterion among a number of candidate solutions [56]. Such local search techniques move in the search space until a solution considered optimal is produced within a bounded period. It is not guaranteed to find the global optimal using this technique. However, a local minima can be guaranteed.

The contents of the chapter, are organized as follows. After introducing the optimization of selected mapping with phase modification, in the next section, we present the PAPR reduction as an optimization problem. We present two methods to solve this optimization problem one of which is not applicable in Wavelet Packet Modulation (WPM) systems. Section 6-2 elucidates the technical details of the optimization of the selected mapping with phase modifications. Then, the results of the simulation studies are discussed in Section 6-3. In Section 6-4, we analyze the convergence and time complexity of the algorithm. Finally, the chapter is concluded in Section 6-5 by drawing on the inferences of the study.

6-1 PAPR Reduction as an Optimization Problem

In Chapter 4, we showed that by creating replicas of the original message whose phases are randomly shifted, we can employ the selected mapping technique to reduce the PAPR of WPM signals. In this chapter, we present how to optimize the PAPR reduction process by selecting the phases in a way that they almost always yield the lowest PAPR.

The PAPR (as in 3-3) is used as the objective $J(\phi)$ of the optimization problem; therefore;

$$J(\phi) = \frac{\max_n(|y[n]|^2)}{\mathbf{E}(|y[n]|^2)}, \quad (6-1)$$

where $y[n]$ depends on the selected phase-shifted signal, X , which are the symbols on each sub-carrier. The optimization problem which we are trying to solve is to minimize the PAPR. Formally, the optimization problem can be stated as

$$\min_{\phi_i} J(\phi) = \frac{\max_n(|y[n]|^2)}{\mathbf{E}(|y[n]|^2)} \quad (6-2)$$

subject to

$$0 \leq \phi_i \leq 2\pi,$$

where $i = 1, 2, \dots, M$, assuming there are M subcarriers. Here,

$$y[n] = IDWPT(X_i e^{j\phi_i})$$

where X_i are the complex symbols after constellation mapping on the i^{th} subcarrier and $j = \sqrt{-1}$. The phase sequences, ϕ_i are determined by this optimization problem. The phase-shifted information bearing streams are then transformed by an Inverse Discrete Wavelet Packet Transform (IDWPT) operation and the objective value which is the PAPR of the transformed composite signal can be calculated.

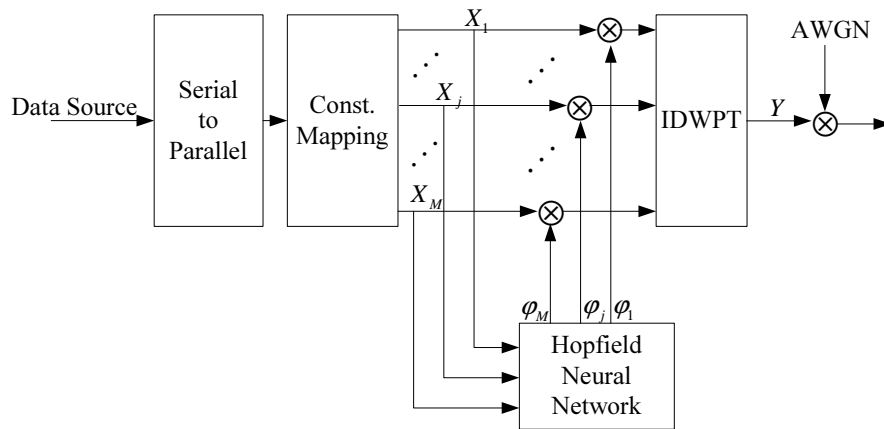


Figure 6-1: Block diagram of the PAPR reduction method using neural network optimizer.

6-1-1 Hopfield neural network (HNN)

In this section, we introduce a method that is already employed in Orthogonal Frequency Division Multiplexing (OFDM) systems to reduce the PAPR using neural networks [57]. In [57], PAPR reduction problem is presented as a combinatorial optimization problem and a solution using the HNN is provided. A Hopfield neural network is a form of recurrent artificial neural network invented by John Hopfield [58]. The proposed solution has a simple structure and is suitable for real-time optimization. The Field-programmable gate array (FPGA) implementation of this solution is presented in [59].

In [57], Yamashita et al. define the objective value of the optimization problem as the sum of the differences between the power of each symbol and the average power of the frame. As has been done in the selected mapping with phase modification, they modify the input symbols with a phase shift. Then, the HNN determines the optimal phase sequence that make the value of the objective function zero. They discuss that when the optimal phase sequence is determined, the objective value becomes zero and this yields the least PAPR.

In this formulation, each OFDM symbol, X_m is multiplied by ϕ_m before the Inverse Discrete Fourier Transform (IDFT) operation. The objective function is defined as in [57]

$$J(\phi) = \sum_{n=0}^{N-1} \left(|\tilde{Y}_n|^2 - \frac{\|\tilde{\mathbf{Y}}_n\|^2}{N} \right)^2 \quad (6-3)$$

where

$$\tilde{Y}_n = \frac{1}{N} \sum_{m=0}^{N-1} e^{j(\phi_m)} X_m e^{j(2\pi/N)nm} \quad (6-4)$$

Here, there are N symbols in an OFDM frame. Assuming that ϕ_m can take values 1 or -1, the objective function (6-3) can be expressed as a polynomial. HNN is not guaranteed to produce the optimal solutions when the objective function has square terms of ϕ_m . For HNN to be able to converge to the optimal phase sequence, ϕ_m^2 must be removed from the objective function. When $\phi_m = \pm 1$, then its square reduces to one and is removed from the objective function.

For details of HNN, readers can refer to [58, 60–62]. The HNN implementation required state motion functions which update the states of the neural network at each iteration of the learning process. For PAPR reduction, the HNN state motion equation of the l^{th} neuron is defined as

$$\frac{\partial J(\phi)}{\partial \phi_l}.$$

As long as the objective function is differentiable with respect to the phase sequence and $\phi \in \{-1, +1\}$ then the solution can be implemented as a HNN. The block diagram of the proposed method is sketched in Figure 6-1. At first sight, it seems to be implementable in WPM systems; however, it is not analytically tractable to take the partial derivative

$$\frac{\partial J(\phi)}{\partial \phi_l}, \quad (6-5)$$

for WPM systems where $J(\phi)$ is defined as in (6-2). Therefore, we revert to the local search based optimization technique which is a good alternative to solving combinatorial problems instead of the HNN when the derivative of the objective function cannot be analytically stated. Specifically, we use the hill climbing algorithm to optimize the PAPR reduction. In the next section, we introduce the details of the hill climbing algorithm and then show how we use it to reduce the PAPR in the subsequent section.

6-1-2 Hill Climbing

Hill climbing is a mathematical optimization technique which belongs to the family of local search. Hill climbing solves combinatorial problems that have many solutions, some of which are better than others. A local search algorithm such as hill climbing starts from a candidate solution. Afterwards, neighboring solutions are checked iteratively. This approach is only feasible if a neighborhood relation can be defined on the search space. When the algorithm cannot see any improvement anymore, it terminates. Ideally, at that point the current solution is close to optimal, but it is not guaranteed that hill climbing will ever come close to the optimal solution.

Assume that the optimization problem is stated as a minimization problem and the solution space is discrete. When the solution space of the combinatorial problem is discrete, the solution space is represented as a graph. The vertices of the graph denoted different states. Hill climbing traverses the vertices always locally decreasing the value of the objective function of the problem. When the solution space is continuous, gradient descent if the function is minimized and gradient ascend if the function is maximized.

Although there are many variants of the hill climbing algorithm, in its simplest case, all possible neighbor solutions are considered. For the discrete optimization problems, the closest vertices to the current state in the solution space (graph) is chosen. In the continuous case, a step size is determined and the incremented states by the step size are considered. The one among the tried incremented states which minimizes the objective function larger is chosen as the current state. The algorithm continues iteratively by changing the state by incrementing it with the step size.

A simple pseudocode of the simple hill climbing is presented in Algorithm 6.1. In this pseudocode, FITNESS function calculates the objective value when a specific solution is selected. MINFITNESS variable keeps track of the achieved least value of the objective function up to that iteration of the pseudocode. Here, the solution points which are in the neighbor set of the current solution is tried and the one producing the least objective value is deemed as the current solution. When, there is no improvement, the pseudocode terminates.

Hill climbing methods, similar to all other local search algorithms, facilitates iterative improvements. This technique is applied to a single point in the search space. At each iteration, a new point is selected from the neighbor set. The variants of the hill climbing method differs in this selection process. Some chose the new point randomly, some tries all the points and selects the one which minimizes the objective value larger. In any case, if the newly selected point produces a solution which is better than the

Algorithm 6.1 Simple Hill Climbing Pseudocode

```

1: solution := randomSolution()
2: MINFITNESS := FITNESS(solution)
3: found := True
4: while found do
5:   found := False
6:   neighbours := Neighbours(solution)
7:   for s IN neighbours do
8:     if FITNESS(s) < MINFITNESS then
9:       MINFITNESS := FITNESS(s)
10:      solution := s
11:      found := True
12:      BREAK
13:   end if
14: end for
15: end while
16: RETURN point

```

previous one, it is selected as the new solution. If there is no improvement, another neighbor solution is tried. The algorithm runs as long as there is improvement. It stops if there is no improvement, or the time of the algorithm is bounded; i.e., if the maximum number of iterations has been exceeded.

Clearly, hill climbing algorithm can only provide locally optimal solutions. The local optimal solution depends on the selection of the initial solution. Usually, the initial solution is selected randomly. The error with respect to the global optimal is not known and cannot be bound. To resolve the problem of converging to a local optimal, several different starting solutions can be tried; however, this comes along with additional cost of complexity. Hill climbing algorithms suffer from several problems [63]:

- The produced solutions are usually locally optimal.
- If we define the error of solution as the deviation from the global optimal, there is no way to determine the error for hill climbing algorithms since the global optimum cannot be determined.
- The performance of the solution depends totally on the initially selected solution.
- The upper bound of the computational time cannot be determined.

Further details of the hill climbing algorithm can be found in [56, 63, 64].

In the next section, we present how we use the hill climbing search algorithm to reduce the PAPR. We optimize the technique presented in Chapter 4. The hill climbing based optimization technique is applied in the problems of the OFDM system due to the disproportionate peak compared to the average. For example, in [65], Kohandani and Khandani propose a modified constellation shaping technique to reduce the PAPR. In

each sub-space, one bit as a dummy bit that does not carry data which gives the flexibility to select dummy bits which reduce the PAPR. They employ hill climbing, exhaustive search and simulated annealing techniques to reduce the PAPR by selecting the dummy bits adequately during constellation mapping. Compared to this technique, we employ the hill climbing based optimization technique that uses phase-shifts after constellation mapping.

6-2 Hill Climbing Based PAPR Reduction for WPM Systems

Assuming that there are M subcarriers in a WPM system as shown in Figure 6-2, for PAPR minimization, the search space is the M -dimensional phase vector where phases can be in between 0 and 2π . The initial candidate solution is determined randomly. More specifically, a vector, ϕ of randomly selected phases is generated where $0 \leq \phi_i \leq 2\pi$, $i = 1, 2, \dots, M$ and M is the number of WPM carriers. Frame elements are multiplied carrier-wise with the M -length phase sequence as in (4-1). The IDWPT transform for the obtained frame sequence is produced and the PAPR per frame of the signal is calculated.

The hill climbing method starts with a random M -dimensional phase vector, ϕ and calculates the objective value which is defined as the PAPR value of the modulated frame. Iteratively, the phase is modified (by adding or subtracting a step size) to new value that produces a lower PAPR value. When this method cannot improve the PAPR anymore, the algorithm terminates. In the ideal case, the PAPR value is close to its optimal value at that point. However, there is no guarantee that this method may produce a global minima. The details of this idea is elaborated in Algorithm 6.2.

We employ the hill climbing technique which is presented in Algorithm 6.2. Initially, an equal step size s_i , $i = 1, 2, \dots, M$ is defined. Step size, s_i determines how much the i^{th} dimension of the phase vector is to be updated. At each epoch, t (iteration, step) of the algorithm, one of the phases, say ϕ_i , is updated by $\phi_i^{(t+1)} = \phi_i^{(t)} + s_i$. The new phase shift $\phi^{(t+1)}$ is applied to the frame, the IDWPT transform for the obtained frame sequence is produced and the PAPR per frame of the signal is calculated as in (3-3). Notice, that this procedure calculates the partial derivative presented in (6-5) if the difference value of the PAPR is divided by the step size; because, while updating any dimension $\phi_i^{(t)}$, we keep the other phases constant. If the objective function value, $J(\phi^{(t+1)})$ decreases, i.e., $J(\phi^{(t+1)}) < J(\phi^{(t)})$, then $\phi_i^{(t+1)}$ becomes $\phi_i^{(t+1)} = \phi_i^{(t)} + s_i$. If the objective function value increases, $J(\phi^{(t+1)}) > J(\phi^{(t)})$, it becomes $\phi_i^{(t+1)} = \phi_i^{(t)} - s_i$. If there is no change in the objective function value, then s_i is set to zero.

$$\phi_i^{(t+1)} = \begin{cases} \phi_i^{(t)} + s_i & \text{if } J(\phi^{(t+1)}) < J(\phi^{(t)}) \\ \phi_i^{(t)} - s_i & \text{if } J(\phi^{(t+1)}) > J(\phi^{(t)}) \\ \phi_i^{(t)} & \text{if } J(\phi^{(t+1)}) = J(\phi^{(t)}). \end{cases} \quad (6-6)$$

With this scheme, at each epoch of the algorithm the PAPR is minimized. However, if the step size is kept constant throughout the epochs, there will be fluctuations when

Algorithm 6.2 Hill Climbing Based PAPR Reduction Algorithm

Require: \mathbf{X} { \mathbf{X} are the symbols on each sub-carrier}

- 1: $stepsize = 0.1$ {how much the phases can be updated at each epoch}
- 2: $maxepochs = 1000$ {maximum number of epochs (iterations)}
- 3: $\phi_i = rand(0, 2\pi)$ where $i = 1, \dots, M$ {initially selected phase vector for each subcarrier}
- 4: $s_i = stepsize$ where $i = 1, \dots, M$ {phase change for local search}
- 5: $d_i = 1$ where $i = 1, \dots, M$ {direction of optimization 1:decreased $J(p)$ 0:increased $J(p)$ }
- 6: Generate $\mathbf{Y} = IDWPT(\mathbf{X}e^{j\phi})$ {Modulate the new frame}
- 7: $J(\phi^{(1)}) = PAPR(\mathbf{Y})$ {Calculate the PAPR (objective value, $J(\phi)$ (6-1))}
- 8: **for** $t = 1$ to $maxepochs$ **do**
- 9: **for** $i = 1$ to M **do**
- 10: $q = \phi^{(t)}$
- 11: $q_i = q_i + s_i$
- 12: Generate $\mathbf{Y} = IDWPT(\mathbf{X}e^{jq})$
- 13: $J(\phi^{(t+1)}) = PAPR(\mathbf{Y})$
- 14: **if** $J(\phi^{(t+1)}) < J(\phi^{(t)})$ **then**
- 15: $\phi_i^{(t+1)} = \phi_i^{(t)} + s_i$
- 16: $d^{t+1} = 1$
- 17: **else**
- 18: **if** $J(\phi^{(t+1)}) > J(\phi^{(t)})$ **then**
- 19: $\phi_i^{(t+1)} = \phi_i^{(t)} - s_i$
- 20: $d^{t+1} = -1$
- 21: **else**
- 22: $s_i = 0$
- 23: $d^{t+1} = 0$
- 24: **end if**
- 25: **end if**
- 26: **if** $d^t + d^{t+1} = 0$ **then**
- 27: $s_i = s_i/2$ {Fluctuations close to minima, decrease the step size}
- 28: **end if**
- 29: **end for**
- 30: $\phi_* = \phi^{(t+1)}$
- 31: Generate $\mathbf{Y} = IDWPT(\mathbf{X}e^{j\phi_*})$
- 32: $J(\phi_*) = PAPR(\mathbf{Y})$
- 33: **if** $\sum_{i=1}^M s_i = 0$ **then**
- 34: Break;
- 35: **end if**
- 36: **end for**

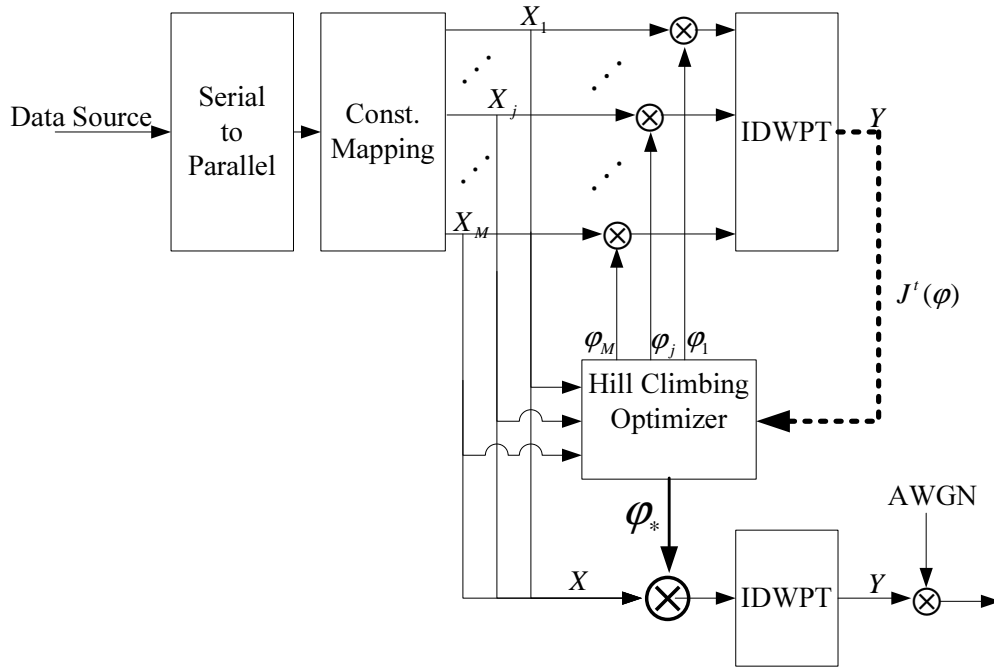


Figure 6-2: Block diagram of the hill climbing based PAPR reduction method.

the solution comes close to the global or one of the local minima. The change in the objective value indicates this situation. If the update of i^{th} phase of $\phi^{(t)}$, $\phi_i^{(t)}$ causes a decrease in $J(\phi^{(t+1)})$ at a epoch and an increase in $J(\phi^{(t+2)})$ at the subsequent epoch (or vice versa), this means that the solution is close to a minima. In other words,

$$J(\phi^{(t-1)}) < J(\phi^{(t)}) \text{ and } J(\phi^{(t)}) > J(\phi^{(t+1)}),$$

or,

$$J(\phi^{(t-1)}) > J(\phi^{(t)}) \text{ and } J(\phi^{(t)}) < J(\phi^{(t+1)}).$$

To converge to the minima, the step size has to be decreased. In Algorithm 6.2, we decrease the step size exponentially. Whenever there is change in the direction of the optimization (decreasing the increased $J(\phi^{(t)})$ value or vice versa) in two subsequent epochs, the step size of the corresponding dimension is halved. If the step size becomes less than a very small threshold, this implies that optimization in that dimension will not be possible anymore and the step size is set to zero. If $s_i = 0, \forall i$, then the optimization algorithm terminates. When the number of epochs is large; in Algorithm 6.2, the number of epochs has to be bounded. When the algorithm stops, the near-optimal phase vector ϕ_* that produces a frame with a smaller PAPR value compared to the original frame is found. Then, the frame elements can be multiplied carrier-wise with the M -length near-optimal phase sequence, ϕ_* as in (4-1). The IDWPT transform for the obtained frame sequence can be produced and sent over the channel.

The two-dimensional demonstration ($M = 2$), of this technique is presented in Figure 6-3 for five different wavelet families, where each axis ($p1$ and $p1$) indicates the selected phase modification for corresponding subcarrier and both axes are expressed

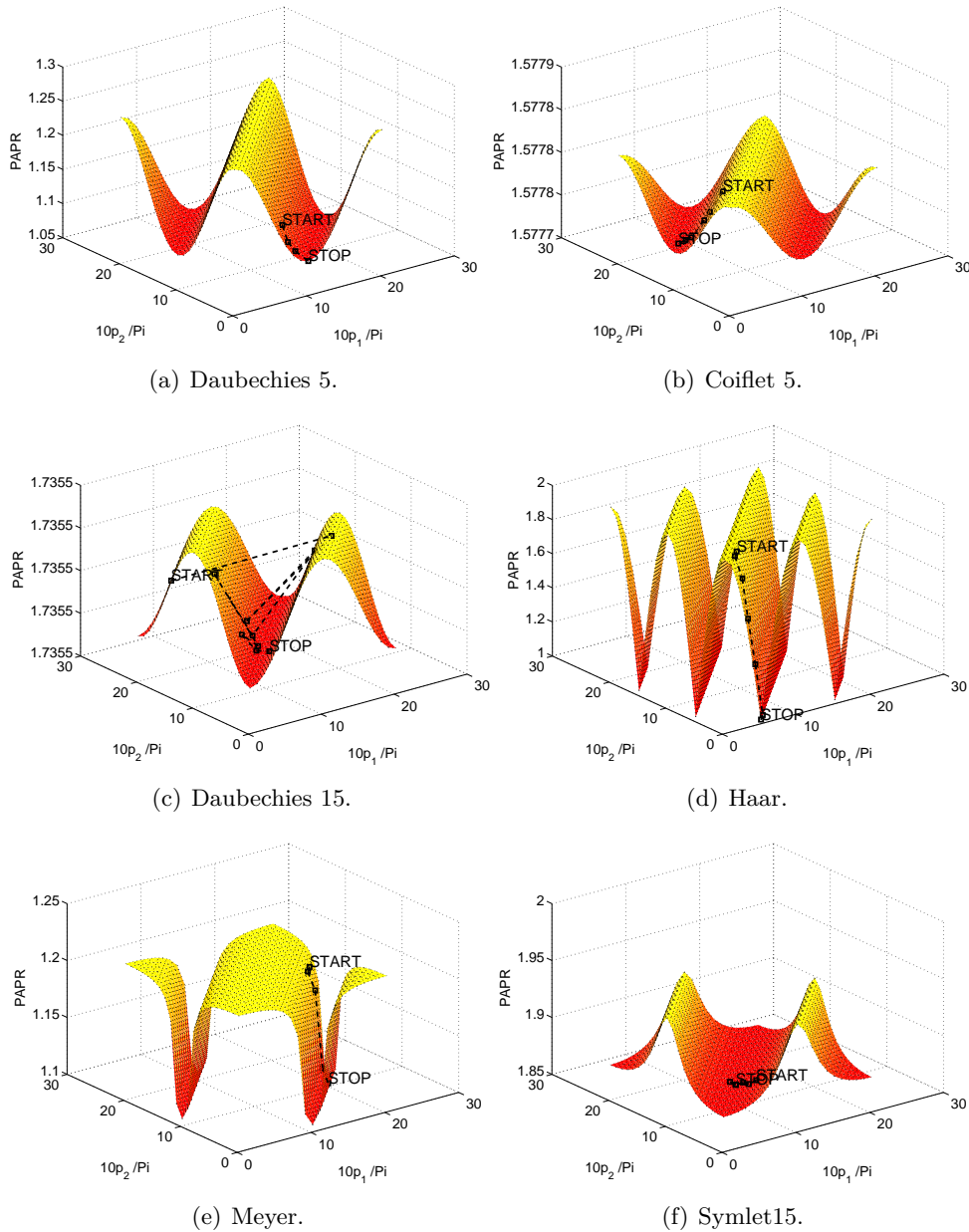


Figure 6-3: Demonstration of Algorithm 6.2 for various wavelet families.

in discrete values for the range 0 to 2π . This figure shows the PAPR surfaces for different wavelet families and demonstrates the steps of the Algorithm 6.2. The initially selected phase vector is marked with *start* in the figure. The updated phase values at each step of the Algorithm 6.2 are marked and the selected near-optimal phase vector is *shown* as *stop* in the figure.

As can be observed in Figure 6-3, the PAPR surface is almost a plane when Coiflet and Daubechies are employed where filter length is larger than 10. When Haar family is employed, there are steep falls in the PAPR surface. When Meyer family is considered,

Table 6-1: The parameter values used in the simulations

Parameter	Value
N	4
M	128
s_j	0.1
Maximum number of epochs	100

there are deep valleys (troughs) and a high plateau (peak). However, Symlets 15 operates exactly the opposite of Meyer. Furthermore, when Symlets are used, the overall PAPR values are larger compared to Meyer, Coiflets and Daubechies. The PAPR peaks of Haar are at the same level as those of Symlets. However, when Haar family is employed there are sharp falls in the PAPR surface which makes a trough at 1 dB as can be seen in Figure 6-3(d).

6-3 Numerical Results

In this section we present results of the computer simulations used to test the algorithm. The parameters used in the study are tabulated in Table 6-1. When we compare the hill climbing based selected mapping technique where phase-shifted copies of the original signal is sent over the channel with the other techniques, it can be concluded that the optimization technique performs better than the other techniques as can be seen in Figure 6-4. Although the PAPR of the frame is significantly reduced with this technique, the disadvantage is the large side information requirement. For each frame, M different phases that are employed to shift the original signal have to be conveyed to the receiver to decode the signal correctly.

Comparison With Other Techniques

In Figure 6-4, the proposed techniques in this thesis are compared to each other. Hill climbing based optimization outperforms in comparison to other techniques such as SLM or scrambling based techniques. When CCDF value is around 10^{-2} , the PAPR of the original frame is around 10 dB; whereas, optimized phase-shifted frame produces a PAPR value around 8.2 dB. All other techniques, which depend on randomization such as randomly phase-shifting or random scrambling, cannot reduce the PAPR below 8.7 dB where the WPM system is realized using a filter bank structure with 4 levels of decomposition and QPSK modulation scheme. The wavelet considered in Figure 6-4 is Daubechies 5 (length 10). For the SLM technique, the number of phase-shifted replicas of the original frame is $N = 4$.

The techniques that depend on some random frame modification allows the receiver to decode the message with a side information. Multiplicative scramble is an exceptional case where no side information is required. However, when there are bit errors in the frame, due to the implicit characteristics of the multiplicative scrambling, the bit

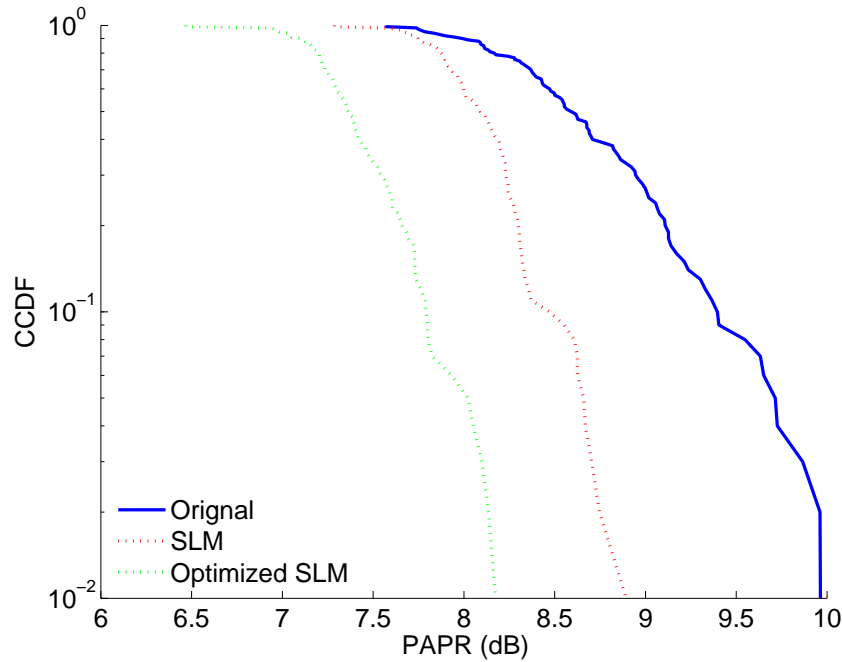


Figure 6-4: CCDF of the PAPR of WPM for several reduction techniques. The WPM system is realized using a filter bank structure with 4 levels of decomposition and QPSK modulation scheme. For SLM, the number of phase-shifted replicas of the original frame, $N = 4$. Reference (original) curves are the PAPR CCDFs where no PAPR reduction technique is employed.

errors are diffused into other bits. When additive scrambling or secure PAPR reduction techniques are employed, additional side information is required and the PAPR reduction performance compared to multiplicative scrambling is almost the same. The required side information is the selected phase values between zero and 2π for each of the M subcarriers. These three techniques manage to reduce the PAPR significantly; however, they are still not able to converge to a minima in the available PAPR space. Hill climbing based optimization technique that is presented in this section, is able to converge to a minima.

Impact of the Synthesis Wavelet Family

In Figure 6-5, the impact of the selected wavelet family on the performance of the PAPR reduction is presented. Daubechies 5 (of length 10), Coiflet 5, Symlet 15 (both of length 30), Meyer (of length 102) and Haar wavelet families are compared with each other. The PAPR of the frame can be significantly reduced with the hill climbing based technique almost independent of the family employed in the transceiver architecture. When CCDF value is around 10^{-2} , the PAPR is around 8.3 dB compared to 10 dB value of the reference implementation where no optimization technique is employed. Two dimensional ($M = 2$) demonstrations of the Algorithm 6.2 when different wavelet families are employed are shown in Figure 6-3.

In Figure 6-6, the impact of the Daubechies wavelet family with various filter lengths

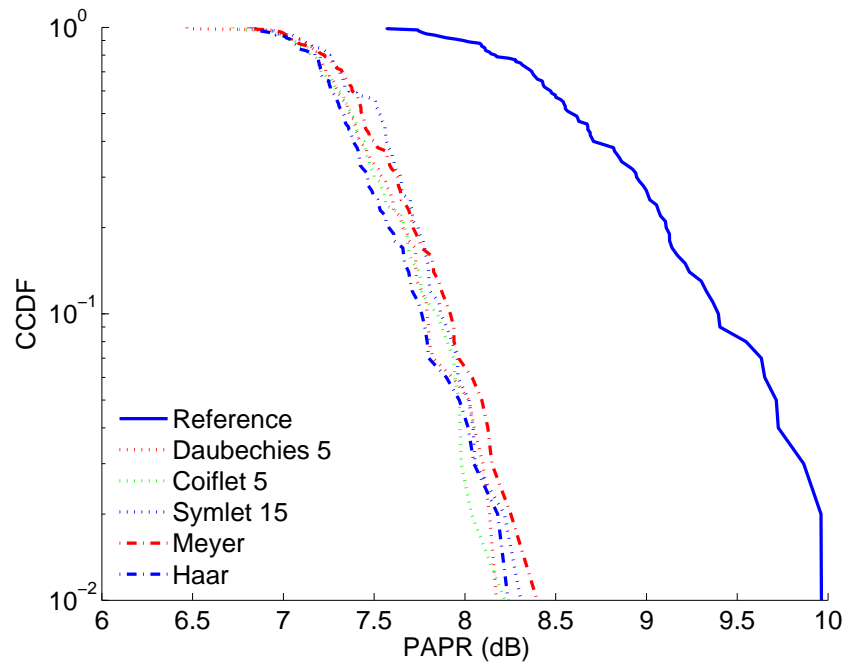


Figure 6-5: CCDF of the PAPR of WPM using Hill Climbing based optimization method. The WPM system is realized using a filter bank structure with 4 levels of decomposition and QPSK modulation scheme, for different wavelet families.

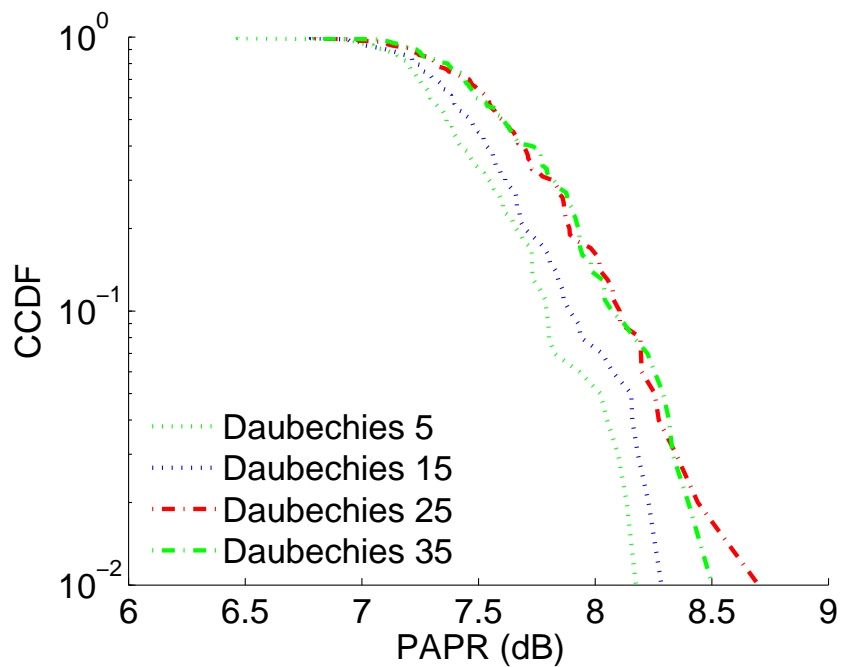


Figure 6-6: CCDF of the PAPR of WPM using Hill Climbing based optimization method with different filter lengths of the Daubechies wavelet family.

are shown. When the CCDF value is around 10^{-2} , the PAPR is around 8.3 to 8.7 dB. Daubechies 2 performs worse compared to the other Daubechies families.

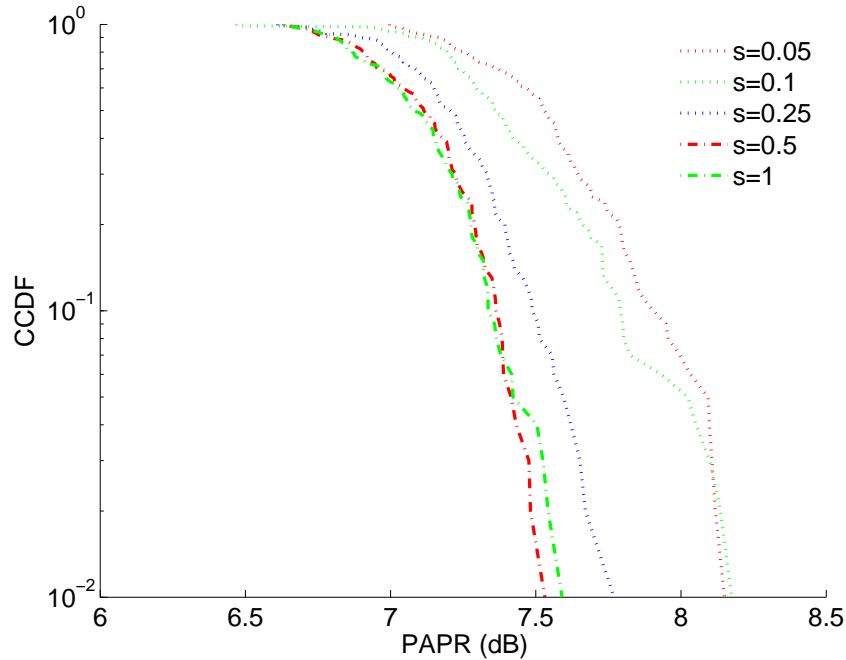


Figure 6-7: Impact of the initially selected step size, s_i on the PAPR reduction.

6-4 Convergence and Complexity

In this section, we present a discussion on the time complexity of the hill climbing based PAPR reduction algorithm and its convergence to a local optimum.

6-4-1 Time Complexity of the Algorithm

The time complexity of this pseudocode presented in Algorithm 6.1 is $O(TK)$ where T is number of iterations of the pseudocode until a local optimum is determined and K is the average number of neighbor solutions of a specific solution. For example, when the solution space is discrete, K is the average number of adjacent vertices of a vertex. For the PAPR reduction, if this simple hill climbing algorithm is considered, K depends on the number of subcarriers, M and it becomes $K = 2M$; because, for each subcarrier we determine a phase shift, for a solution point, there are two directions of the phase updates. Either the phase can be incremented or decremented with the step size. When considering the time complexity of the algorithm, constant terms are not influential. Therefore, $K = M$. Consequently, the time complexity of the simple hill climbing pseudocode presented in Algorithm 6.1, the time complexity is $O(TM)$ where T is still the number of iterations till convergence.

Algorithm 6.2 that we propose for PAPR reduction, is based on the simple pseudocode presented in Algorithm 6.1. Hence, the time complexity is the same except the time requirement for IDWPT. The time complexity of the IDWPT is $O(M \log_2 M)$. Therefore, the complexity of Algorithm 6.2 becomes $O(TM^2 \log_2 M)$.

6-4-2 Convergence of the Algorithm

The hill climbing based optimization of the PAPR reduction searches the space around a randomly selected phase vector, ϕ . The neighbor scanning depends on the step size as shown in Algorithm 6.2. If a large step size is selected, large jumps in the search space occurs. If the step size is too small, then the required number of epochs to converge to the minima increases. The exponential step size update dismisses the fine-tuning of the step size. The impact of the step size on the PAPR reduction is shown in Figure 6-7. As can be seen in this figure, a large step size; e.g., 1, produces a smaller PAPR. To avoid large running times of the algorithm, we bound the maximum number of epochs. The algorithm consumes all the search attempts by small steps (i.e., small step size) in the search domain before converging to the minima. If the maximum number of epochs increases, the running time of the algorithm is enlarged. However, it will be possible to converge a minima thanks to the exponential updates of the step sizes. When, by chance, a jump is made some where close to a minima, fluctuations around the minima (small jumps around the minima) will start and step size will be further halved. Consequently, as the step size decreases, convergence will be possible. This phenomenon is depicted in Figure 6-3(c); randomly selected initial phase vector is marked with *start*. After several large jumps, Algorithm 6.2 manages to reduce the step size and converge to a minima which is marked with *stop*. If a very small step size is selected, then the converge time increases as shown in Figure 6-8. In this demonstrative figure, Algorithm 6.2 converges to a minima in around 2000 epochs.

6-5 Summary

In this chapter, we extend the selected mapping technique by proposing a novel optimization scheme using the phase shifts of the selected mapping technique. The hill climbing based optimization outperforms in comparison to other techniques such as SLM or scrambling based techniques. When we compare the hill climbing based selected mapping technique where phase-shifted copies of the original signal is sent over the channel with the signal scrambling techniques which are mentioned in the previous chapters, it can be concluded that the optimization technique performs better.

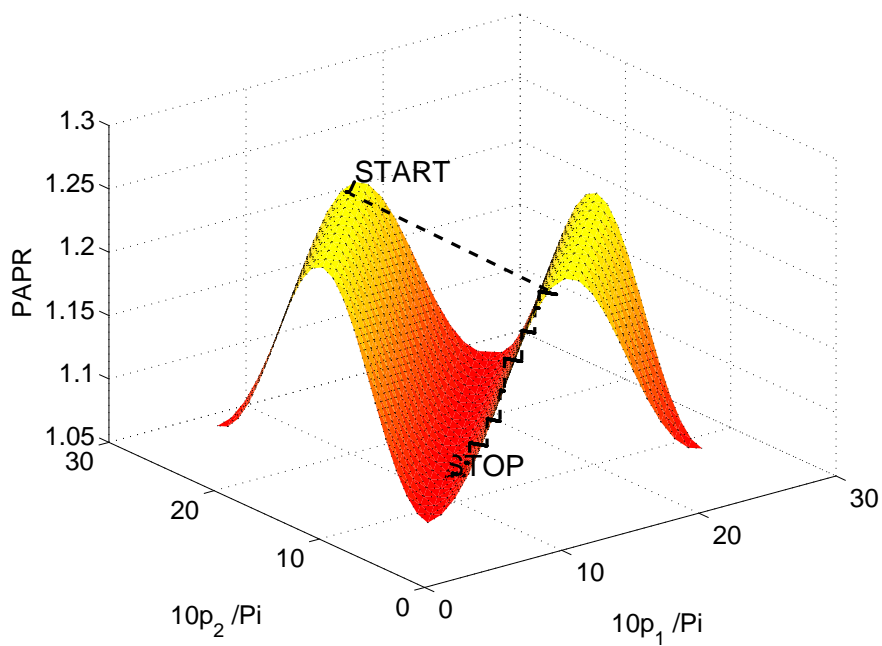


Figure 6-8: Demonstration of the impact of the initially selected step size where $s_j = 0.01$, $\forall j$ on the PAPR reduction. The wavelet considered is Daubechies 5 (length 10). Algorithm 6.2 converges to a minima in around 2000 epochs which are marked with black dots.

Conclusions and Future Research

In this thesis report we presented how to employ selected mapping technique with scrambling and with phase modification, respectively to reduce the Peak-to-Average-Power-Ratio (PAPR) of the developmental Wavelet Packet Modulation (WPM) system. As a novelty, we propose to employ an encryption system which is similar to additive scrambling technique to reduce the Peak-to-Average Power Ratio (PAPR). Furthermore, we extend the selected mapping technique by proposing a novel optimization scheme using the phase shifts of the selected mapping technique. The conclusions of the proposed techniques will be summarized in Section 7-1 and the recommendations on future research topics will be discussed in Section 7-2.

7-1 Conclusions

In Chapter 3, a study on the effect of PAPR on the developmental Wavelet Packet Modulation (WPM) scheme was presented. The stochastic of WPM signal and its power variations were simulated. We showed that the envelope of the WPM signal follows the Gaussian distribution and its power has Chi-squared distribution. In this chapter, we also presented the analysis of the PAPR performance for WPM systems with different wavelets, pulse shapes and lengths. Almost all the wavelets performed similarly with regard to their PAPR performances.

In Chapter 4, selected mapping with phase modification technique to reduce the PAPR in the Wavelet Packet Modulation system is presented. By altering the phase of the WPM sub-carriers, the PAPR of the transmitted signal is changed. By creating replicas of the original message by randomly altering the phases of the sub-carriers that modulate the information, different WPM frames with different PAPR values is obtained. The WPM frame having least PAPR is transmitted. The possibility of the WPM system slipping into non-linear region is considerably reduced. The importance of the method is in its simplicity and elegance of implementation.

In Chapter 5, the selected mapping with scrambling techniques used to reduce the PAPR is presented. In the selected mapping with scrambling based techniques, replicas of the original input signal is created by scrambling the original message with different scrambling sequences. Additive and multiplicative scramblers are considered in this study. As a novelty of this chapter, we propose to employ an encryption system which is similar to additive scrambling technique to reduce the PAPR. The proposed encryption based system enhances the security of the system, performs as well as additive scrambler and incurs no additional cost. Since all telecommunications systems employ some kind of stream ciphers to secure the signals transmitted over an insecure channel, using the same block for PAPR reduction does not introduce additional implementation or permutational costs. To the best of our knowledge, this technique has never been employed in Orthogonal Frequency Division Multiplexing (OFDM) or WPM systems.

When secure PAPR reduction technique is used, multiple encrypted replicas of the original message with different keys are used in the selected mapping. Among these generated scrambled signals containing the original signal, the one producing the least PAPR is selected after modulation and transmitted. When additive scrambler or secure PAPR is employed, additional side information, namely, the initialization state (seed) or the index of the ciphering key is transmitted to the receivers, respectively. When multiplicative scrambler is used, no side information is required. However, a prefix has to be inserted in front of the signal to change the output of the scrambler such that various scrambled copies of the same original signal can be generated. Since original signal is used to alter the state of the multiplicative scrambler, the output signal consists of the diffused original signal which implies that a symbol error will also be diffused to the other symbol positions. In selected mapping with multiplicative scrambling, symbol errors disperse onto the other symbol positions resulting in a larger Bit Error Rate (BER).

In Chapter 6, we extend the selected mapping technique by proposing a novel optimization scheme using the phase shifts of the selected WPM signal mapping technique. Neural network optimizers; specifically the Hopfield neural networks are discussed. Because of the intractability of differentiating the phase-shifted WPM frame; instead of employing neural optimizer, we digressed to a numerical local search technique; namely, the hill climbing based optimization. The hill climbing based optimization outperforms in comparison to other techniques such as SLM or scrambling based techniques. When we compare the hill climbing based selected mapping technique where phase-shifted copies of the original signal is sent over the channel with the signal scrambling techniques, it can be concluded that the optimization technique performs better. The large side information requirement of this optimization technique reduces the applicability of this technique. However, by bounding the phase alphabet the side information requirement can be overcome with a trade-off with the PAPR reduction performance.

To summarize the conclusions:

- We showed that the envelope of the WPM signal follows the Gaussian distribution and its power has Chi-squared distribution.
- In this thesis, the secure PAPR reduction technique is proposed for the first time

to the best of our knowledge.

- By employing the selected mapping with phase modifications, we showed that the PAPR of the WPM system can be significantly reduced.
- We optimized the selected mapping with phase modification technique using the hill climbing local search to further reduce the PAPR of the WPM system.
- When we compare the hill climbing based selected mapping technique where phase-shifted copies of the original signal is sent over the channel with the signal scrambling techniques which are mentioned in the previous chapters, it can be concluded that the optimization technique performs better.
- In this thesis, we showed that the PAPR of the WPM system can be reduced 2-3 dB using selected mapping techniques. By optimizing the selected mapping technique 1 dB further reduction can be achieved.

7-2 Future Research Topics

Future efforts in this area can broadly be in the lines of:

- Exploiting the unique tree structure of WPM to come out with the best tree formation with minimum PAPR. Unlike OFDM which divides the communication channel into orthogonal subchannels of equal bandwidths, WPM uses an arbitrary time-frequency plane tiling to create orthogonal subchannels of different bandwidths and symbol rates. When transmitting the same data in WPM, alternative tree representations can be used resulting in different subchannel spacing in time and frequency which are not necessarily uniform. This feature of WPM can be utilized for the reduction of PAPR. In particular, each of the alternative (pruned) trees could result in a different value for PAPR, and an algorithm to choose the optimum tree structure can be devised such that the structure achieves the minimum PAPR.
- Carrying out research with the aim to obviate the need to send side information (or the index of the phase vector with least PAPR). In selected mapping with multiplicative scrambling, symbol errors disperse onto the other symbol positions resulting in a larger BER. Since the channel decoder usually emits errors in bursts, the error multiplication is in practice even less severe. By implementing a convolutional code as the channel code, the scrambler and the channel encoder as well as the channel decoder and the descrambler can be integrated into a single device without further cost, respectively to avoid this problem.
- Hill-Climbing (local search algorithm) can be extended further by finding the optimum set of phase values that result in the lowest possible PAPR at all instances via locating a good approximation to the global optimum of a given function using a large search space technique.

- A complexity analysis study which considers the cost of implementing the reduction technique along with the loss in data-rate.
- A comparison study between the performances of different PAPR reduction techniques in the field of signal scrambling and signal distortion.

Bibliography

- [1] A. Lindsey, “Wavelet packet modulation for orthogonally multiplexed communication,” *IEEE Transactions on Signal Processing*, vol. 45, no. 5, pp. 1336 – 1339, May 1997.
- [2] J. Bingham, “Multicarrier modulation for data transmission: an idea whose time has come,” *Communications Magazine, IEEE*, vol. 28, no. 5, pp. 5 –14, May 1990.
- [3] B. Hubbard and F. Meyer, *The world according to wavelets: the story of a mathematical technique in the making*. AK Peters Wellesley, 1998.
- [4] M. Lakshmanan and H. Nikookar, “A review of wavelets for digital wireless communication,” *Wireless Personal Communications*, vol. 37, no. 3, pp. 387–420, 2006.
- [5] I. Daubechies, *Ten Lectures on Wavelets*. Philadelphia: SIAM, 1992.
- [6] S. Mallat, “A theory for multiresolution signal decomposition: the wavelet representation,” *Pattern Analysis and Machine Intelligence, IEEE Transactions on*, vol. 11, no. 7, pp. 674 –693, jul 1989.
- [7] ———, “Multiresolution approximations and wavelet orthonormal bases of $L^2(\mathbb{R})$,” *Transactions of the American Mathematical Society*, vol. 315, no. 1, pp. 69–87, 1989.
- [8] C. Burrus, R. Gopinath, H. Guo, J. Odegard, and I. Selesnick, *Introduction to wavelets and wavelet transforms: a primer*. Prentice Hall Upper Saddle River, NJ, 1997.
- [9] *DVB Standards and Specifications*, European Telecommunications Standards Institute Std.
- [10] B. Crow, I. Widjaja, L. Kim, and P. Sakai, “IEEE 802.11 wireless local area networks,” *IEEE Communications magazine*, vol. 35, no. 9, pp. 116–126, 1997.

- [11] C. Bernardos, I. Soto, and A. Banchs, "IEEE 802.11 standards," *Medium Access Control in Wireless Networks*, p. 235, 2008.
- [12] *IEEE 802.11 Specifications*, IEEE 802 LAN/MAN Standards Committee Std.
- [13] *IEEE 802.15 Specifications*, IEEE 802 LAN/MAN Standards Committee, WPAN WG Std.
- [14] *IEEE 802.20 Specifications*, IEEE 802 LAN/MAN Standards Committee, Mobile Broadband Wireless Access Std.
- [15] A. Jamin and P. Mahonen, "Wavelet packet modulation for wireless communications," *Wireless Communications and Mobile Computing Journal*, vol. 5, no. 2, pp. 123 – 137, Mar. 2005.
- [16] K. Anwar, A. Priantoro, M. Saito, T. Hara, M. Okada, and H. Yamamoto, "On the PAPR reduction for wavelet based transmultiplexer," in *IEEE International Symposium on Communications and Information Technology, 2004. ISCIT 2004*, 2004, pp. 812–815.
- [17] M. Gautier and J. Lienard, "Performances of complex wavelet packet based multicarrier transmission through double dispersive channel," in *Proceedings of the 7th Nordic Signal Processing Symposium, NORSIG 2006.*, 7-9 2006, pp. 74 –77.
- [18] M. Vetterli and J. Kovacevic, *Wavelets and Subband Coding*. Englewood Cliffs, New Jersey: Prentice Hall PTR, 1995.
- [19] A. Jones, T. Wilkinson, and S. Barton, "Block coding scheme for reduction of peak to mean envelope power ratio of multicarrier transmission schemes," *Electronics Letters*, vol. 30, p. 2098, 1994.
- [20] R. Bauml, R. Fischer, and J. Huber, "Reducing the peak-to-average power ratio of multicarrier modulation by selected mapping," *Electronics Letters*, vol. 32, pp. 2056 – 2057, 1996.
- [21] P. Van Eetvelt, G. Wade, and M. Tomlinson, "Peak to average power reduction for OFDM schemes by selective scrambling," *Electronics letters*, vol. 32, p. 1963, 1996.
- [22] S. Muller and J. Huber, "OFDM with reduced peak-to-average power ratio by optimum combination of partial transmit sequences," *Electronics letters*, vol. 33, no. 5, 1997.
- [23] M. Friese, "Multitone signals with low crest factor," *IEEE Transactions on Communications*, vol. 45, no. 10, pp. 1338–1344, 1997.
- [24] R. van Nee and A. de Wild, "Reducing the peak-to-average power ratio of ofdm," in *Proc. of the 48th IEEE Vehicular Technology Conference, VTC 98*, vol. 3, 18-21 1998, pp. 2072 –2076 vol.3.

-
- [25] O. Muta, T. Takada, and Y. Akaiwa, "Peak power suppression with parity carrier for multicarrier transmission," in *IEEE conf. proc. VTC*, vol. 99, 1999, pp. 2923–2928.
- [26] D. Kim and G. Stuber, "Clipping noise mitigation for OFDM by decision-aided reconstruction," *IEEE Communications Letters*, vol. 3, no. 1, pp. 4–6, 1999.
- [27] X. Wang, T. Tjhung, and C. Ng, "Reduction of peak-to-average power ratio of OFDM systems using a companding technique," *IEEE Transactions on Broadcasting*, vol. 45, no. 3, 1999.
- [28] H. W. Kang, Y. S. Cho, and D. H. Youn, "On compensating nonlinear distortions of an ofdm system using an efficient adaptive predistorter," *Communications, IEEE Transactions on*, vol. 47, no. 4, pp. 522–526, apr 1999.
- [29] R. Van Nee and R. Prasad, *OFDM for wireless multimedia communications*. Artech House, Inc. Norwood, MA, USA, 2000.
- [30] J. Tellado, *Multicarrier modulation with low PAR: applications to DSL and wireless*. Springer Netherlands, 2000.
- [31] S. Slimane, "Peak-to-average power ratio reduction of ofdm signals using pulse shaping," in *Proc. of the IEEE Global Telecommunications Conference, GLOBECOM*, vol. 3, 2000, pp. 1412 – 1416.
- [32] H. Nikookar and K. Lidsheim, "Random phase updating algorithm for OFDM transmission with low PAPR," *IEEE Transactions on Broadcasting*, vol. 48, no. 2, pp. 123–128, 2002.
- [33] S. H. Han and J. H. Lee, "An overview of peak-to-average power ratio reduction techniques for multicarrier transmission," *IEEE Wireless Communications*, vol. 12, no. 2, pp. 56 – 65, Apr. 2005.
- [34] H. Nikookar and D. Soehartono, "Complex-weighted ofdm transmission with low papr," in *Proc. of the European Conference on Wireless Technologies*, Munich, Germany, 8-10 Oct. 2007, pp. 8 – 11.
- [35] S. Litsyn, *Peak power control in multicarrier communications*. Cambridge Univ Pr, 2007.
- [36] M. Gautier, C. Lereau, M. Arndt, and J. Lienard, "Papr analysis in wavelet packet modulation," in *Communications, Control and Signal Processing, 2008. ISCCSP 2008. 3rd International Symposium on*, St Julians, Portugal, 12-14 Mar. 2008, pp. 799 – 803.
- [37] B. Torun, M. Lakshmanan, and H. Nikookar, "On the analysis of peak-to-average power ratio of wavelet packet modulation," in *Proc. of European Wireless Technology Conference*, Roma, Italy, 29 Sept. – 1 Oct. 2009, pp. 1 – 4.

- [38] A. Jayalath and C. Tellambura, "The use of interleaving to reduce the peak-to-average power ratio of an ofdm signal," in *Global Telecommunications Conference, 2000. GLOBECOM '00. IEEE*, vol. 1, 2000, pp. 82–86 vol.1.
- [39] T. May and H. Rohling, "Reducing the peak-to-average power ratio in OFDM radio transmission systems," *Proc. of IEEE Vehicular Technology Conference, VTC 98*, pp. 2774–2778, 1998.
- [40] V. Kumbasar and O. Kucur, *Digital Signal Processing*. Elsevier, Nov. 2008, vol. 18, no. 6, ch. Better wavelet packet tree structures for PAPR reduction in WOFDM systems, pp. 885 – 891.
- [41] M. Baro and J. Ilow, "Improved papr reduction for wavelet packet modulation using multi-pass tree pruning," in *Proc. of the IEEE 18th International Symposium on Personal, Indoor and Mobile Radio Communications, PIMRC*, Athens, Greece, 3-7 Sept. 2007, pp. 1 – 5.
- [42] J. Davis and J. Jedwab, "Peak-to-mean power control and error correction for ofdm transmission using golay sequences and reed-muller codes," *Electronics Letters*, vol. 33, no. 4, pp. 267–268, Feb. 1997.
- [43] —, "Peak-to-mean power control in OFDM, Golay complementary sequences, and Reed–Muller codes," *IEEE Transactions on Information Theory*, vol. 45, no. 7, p. 2397, 1999.
- [44] M. Breiling, S. Müller-Weinfurtner, and J. Huber, "Peak–Power Reduction in OFDM without Explicit Side Information," in *5th International OFDM-Workshop*. Hamburg/Germany: Citeseer, Sept. 2000, pp. 28–1.
- [45] M. Breiling, S. Müller-Weinfurtner, and J. Huber, "Distortionless reduction of peak power without explicit side information," in *IEEE GLOBECOM*, vol. 3, 2000, pp. 1494 – 1498.
- [46] H. Breiling, S. Müller-Weinfurtner, and J. Huber, "SLM peak-power reduction without explicit side information," *IEEE Communications Letters*, vol. 5, no. 6, pp. 239–241, 2001.
- [47] A. Vallavaraj, B. G. Stewart, D. K. Harrison, and F. G. McIntosh, "Reducing the papr of ofdm using a simplified scrambling slm technique with no explicit side information," in *ICPADS '08: Proceedings of the 2008 14th IEEE International Conference on Parallel and Distributed Systems*. Washington, DC, USA: IEEE Computer Society, 2008, pp. 902–907.
- [48] P.-Y. Tsai, H.-Y. Kang, and T.-D. Chiueh, "Design of a baseband transceiver for multicarrier cdma communications," *EURASIP J. Appl. Signal Process.*, vol. 2005, pp. 1645–1655, 2005.
- [49] C.-Y. Hsu and H.-C. Chao, "Peak power reduction scheme base on transform kernel scrambling for ofdm systems," *Wirel. Pers. Commun.*, vol. 43, no. 4, pp. 1499–1509, 2007.

-
- [50] H. Ochiai and H. Imai, "Performance of OFDM-CDMA with simple peak power reduction," *European Transactions on Telecommunications*, vol. 10, no. 4, pp. 391–398, 1999.
- [51] H. Beker and F. Piper, *Cipher systems: the protection of communications*. Northwood Books, 1982.
- [52] C. Ding, G. Xiao, and W. Shan, *The stability theory of stream ciphers*. Springer, 1991.
- [53] K. Zeng, C.-H. Yang, D.-Y. Wei, and T. Rao, "Pseudorandom bit generators in stream-cipher cryptography," *Computer*, vol. 24, no. 2, pp. 8–17, feb 1991.
- [54] C. Shannon, "Communication theory of secrecy systems," *Journal*, vol. 28, no. 4, pp. 656–715, 1949.
- [55] B.Torun, M. Lakshmanan, and H. Nikookar, "Peak-to-average power ratio reduction of wavelet packet modulation by adaptive phase selection," *PIMRC, Sept., Istanbul, Turkey*, 2010.
- [56] S. J. Russell and P. Norvig, *Artificial Intelligence: A Modern Approach*, 2nd ed. Upper Saddle River, New Jersey: Prentice Hall, 2003.
- [57] K. Yamashita, M. Ohta, and W. Jiang, "Reducing peak-to-average power ratio of multicarrier modulation by Hopfield neural network," *Electronics letters*, vol. 38, p. 1370, 2002.
- [58] J. Hopfield, "Neural networks and physical systems with emergent collective computational abilities," *Proceedings of the National Academy of Sciences of the United States of America*, vol. 79, no. 8, p. 2554, 1982.
- [59] M. Ohta, A. Mori, and K. Yamashita, "An FPGA implementation of 1,024-neuron system for PAPR reduction of OFDM signal," in *Proc of the IEEE International Joint Conference on Neural Networks*, vol. 4, 2004.
- [60] R. Rojas, *Neural networks: a systematic introduction*. Springer, 1996.
- [61] K. Priddy and P. Keller, *Artificial neural networks: An introduction*. Society of Photo Optical, 2005.
- [62] J. Heaton, *Introduction to Neural Networks for Java*. Heaton Research Inc, 2008.
- [63] Z. Michalewicz and D. Fogel, *How to solve it: modern heuristics*. Springer-Verlag New York Inc, 2004.
- [64] W. Press, S. Teukolsky, W. Vetterling, and B. Flannery, *Numerical recipes in Fortran; the art of scientific computing*. New York, NY, USA: Cambridge University Press New York, NY, USA, 1993.
- [65] F. Kohandani and A. Khandani, "A new algorithm for peak/average power reduction in OFDM systems," *IEEE Transactions on Broadcasting*, vol. 54, no. 1, pp. 159–165, Mar. 2008.

Publications

1. Berna Torun, Madan Kumar Lakshmanan, and Homayoun Nikookar, "On the analysis of peak-to-average power ratio of wavelet packet modulation," in *Proc. of the European Wireless Technology Conference*, Rome, Italy, September 2009, pp. 1 - 4.
2. Berna Torun, Madan Kumar Lakshmanan, and Homayoun Nikookar, "Peak-to-Average Power Ratio Reduction of Wavelet Packet Modulation by Adaptive Phase Selection," in *Proc. of the 21st IEEE PIMRC*, Istanbul, Turkey, September 2010.
3. Berna Torun, Madan Kumar Lakshmanan, and Homayoun Nikookar, "Phase Optimization for PAPR Reduction of Wavelet Packet Modulation," *submitted to the ICC 2011*, Kyoto, Japan.

Glossary

List of Acronyms

BER	Bit Error Rate
BPSK	Binary Phase Shift Keying
CCDF	Complementary Cumulative Distribution Function
CDF	Cumulative Distribution Function
CLT	Central Limit Theorem
CWT	Continuous Wavelet Transform
DAB	European Digital Audio Broadcasting
DFT	Discrete Fourier Transform
DVB	Digital Video Broadcasting
DWT	Discrete Wavelet Transform
DWPT	Discrete Wavelet Packet Transform
FDM	Frequency Division Multiplexing
FIR	Finite Impulse Response
FFT	Fast Fourier Transform
FPGA	Field-programmable gate array
HNN	Hopfield neural network
HPF	High-Pass Filter
IDFT	Inverse Discrete Fourier Transform

IDWPT	Inverse Discrete Wavelet Packet Transform
IDWT	Inverse Discrete Wavelet Transform
LFSR	Linear Feedback Shift Register
LPF	Low-Pass Filter
MBWA	Mobile Broadband Wireless Access
MCM	Multi-carrier Modulation
MRA	Multi-Resolution Analysis
OFDM	Orthogonal Frequency Division Multiplexing
OTP	One-time Pad
PAN	Personal Area Network
PAPR	Peak-to-Average Power Ratio
SNR	Signal-to-Noise Ratio
QMF	Quadrature Mirror Filters
QPSK	Quadratic Phase Shift Keying
UWB	Ultrawideband
WEP	Wired Equivalent Privacy
WPM	Wavelet Packet Modulation
WPT	Wavelet Packet Transform